

A Nonconvex Approach for Exact and Efficient Multichannel Sparse Blind Deconvolution

Qing Qu[#], Xiao Li[†], and Zhihui Zhu[◇]

[#]Center for Data Science, New York University

[†]Department of Electronic Engineering, the Chinese University of Hong Kong

[◇]Mathematical Institute for Data Science, Johns Hopkins University

December 12, 2021

Abstract

We study the multi-channel sparse blind deconvolution (MCS-BD) problem, whose task is to simultaneously recover a kernel \mathbf{a} and multiple sparse inputs $\{\mathbf{x}_i\}_{i=1}^p$ from their circulant convolution $\mathbf{y}_i = \mathbf{a} \circledast \mathbf{x}_i$ ($i = 1, \dots, p$). We formulate the task as a nonconvex optimization problem over the sphere. Under mild statistical assumptions of the data, we prove that the vanilla Riemannian gradient descent (RGD) method, with random initializations, provably recovers both the kernel \mathbf{a} and the signals $\{\mathbf{x}_i\}_{i=1}^p$ up to a signed shift ambiguity. In comparison with state-of-the-art results, our work shows significant improvements in terms of sample complexity and computational efficiency. Our theoretical results are corroborated by numerical experiments, which demonstrate superior performance of the proposed approach over the previous methods on both synthetic and real datasets.

Keywords. Nonconvex optimization, blind deconvolution, sparsity, Riemannian manifold/optimization, inverse problem, nonlinear approximation.

1 Introduction

We study the blind deconvolution problem with multiple inputs: given *circulant* convolutions

$$\mathbf{y}_i = \mathbf{a} \circledast \mathbf{x}_i \in \mathbb{R}^n, \quad i \in [p] := \{1, \dots, p\}, \quad (1)$$

we aim to recover both the kernel $\mathbf{a} \in \mathbb{R}^n$ and the signals $\{\mathbf{x}_i\}_{i=1}^p \in \mathbb{R}^n$ using efficient methods. Blind deconvolution is an *ill-posed* problem in its most general form. Nonetheless, problems in practice often exhibit *intrinsic* low-dimensional structures, showing promises for efficient optimization. One such useful structure is the *sparsity* of the signals $\{\mathbf{x}_i\}_{i=1}^p$. The multichannel sparse blind deconvolution (MCS-BD) broadly appears in the context of communications [ADCY97, TBSR17], computational imaging [BPS⁺06, SCL⁺15], seismic imaging [KT98, NFTLR15, RPD⁺15], neuroscience [GPAF03, ETS11, WLS⁺13, FZP17, PSG⁺16], computer vision [LWDF11, ZWZ13, SM12], and more.

- **Neuroscience.** Detections of neuronal spiking activity is a prerequisite for understanding the mechanism of brain function. Calcium imaging [FZP17, PSG⁺16] and functional MRI [GPAF03, WLS⁺13] are two widely used techniques, which record the convolution of unknown neuronal transient response and sparse spike trains. The spike detection problem can be naturally cast as a MCS-BD problem.

Table 1: Comparison with existing methods for solving MCS-BD¹

Methods	Wang et al. [WC16]	Li et al. [LB18]	Ours
Assumptions	\mathbf{a} spiky & invertible, $\mathbf{x}_i \sim \text{i.i.d. } \mathcal{BG}(\theta)$	\mathbf{a} invertible, $\mathbf{x}_i \sim \text{i.i.d. } \mathcal{BR}(\theta)$	\mathbf{a} invertible, $\mathbf{x}_i \sim \text{i.i.d. } \mathcal{BG}(\theta)$
Formulation	$\min_{q_1=1} \ \mathbf{C}_q \mathbf{Y}\ _1$	$\max_{q \in \mathbb{S}^{n-1}} \ \mathbf{C}_q \mathbf{P} \mathbf{Y}\ _4^4$	$\min_{q \in \mathbb{S}^{n-1}} H_\mu(\mathbf{C}_q \mathbf{P} \mathbf{Y})$
Algorithm	interior point	noisy RGD	vanilla RGD
Recovery Condition	$\theta \in \mathcal{O}(1/\sqrt{n})$, $p \geq \tilde{\Omega}(n)$	$\theta \in \mathcal{O}(1)$, $p \geq \tilde{\Omega}(\max\{n, \kappa^8\} \frac{n^8}{\varepsilon^8})$	$\theta \in \mathcal{O}(1)$, $p \geq \tilde{\Omega}(\max\{n, \frac{\kappa^8}{\mu^2}\} n^4)$
Time Complexity	$\tilde{\mathcal{O}}(p^4 n^5 \log(1/\varepsilon))$	$\tilde{\mathcal{O}}(pn^{13}/\varepsilon^8)$	$\tilde{\mathcal{O}}(pn^5 + pn \log(1/\varepsilon))$

- **Computational (microscopy) imaging.** Super-resolution fluorescent microscopy imaging [BPS⁺06,HGM06,RBZ06] conquers the resolution limit by solving sparse deconvolution problems. Its basic principle is using photoswitchable fluorophores that stochastically activate fluorescent molecular, creating a video sequence of sparse superpositions of point spread function (PSF). In many scenarios (especially in 3D imaging), as it is often difficult to obtain the PSF due to defocus and unknown aberrations [SN06], it is preferred to estimate the point-sources and PSF jointly by solving MCS-BD.
- **Image deblurring.** Sparse blind deconvolution problems also arise in natural image processing: when a blurry image is taken due to the resolution limit or malfunction of imaging procedure, it can be modeled as a blur pattern convolved with visually plausible sharp images (whose gradient are sparse) [ZWZ13,SM12].

Prior arts on MCS-BD. Recently, there have been a few attempts to solve MCS-BD with guaranteed performance. Wang et al. [WC16] formulated the task as finding the sparsest vector in a subspace problem [QSW14]. They considered a convex objective, showing that the problem can be solved to exact solutions when $p \geq \Omega(n \log n)$ and the sparsity level $\theta \in \mathcal{O}(1/\sqrt{n})$. A similar approach has also been investigated by [Cos17]. Li et al. [LB18] consider a nonconvex ℓ^4 -maximization problem over the sphere², revealing benign global geometric structures of the problem. Correspondingly, they introduced a *noisy* Riemannian gradient descent (RGD) that solves the problem to approximate solutions in polynomial time.

These results are very inspiring but still suffer from quite a few limitations. The theory and method in [WC16] *only* applies to cases when \mathbf{a} is approximately a delta function (which excludes most problems of interest) and $\{\mathbf{x}_i\}_{i=1}^p$ are *very* sparse. Li et al. [LB18] suggests that more generic kernels \mathbf{a} can be handled via preconditioning of the data. However, due to the *heavy-tailed* behavior of ℓ^4 -loss, the sample complexity provided in [LB18] is quite *pessimistic*³. Moreover, noisy RGD is proved to converge with huge amounts of iterations [LB18], and it requires additional efforts to tune the noise parameters which is often unrealistic in practice. As mentioned in [LB18], one may use vanilla RGD which almost surely converges to a global minimum, but without guarantee on the number of iterations. On the other hand, Li et al. [LB18] only considered the Bernoulli-Rademacher model⁴ which is restrictive for many problems.

¹Here, (i) $\mathcal{BG}(\theta)$ and $\mathcal{BR}(\theta)$ denote Bernoulli-Gaussian and Bernoulli-Rademacher distribution, respectively; (ii) $\theta \in [0, 1]$ is the Bernoulli parameter controlling the sparsity level of \mathbf{x}_i ; (iii) ε denotes the recovery precision of global solution \mathbf{a}_* , i.e., $\min_{\ell} \|\mathbf{a} - s_{\ell}[\mathbf{a}_*]\| \leq \varepsilon$; (iv) $\tilde{\mathcal{O}}$ and $\tilde{\Omega}$ hides $\log(n)$, θ and other factors. For [WC16], we may get rid of the spiky assumption by solving a preconditioned problem $\min_{q_1=1} \|\mathbf{C}_q \mathbf{P} \mathbf{Y}\|_1$, where \mathbf{P} is a preconditioning matrix defined in (6).

²Recently, similar loss has been considered for short and sparse deconvolution [ZKW18] and complete dictionary learning [ZYL⁺19].

³As the tail of $\mathcal{BG}(\theta)$ distribution is heavier than that of $\mathcal{BR}(\theta)$, their sample complexity would be even worse if $\mathcal{BG}(\theta)$ model was considered.

⁴We say \mathbf{x} obeys a Bernoulli-Rademacher distribution when $\mathbf{x} = \mathbf{b} \odot \mathbf{r}$ where \odot denotes point-wise product, \mathbf{b} follows i.i.d. Bernoulli distribution and \mathbf{r} follows i.i.d. Rademacher distribution.

Contributions of this paper. In this work, we introduce an efficient optimization method for solving MCS-BD. We consider a natural nonconvex formulation based on a smooth relaxation of ℓ^1 -loss. Under mild assumptions of the data, we prove the following result.

With *random* initializations, a *vanilla* RGD efficiently finds an approximate solution, which can be refined by a subgradient method that converges exactly to the target solution in a *linear* rate.

We summarize our main result in Table 1. By comparison⁵ with [LB18], our approach demonstrates *substantial* improvements for solving MCS-BD in terms of both sample and time complexity. Moreover, our experimental results imply that our analysis is still far from tight – the phase transitions suggest that $p \geq \Omega(\text{poly log}(n))$ samples might be sufficient for exact recovery, which is favorable for applications (as real data in form of images can have millions of pixels, resulting in huge dimension n). Our analysis is inspired by recent results on orthogonal dictionary learning [GBW18, BJS18], but much of our theoretical analysis is tailored for MCS-BD with a few extra new ingredients. Our work is the first result provably showing that *vanilla* gradient descent type methods with random initialization solve MCS-BD efficiently. Moreover, our ideas could potentially lead to new algorithmic guarantees for other nonconvex problems such as blind gain and phase calibration [LLB17, LS18] and convolutional dictionary learning [BEL13, GCW18].

Organizations, notations, and reproducible research. We organize the rest of the paper as follows. In Section 2, we introduce the basic assumptions and nonconvex problem formulation. Section 3 presents the main results and sketch of analysis. In Section 4, we demonstrate the proposed approach by experiments on both synthetic and real datasets. We conclude the paper in Section 5. The basic notations are introduced in Appendix A, and all the detailed analysis are deferred to the appendices. For reproducing the experimental results in this work, we refer readers to

<https://github.com/qingqu06/MCS-BD>.

2 Problem Formulation

2.1 Assumptions and Intrinsic Properties

Assumptions To begin, we list our assumptions on the kernel $\mathbf{a} \in \mathbb{R}^n$ and sparse inputs $\{\mathbf{x}_i\}_{i=1}^p \in \mathbb{R}^n$:

1. *Invertible kernel.* We assume the kernel \mathbf{a} to be *invertible* in the sense that its spectrum $\hat{\mathbf{a}} = \mathbf{F}\mathbf{a}$ does not have zero entries, where $\hat{\mathbf{a}} = \mathbf{F}\mathbf{a}$ is the discrete Fourier transform (DFT) of \mathbf{a} with $\mathbf{F} \in \mathbb{C}^{n \times n}$ being the DFT matrix. Let $\mathbf{C}_{\mathbf{a}} \in \mathbb{R}^{n \times n}$ be an $n \times n$ circulant matrix whose first column is \mathbf{a} ; see (17) for the formal definition. Since this circulant matrix $\mathbf{C}_{\mathbf{a}}$ can be decomposed as $\mathbf{C}_{\mathbf{a}} = \mathbf{F}^* \text{diag}(\hat{\mathbf{a}}) \mathbf{F}$ [G⁺06], it is also invertible and we define its condition number

$$\kappa(\mathbf{C}_{\mathbf{a}}) := \max_i |\hat{a}_i| / \min_i |\hat{a}_i|.$$

2. *Random sparse signal.* We assume the input signals $\{\mathbf{x}_i\}_{i=1}^p$ follow i.i.d. Bernoulli-Gaussian ($\mathcal{BG}(\theta)$) distribution:

$$\mathbf{x}_i = \mathbf{b}_i \odot \mathbf{g}_i, \quad \mathbf{b}_i \sim \text{i.i.d. } \mathcal{B}(\theta), \quad \mathbf{g}_i \sim \text{i.i.d. } \mathcal{N}(\mathbf{0}, \mathbf{I}),$$

where $\theta \in [0, 1]$ is the Bernoulli-parameter which controls the sparsity level of each \mathbf{x}_i .

As aforementioned, this assumption generalizes those used in [WC16, LB18]. In particular, the first assumption on kernel \mathbf{a} is much more practical than that of [WC16], in which \mathbf{a} is assumed to be approximately a delta function. The second assumption is a generalization of the Bernoulli-Rademacher model adopted in [LB18].

⁵We do not find a direct comparison with [WC16] meaningful, mainly due to its limitations of the kernel assumption and sparsity level $\theta \in \mathcal{O}(1/\sqrt{n})$ discussed above.

Intrinsic symmetry. Note that the MCS-BD problem exhibits intrinsic *signed scaling-shift* symmetry, i.e., for any $\alpha \neq 0$,

$$\mathbf{y}_i = \mathbf{a} \circledast \mathbf{x}_i = s_{-\ell}[\pm\alpha\mathbf{a}] \circledast s_{\ell}[\pm\alpha^{-1}\mathbf{x}_i], \quad i \in \{0, 1, \dots, p-1\}, \quad (2)$$

where $s_{\ell}[\cdot]$ denotes a cyclic shift operator of length ℓ . Thus, we only hope to recover \mathbf{a} and $\{\mathbf{x}_i\}_{i=1}^p$ up to a *signed shift ambiguity*. Without loss of generality, for the rest of the paper we assume that the kernel \mathbf{a} is normalized with $\|\mathbf{a}\| = 1$.

2.2 A Nonconvex Formulation

Let $\mathbf{Y} = [\mathbf{y}_1 \ \mathbf{y}_2 \ \dots \ \mathbf{y}_p]$ and $\mathbf{X} = [\mathbf{x}_1 \ \mathbf{x}_2 \ \dots \ \mathbf{x}_p]$. We can rewrite the measurement (1) in a matrix-vector form via circulant matrices,

$$\mathbf{y}_i = \mathbf{a} \circledast \mathbf{x}_i = \mathbf{C}_a \mathbf{x}_i, \quad i \in [p] \implies \mathbf{Y} = \mathbf{C}_a \mathbf{X},$$

Since \mathbf{C}_a is assumed to be invertible, we can define its corresponding *inverse kernel* $\mathbf{h} \in \mathbb{R}^n$ by $\mathbf{h} := \mathbf{F}^{-1} \hat{\mathbf{a}}^{\odot -1}$ whose corresponding circulant matrix satisfies

$$\mathbf{C}_h := \mathbf{F}^* \text{diag}(\hat{\mathbf{a}}^{\odot -1}) \mathbf{F} = \mathbf{C}_a^{-1},$$

where $(\cdot)^{\odot -1}$ denotes entrywise inversion. Observing

$$\mathbf{C}_h \cdot \mathbf{Y} = \underbrace{\mathbf{C}_h \cdot \mathbf{C}_a}_{=\mathbf{I}} \cdot \mathbf{X} = \underbrace{\mathbf{X}}_{\text{sparse}},$$

it leads us to consider the following objective

$$\min_{\mathbf{q}} \frac{1}{np} \|\mathbf{C}_q \mathbf{Y}\|_0 = \frac{1}{np} \sum_{i=1}^p \|\mathbf{C}_{y_i} \mathbf{q}\|_0, \quad \text{s.t. } \mathbf{q} \neq \mathbf{0}. \quad (3)$$

Obviously, when the solution of (3) is unique, the *only* minimizer is the inverse kernel \mathbf{h} up to signed scaling-shift (i.e., $\mathbf{q}_{\star} = \pm \alpha s_{\ell}[\mathbf{h}]$), producing $\mathbf{C}_h \mathbf{Y} = \mathbf{X}$ with the highest sparsity. The nonzero constraint $\mathbf{q} \neq \mathbf{0}$ is enforced simply to prevent the trivial solution $\mathbf{q} = \mathbf{0}$. Ideally, if we could solve (3) to obtain one of the target solutions $\mathbf{q}_{\star} = s_{\ell}[\mathbf{h}]$ up to a signed scaling, the kernel \mathbf{a} and sparse signals $\{\mathbf{x}_i\}_{i=1}^p$ can be exactly recovered up to signed shift via

$$\mathbf{a}_{\star} = \mathbf{F}^{-1} \left[(\mathbf{F} \mathbf{q}_{\star})^{\odot -1} \right], \quad \mathbf{x}_i^{\star} = \mathbf{C}_{y_i} \mathbf{q}_{\star}, \quad (1 \leq i \leq p).$$

However, it has been known for decades that optimizing the basic ℓ_0 -formulation (3) is an NP-hard problem [CP86, Nat95]. Instead, we consider the following *nonconvex*⁶ relaxation of the original problem (3):

$$\boxed{\min_{\mathbf{q}} \varphi_h(\mathbf{q}) := \frac{1}{np} \sum_{i=1}^p H_{\mu}(\mathbf{C}_{y_i} \mathbf{P} \mathbf{q}), \quad \text{s.t. } \mathbf{q} \in \mathbb{S}^{n-1},} \quad (4)$$

where $H_{\mu}(\cdot)$ is the Huber loss [Hub92] and \mathbf{P} is a preconditioning matrix, both of which will be defined and discussed in detail as follows.

⁶It is nonconvex because of the spherical constraint $\mathbf{q} \in \mathbb{S}^{n-1}$.

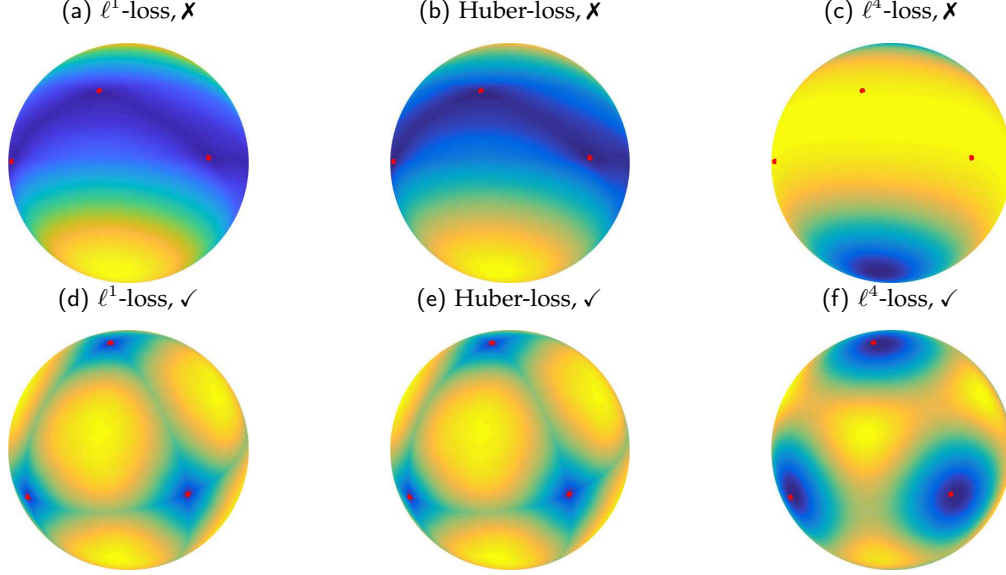


Figure 1: Comparison of optimization landscapes for different loss functions. Here \times and \checkmark mean without and with the preconditioning matrix \mathbf{P} , respectively. Each figure plots the function values of the loss over \mathbb{S}^2 , where the function values are all normalized between 0 and 1 (darker color means smaller value, and vice versa). The small red dots on the landscapes denote shifts of the ground truths.

Smooth sparsity surrogate. It is well-known that ℓ^1 -norm serves as a natural sparsity surrogate for ℓ^0 -norm, but its nonsmoothness often makes it difficult for analysis⁷. Here, we consider the Huber loss⁸ $H_\mu(\cdot)$ which is widely used in robust optimization [Hub92]. It acts as a *smooth* sparsity surrogate of ℓ^1 penalty and is defined as:

$$H_\mu(\mathbf{Z}) := \sum_{i=1}^n \sum_{j=1}^p h_\mu(Z_{ij}), \quad h_\mu(z) := \begin{cases} |z| & |z| \geq \mu \\ \frac{z^2}{2\mu} + \frac{\mu}{2} & |z| < \mu \end{cases}, \quad (5)$$

where $\mu > 0$ is a smoothing parameter. Our choice $h_\mu(z)$ is first-order smooth, and behaves exactly same as the ℓ^1 -norm for all $|z| \geq \mu$. In contrast, although the ℓ^4 objective in [LB18] is smooth, it only promotes sparsity in special cases. Moreover, it results in a heavy-tailed process, producing flat landscape around target solutions, and requiring substantially more samples for measure concentration. Figure 1 shows a comparison of optimization landscapes of all losses in low dimension: the Huber-loss produces an almost identical landscape as the ℓ^1 -loss, while optimizing the ℓ^4 -loss could result in large approximation error.

Preconditioning. An ill-conditioned kernel \mathbf{a} can result in poor optimization landscapes (see Figure 1 for an illustration). To alleviate this effect, we introduce a preconditioning matrix $\mathbf{P} \in \mathbb{R}^{n \times n}$ [SQW16, ZKW18, LB18], defined as follows⁹

$$\mathbf{P} = \left(\frac{1}{\theta np} \sum_{i=1}^p \mathbf{C}_{\mathbf{y}_i}^\top \mathbf{C}_{\mathbf{y}_i} \right)^{-1/2}, \quad (6)$$

⁷The subgradient of ℓ^1 -loss is *non-Lipschitz*, which introduces tremendous difficulty in controlling suprema of random process and perturbation analysis for preconditioning

⁸Actually, $h_\mu(\cdot)$ is a scaled and elevated version of the standard Huber function $h_\mu^s(z)$, with $h_\mu(z) = \frac{1}{\mu} h_\mu^s(z) + \frac{\mu}{2}$. Hence in our framework minimizing with $h_\mu(z)$ is equivalent to minimizing with $h_\mu^s(z)$.

⁹Here, the sparsity θ serves as a normalization purpose. It is often not known ahead of time, but the scaling here does not change the optimization landscape.

which refines the optimization landscapes by orthogonalizing the circulant matrix C_a as

$$\underbrace{C_a P}_R \approx \underbrace{C_a (C_a^\top C_a)^{-1/2}}_{Q \text{ orthogonal}}. \quad (7)$$

Since $P \approx (C_a^\top C_a)^{-1/2}$, R can be proved to be very close to the orthogonal matrix Q . Thus, R is much more well-conditioned than C_a . As illustrated in Figure 1, a comparison of optimization landscapes without and with preconditioning shows that preconditioning symmetrifies the optimization landscapes and eliminates *spurious* local minimizers. Therefore, it makes the problem more amenable to optimization algorithms.

Constrain over the sphere \mathbb{S}^{n-1} . We relax the nonconvex constraint $q \neq 0$ in (3) by a unit norm constraint on q . The norm constraint removes the scaling ambiguity as well as prevents the trivial solution $q = 0$. Note that the choice of the norm has strong implication for computation. When q is constrained over ℓ^∞ -norm, the ℓ^1/ℓ^∞ optimization problem breaks beyond sparsity level $\theta \geq \Omega(1/\sqrt{n})$ [WC16]. In contrast, the sphere \mathbb{S}^{n-1} is a smooth homogeneous Riemannian manifold and it has been shown recently that optimizing over the sphere leads to optimal sparsity $\theta \in \mathcal{O}(1)$ for several sparse learning problems [QSW14, SQW16, SQW17, LB18]. Therefore, we choose to work with a nonconvex spherical constraint $q \in \mathbb{S}^{n-1}$ and we will also show similar results for MCS-BD.

Next, we develop efficient first-order methods and provide guarantees for exact recovery.

3 Main Results and Analysis

In this section, we show that the underlying benign *first-order geometry* of the optimization landscapes of Equation (4) enables efficient and exact recovery using *vanilla* gradient descent methods, even with *random* initialization. Our main result can be captured by the following theorem, with details described in the following subsections.

Theorem 3.1 *We assume that the kernel a is invertible with condition number κ , and $\{x_i\}_{i=1}^p \sim \mathcal{BG}(\theta)$. Suppose $\theta \in (\frac{1}{n}, \frac{1}{3})$ and $\mu \leq c \min\left\{\theta, \frac{1}{\sqrt{n}}\right\}$. Whenever*

$$p \geq C \max\left\{n, \frac{\kappa^8}{\theta \mu^2 \sigma_{\min}^2} \log^4 n\right\} \theta^{-2} n^4 \log^3(n) \log\left(\frac{\theta n}{\mu}\right), \quad (8)$$

w.h.p. the function (4) satisfies certain regularity conditions (see Theorem 3.2), allowing us to design an efficient vanilla first-order method. In particular, with probability at least $\frac{1}{2}$, by using a random initialization, the algorithms provably recover the target solution up to a signed shift with ε -precision in a linear rate

$$\#Iter \leq C' \left(\theta^{-1} n^4 \log\left(\frac{1}{\mu}\right) + \log(np) \log\left(\frac{1}{\varepsilon}\right) \right).$$

Remark 1. The detailed proofs are detained to Appendix C and Appendix D. In the following, we explain our results in several aspects.

- **Conditions and Assumptions.** Here, as the MCS-BD problem becomes trivial¹⁰ when $\theta \leq 1/n$, we only focus on the regime $\theta > 1/n$. Similar to [LB18], our result only requires the kernel a to be invertible and sparsity level θ to be constant. In contrast, the method in [WC16] only works when the kernel a is spiky and $\{x_i\}_{i=1}^p$ are very sparse $\theta \in \mathcal{O}(1/\sqrt{n})$, excluding most problems of interest.

¹⁰The problem becomes trivial when $\theta \leq 1/n$ because $\theta n = 1$ so that each x_i tends to be an one sparse δ -function.

- *Sample Complexity.* As shown in Table 1, our sample complexity $p \geq \tilde{\Omega}(\max\{n, \kappa^8/\mu^2\} n^4)$ in Equation (8) improves upon the result $p \geq \tilde{\Omega}(\max\{n, \kappa^8\} n^8/\varepsilon^8)$ in [LB18]. As aforementioned, this improvement partly owes to the similarity of the Huber-loss to ℓ^1 -loss, so that the Huber-loss is much less heavy-tailed than the ℓ^4 -loss studied in [LB18], requiring fewer samples for measure concentration. Still, our result leaves much room for improvement – we believe the sample dependency on θ^{-1} is an artifact of our analysis¹¹, and the phase transition in Figure 5 suggests that $p \geq \Omega(\text{poly log}(n))$ samples might be sufficient for exact recovery.
- *Algorithmic Convergence.* Finally, it should be noted that the number of iteration $\tilde{O}(n^4 + \log(1/\varepsilon))$ for our algorithm substantially improves upon that $\tilde{O}(n^{12}/\varepsilon^2)$ of the noisy RGD in [LB18, Theorem IV.2]. This has been achieved via a two-stage approach: (i) we first run $\mathcal{O}(n^4)$ iterations of vanilla RGD to obtain an approximate solution; (ii) then perform a subgradient method with linear convergence to the ground-truth. Moreover, without any noise parameters to tune, vanilla RGD is more practical than the noisy RGD in [LB18].

3.1 A glimpse of high dimensional geometry

To study the optimization landscape of the MCS-BD problem (4), we simplify the problem by a change of variable $\bar{\mathbf{q}} = \mathbf{Q}\mathbf{q}$, which rotates the space by the orthogonal matrix \mathbf{Q} in (7). Since the rotation \mathbf{Q} does not change the optimization landscape, by an abuse of notation of \mathbf{q} and $\bar{\mathbf{q}}$, we can rewrite the problem (4) as

$$\min_{\mathbf{q}} f(\mathbf{q}) := \frac{1}{np} \sum_{i=1}^p H_{\mu}(C_{x_i} \mathbf{R} \mathbf{Q}^{-1} \mathbf{q}), \quad \text{s.t.} \quad \|\mathbf{q}\| = 1, \quad (9)$$

where we also used the fact that $C_{y_i} \mathbf{P} = C_{x_i} \mathbf{R}$ in (7). Moreover, since $\mathbf{R} \approx \mathbf{Q}$ is *near orthogonal*, by assuming $\mathbf{R} \mathbf{Q}^{-1} = \mathbf{I}$, for *pure analysis* purposes we can further reduce (9) to

$$\min_{\mathbf{q}} \tilde{f}(\mathbf{q}) = \frac{1}{np} \sum_{i=1}^p H_{\mu}(C_{x_i} \mathbf{q}), \quad \text{s.t.} \quad \|\mathbf{q}\| = 1. \quad (10)$$

The reduction in (10) is simpler and much easier for parsing. By a similar analysis as [SQW16, GBW18], it can be shown that asymptotically the landscape is highly symmetric and the standard basis vectors $\{\pm \mathbf{e}_i\}_{i=1}^n$ are approximately¹² the only global minimizers. Hence, as $\mathbf{R} \mathbf{Q}^{-1} \approx \mathbf{I}$, we can study the optimization landscape of $f(\mathbf{q})$ via studying the landscape of $\tilde{f}(\mathbf{q})$ followed by a perturbation analysis. As illustrated in Figure 2, based on the target solutions of $\tilde{f}(\mathbf{q})$, we partition the sphere into $2n$ symmetric regions, and consider $2n$ (disjoint) subsets of each region¹³ [GBW18, BJS18]

$$\mathcal{S}_{\xi}^{i\pm} := \left\{ \mathbf{q} \in \mathbb{S}^{n-1} \mid \frac{|q_i|}{\|\mathbf{q}_{-i}\|_{\infty}} \geq \sqrt{1+\xi}, q_i \gtrless 0 \right\}, \quad \xi \in [0, \infty),$$

where \mathbf{q}_{-i} is a subvector of \mathbf{q} with i -th entry removed. For every $i \in [n]$, \mathcal{S}_{ξ}^{i+} (or \mathcal{S}_{ξ}^{i-}) contains exactly one of the target solution \mathbf{e}_i (or $-\mathbf{e}_i$), and all points in this set have one unique largest entry with index i , so that they are closer to \mathbf{e}_i (or $-\mathbf{e}_i$) in ℓ^{∞} distance than all the other standard basis vectors. As shown in Figure 2, the union of these sets form a full partition of the sphere only when $\xi = 0$. While for small $\xi > 0$, each disjoint set excludes all the saddle points and maximizers, but their union covers most measure of the sphere: when $\xi = (5 \log n)^{-1}$, their union covers at least half of the sphere, and hence a random initialization

¹¹The same θ^{-1} dependency also appears in [SQW16, LB18, BJS18, ZKW18, GBW18].

¹²The standard basis $\{\pm \mathbf{e}_i\}_{i=1}^n$ are exact global solutions for ℓ^1 -loss. The Huber loss we considered here introduces small approximation errors due to its smoothing effects.

¹³Here, we define $\|\mathbf{q}_{-i}\|_{\infty}^{-1} = +\infty$ when $\|\mathbf{q}_{-i}\|_{\infty} = 0$, so that the set $\mathcal{S}_{\xi}^{i\pm}$ is compact and \mathbf{e}_i is also contained in the set.

been proved for phase retrieval [CLS15], dictionary learning [BJS18], etc. Such condition implies that the negative gradient direction coincides with the direction to the target solution. Even when it is close to the target, the lower bound on Riemannian gradient ensures that the gradient is large enough so that the iterate still makes rapid progress to the target solution. Finally, it should be noted that the regularity condition holds within all S_ξ^{i-} excluding a ball around e_i of radius $\mathcal{O}(\mu)$ (see Figure 2). This is due to the smoothing effect of the Huber. In the subsequent section, we will show how to obtain the exact solution within the ball via a rounding procedure.

To ensure convergence of RGD, we also need to show the following property, so that once initialized in S_ξ^{i+} the iterates of the RGD method *implicitly* regularize themselves staying in the set S_ξ^{i+} . This ensures that the regularity condition (11) holds through the solution path of the RGD method.

Proposition 3.3 (Implicit Regularization) *Under the same condition of Proposition 3.2, w.h.p. over the randomness of $\{x_i\}_{i=1}^p$, the Riemannian gradient of $f(q)$ satisfies*

$$\left\langle \text{grad } f(q), \frac{1}{q_j} e_j - \frac{1}{q_i} e_i \right\rangle \geq c_4 \frac{\theta(1-\theta)}{n} \frac{\xi}{1+\xi}, \quad (12)$$

for all $q \in S_\xi^{i+}$ and any q_j such that $j \neq i$ and $q_j^2 \geq \frac{1}{3} q_i^2$.

Remark 3. We defer detailed proofs to Appendix C. In a nutshell, (12) guarantees that the negative gradient direction points towards e_i component-wisely for relatively large components (i.e., $q_j^2 \geq \frac{1}{3} q_i^2$, $\forall j \neq i$). With this, we can prove that those components will not increase after gradient update, ensuring the iterates stay within the region S_ξ^{i+} . This type of implicit regularizations for the gradient has also been discovered for many nonconvex optimization problems, such as low-rank matrix factorizations [GWB⁺17, MWCC17, CLC18, CC18], phase retrieval [CCFM19], and neural network training [NTSS17].

3.2 From geometry to efficient optimization

Based on the geometric properties of the function we characterized in the previous section, we show how they lead to efficient optimization via a two-stage optimization method. All the detailed proofs of convergence are postponed to Appendix D, and the implementation details of our methods can be found in Appendix I.

Phase 1: Finding an approximate solution via RGD.

Starting from a *random* initialization $q^{(0)}$ uniformly drawn from \mathbb{S}^{n-1} , we solve the problem (4) via *vanilla* RGD

$$q^{(k+1)} = \mathcal{P}_{\mathbb{S}^{n-1}} \left(q^{(k)} - \tau \cdot \text{grad } f(q^{(k)}) \right), \quad (13)$$

where $\tau > 0$ is the stepsize, and $\mathcal{P}_{\mathbb{S}^{n-1}}(\cdot)$ is a projection operator onto the sphere \mathbb{S}^{n-1} .

Proposition 3.4 (Linear convergence of gradient descent) *Suppose Proposition 3.2 and Proposition 3.3 hold. With probability at least $1/2$, the random initialization $q^{(0)}$ falls into one of the regions $S_\xi^{i\pm}$ for some $i \in [n]$. Choosing a fixed step size $\tau \leq \frac{c}{n} \min \{\mu, n^{-3/2}\}$ in (13), we have*

$$\|q^{(k)} - e_i\| \leq 2\mu, \quad \forall k \geq N := \frac{C}{\theta} n^4 \log \left(\frac{1}{\mu} \right).$$

Because of the preconditioning and smoothing via Huber loss in (5), the geometry structure in Proposition 3.2 implies that the gradient descent method can only produce an approximate solution q_s up to a precision $\mathcal{O}(\mu)$. Moreover, as we can show that $\|e_i - \beta(RQ^{-1})^{-1}e_i\| \leq \mu/2$, it does not make much difference of stating the result in terms of either e_i or $\beta(RQ^{-1})^{-1}e_i$. Next, we show that, by using q_s as a *warm start*, an extra linear program (LP) rounding procedure produces an exact solution $(RQ^{-1})^{-1}e_i$ up to a scaling factor in a few iterations.

Phase 2: Exact solutions via projected subgradient method for LP rounding.

Given the solution $\mathbf{r} = \mathbf{q}_s$ of running the RGD, we recover the exact solution by solving the following LP problem¹⁴

$$\min_{\mathbf{q}} \zeta(\mathbf{q}) := \frac{1}{np} \sum_{i=1}^p \|C_{\mathbf{x}_i} RQ^{-1} \mathbf{q}\|_1 \quad \text{s.t.} \quad \langle \mathbf{r}, \mathbf{q} \rangle = 1. \quad (14)$$

Since the feasible set $\langle \mathbf{r}, \mathbf{q} \rangle = 1$ is essentially the tangent space of the sphere \mathbb{S}^{n-1} at \mathbf{r} , and $\mathbf{r} = \mathbf{q}_s$ is pretty close to the target solution, one should expect that the optimizer \mathbf{q}_r of (14) exactly recovers the inverse kernel \mathbf{h} up to a scaled-shift. The problem (14) is *convex* and can be directly solved using standard tools such as CVX [GBY08], but it will be time consuming for large dataset. Instead, we introduce an efficient projected subgradient method for solving (14),

$$\mathbf{q}^{(k+1)} = \mathbf{q}^{(k)} - \tau^{(k)} \mathcal{P}_{\mathbf{r}^\perp} \partial \zeta(\mathbf{q}^{(k)}), \quad (15)$$

where $\partial \zeta(\mathbf{q})$ is the subgradient of $\zeta(\cdot)$ at \mathbf{q} . For convenience, let $\tilde{\mathbf{r}} := (RQ^{-1})^{-\top} \mathbf{r}$, and define the distance $d(\mathbf{q})$ between \mathbf{q} and the truth

$$\text{dist}(\mathbf{q}) := \|\mathbf{d}(\mathbf{q})\|, \quad \mathbf{d}(\mathbf{q}) := \mathbf{q} - (RQ^{-1})^{-1} \frac{\mathbf{e}_i}{\tilde{r}_i}.$$

Proposition 3.5 Suppose $\mu \leq \frac{1}{25}$ and let $\mathbf{r} = \mathbf{q}_s$ which satisfies $\|\mathbf{r} - \mathbf{e}_i\| \leq 2\mu$. Choose $\tau^{(k)} = \eta^k \tau^{(0)}$ with $\tau^{(0)} = c_1 \log^{-2}(np)$ and $\eta \in [(1 - c_2 \log^{-2}(np))^{1/2}, 1)$. Under the same condition of Theorem 3.1, w.h.p. the sequence $\{\mathbf{q}^{(k)}\}$ produced by (15) with $\mathbf{q}^{(0)} = \mathbf{r}$ converges to the target solution in a linear rate, i.e.,

$$\text{dist}(\mathbf{q}^{(k)}) \leq C\eta^k, \quad \forall k = 0, 1, 2, \dots$$

Remark 4. Unlike smooth problems, in general, subgradient methods for nonsmooth problems have to use *geometrically* diminishing stepsize to achieve linear convergence¹⁵ [Gof77, LZSV18, DDMP18, LZSL19]. The underlying geometry that supports the use of geometric diminishing step size and linear convergence in the above proposition is the so-called *sharpness* property [BF93, DDMP18] of the problem (14). In particular, we prove that w.h.p. $\zeta(\mathbf{q})$ is sharp in the sense that

$$\zeta(\mathbf{q}) - \zeta\left((RQ^{-1})^{-1} \frac{\mathbf{e}_i}{\tilde{r}_i}\right) \geq \frac{1}{50} \sqrt{\frac{2}{\pi}} \theta \cdot \text{dist}(\mathbf{q}), \quad \forall \langle \mathbf{r}, \mathbf{q} \rangle = 1.$$

In a nutshell, the above sharpness implies that (i) a scaled version of \mathbf{e}_i is the unique global minimum of (14), and (ii) the objective function $\zeta(\mathbf{q})$ increases at least proportional to the distance that \mathbf{q} moves away from the global minimum. This sharpness along with the convexity of (14) enables us to develop efficient projected subgradient method that converges in a linear rate with geometrically diminishing step size.

Remark 5. It should be noted that the LP rounding problem (14) is stated in the same rotated space as (9), which is only for analysis purposes. By plugging $\mathbf{q} = Q\mathbf{q}'$ into (9) and abusing notations of \mathbf{q} and \mathbf{q}' , we get back the *actual* rounding problem in the same space as the problem (4),

$$\min_{\mathbf{q}} \frac{1}{np} \sum_{i=1}^p \|C_{\mathbf{y}_i} P\mathbf{q}\|_1, \quad \text{s.t.} \quad \langle \mathbf{r}', \mathbf{q} \rangle = 1,$$

¹⁴Here, we state this problem in the same rotated space as (9). Since our geometric analysis is conducted in the rotated space, this is for convenience of stating our result. We will state the original problem subsequently.

¹⁵Typical choices such as $\tau^{(k)} = \mathcal{O}(1/k)$ and $\tau^{(k)} = \mathcal{O}(1/\sqrt{k})$ lead to sublinear convergence [BXM03].

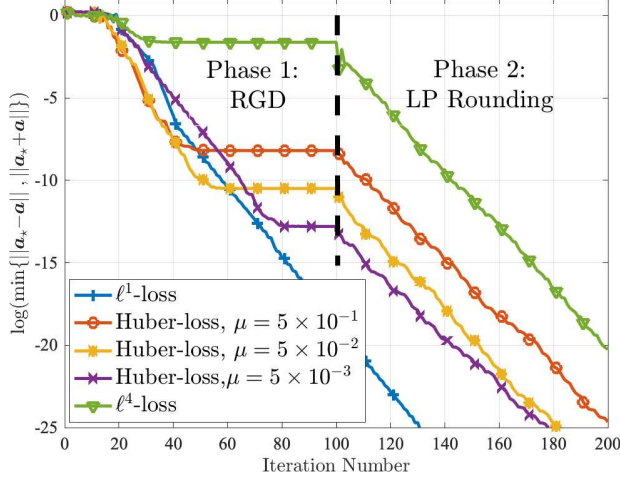


Figure 3: Comparison of iterate convergence. $p = 50, n = 200, \theta = 0.25$.

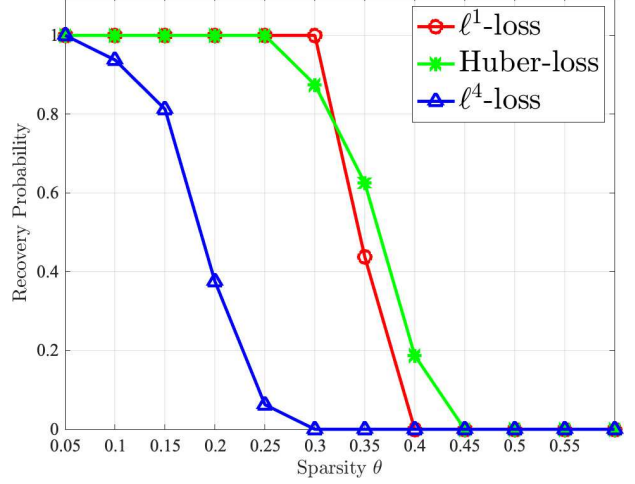


Figure 4: Comparison of recovery probability with varying θ . $p = 50, n = 500$.

where $r' = Qr = Qq_s$ is the *actual* solution produced by running the RGD.

Finally, we end this section by noting that although we use the matrix-vector form of convolutions in (13) and (15), all the matrix-vector multiplications can be efficiently implemented by FFT, including the preconditioning matrix in (6) which is also a circulant matrix. With FFT, the complexities of implementing one gradient update in (13) and subgradient in (15) are both $\mathcal{O}(pn \log n)$ for 1D problems.

4 Experiment

In this section, we demonstrate the performance of the proposed methods on both synthetic and real dataset. On the synthetic dataset, we compare the iterate convergence and phase transition for optimizing Huber, ℓ^1 , and ℓ^4 losses; for the real dataset, we demonstrate the effectiveness of our methods on sparse deconvolution for super-resolution microscopy imaging.

4.1 Experiments on 1D synthetic dataset

First, we conduct a series of experiments on synthetic dataset to demonstrate the superior performance of the vanilla RGD method (13). For all synthetic experiments, we generate the measurements $y_i = a \circledast x_i$ ($1 \leq i \leq p$), where the ground truth kernel $a \in \mathbb{R}^n$ is drawn uniformly random from the sphere \mathbb{S}^{n-1} (i.e., $a \sim \mathcal{U}(\mathbb{S}^{n-1})$), and sparse signals $x_i \in \mathbb{R}^n, i = [p]$ are drawn from i.i.d. Bernoulli-Gaussian distribution $x_i \sim i.i.d. \mathcal{BG}(\theta)$.

We compare the performances of RGD¹⁶ with random initialization on ℓ^1 -loss, Huber-loss, and the ℓ^4 -loss considered in [LB18]. We use line-search for adaptively choosing stepsize. For more implementation details, we refer the readers to Appendix I. For a fair comparison of optimizing all losses, we refine solutions with the LP rounding procedure (14) optimized by projected subgradient descent (15), and use the same random initialization uniformly drawn from the sphere.

For judging the success of recovery, let q_\star be a solution produced by the two-stage algorithm and we define

$$\rho_{acc}(q_\star) := \|C_a P q_\star\|_\infty / \|C_a P q_\star\| \in [0, 1].$$

¹⁶For ℓ^1 -loss, we use Riemannian subgradient method.

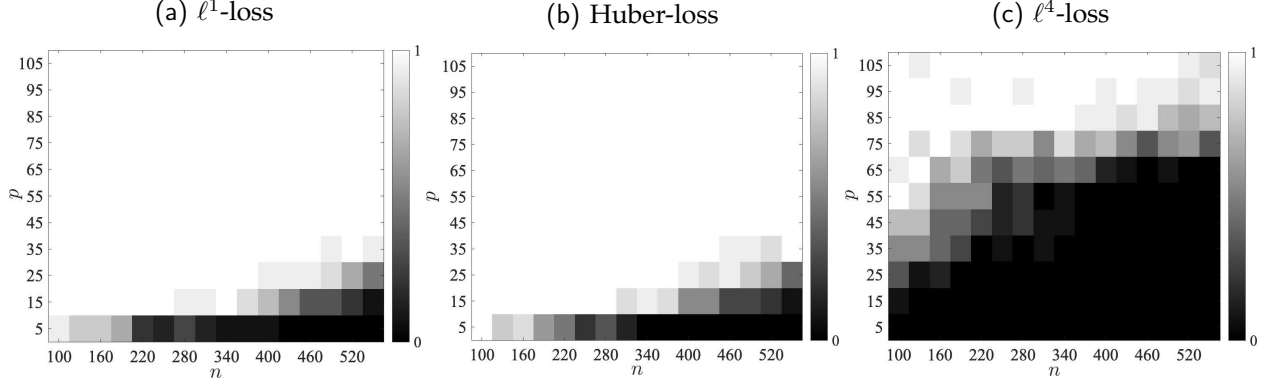


Figure 5: Comparison of phase transition on (p, n) with fixed $\theta = 0.25$. Here white denotes successful recovery while black indicates failure.

If \mathbf{q}_\star achieves the target solution, it should satisfy $\mathbf{P}\mathbf{q}_\star = \mathbf{s}_\ell[\mathbf{h}]$, with $\mathbf{s}_\ell[\mathbf{h}]$ being some circulant shift of the inverse kernel of \mathbf{a} and thus $\rho_{acc}(\mathbf{q}_\star) = 1$. Therefore, we should expect $\rho_{acc}(\mathbf{q}_\star) \approx 1$ when an algorithm produces a correct solution. For the following simulations, we assume successful recovery whenever $\rho_{acc}(\mathbf{q}_\star) \geq 0.95$.

Comparison of iterate convergence. We first compare the convergence of our two-stage approach in terms of the distance from the iterate to the target solution (up to a shift ambiguity) for all losses using RGD. For Huber and ℓ^4 losses, we run RGD for 100 iterations in Phase 1 and use the solution as warm start for solving LP rounding in Phase 2. For ℓ^1 -loss, we run Riemannian subgradient descent without rounding. As shown in Figure 3, in Phase 1, optimizing ℓ^4 -loss can only produce an approximate solution up to precision 10^{-2} . In contrast, optimizing Huber-loss converges with much faster linear rate before iterates stagnate, and produces much more accurate solutions as μ decreases, even without LP rounding. In Phase 2, for both losses, projected subgradient descent converges linearly to the target solution. For ℓ^1 loss, the experiments tend to suggest that Riemannian subgradient exactly recovers the target solution in a linear rate even without LP rounding. We leave analyzing ℓ^1 -loss for future research.

Recovery with varying sparsity. Fixing $n = 500$ and $p = 50$, we compare the recovery probability with varying sparsity level $\theta \in (0, 0.6]$. For Huber loss, we use $\mu = 10^{-2}$. For each value of θ and each loss, we run our two-stage optimization method and repeat the simulation 15 times. As illustrated in Figure 4, optimizing Huber-loss enables successful recovery for much larger θ in comparison with that of ℓ^4 -loss. The performances of optimizing ℓ^1 -loss and Huber-loss are quite similar, which achieves constant sparsity level $\theta \approx 1/3$ as suggested by our theory.

Phase transition on (p, n) . Finally, we fix $\theta = 0.25$, and test the dependency of sample number p on the dimension n via phase transition plots. For Huber loss, we use $\mu = 10^{-2}$. For each individual (p, n) , we run our two-stage optimization method and repeat the simulation 15 times. In Figure 5, whiter pixels indicate higher success probability, and vice versa. As illustrated in Figure 5, for each individual n , optimizing Huber-loss requires much fewer samples p for recovery in comparison with that of ℓ^4 -loss. The performances of optimizing ℓ^1 -loss and Huber-loss are comparable; we conjecture sample dependency for optimizing both losses is $p \geq \Omega(\text{poly}(\log(n)))$, which is much better than our theory predicted. In contrast, optimizing ℓ^4 -loss might need $p \geq \Omega(n)$ samples. This is mainly due to the heavy-tailed behavior for high order polynomial of random variables.

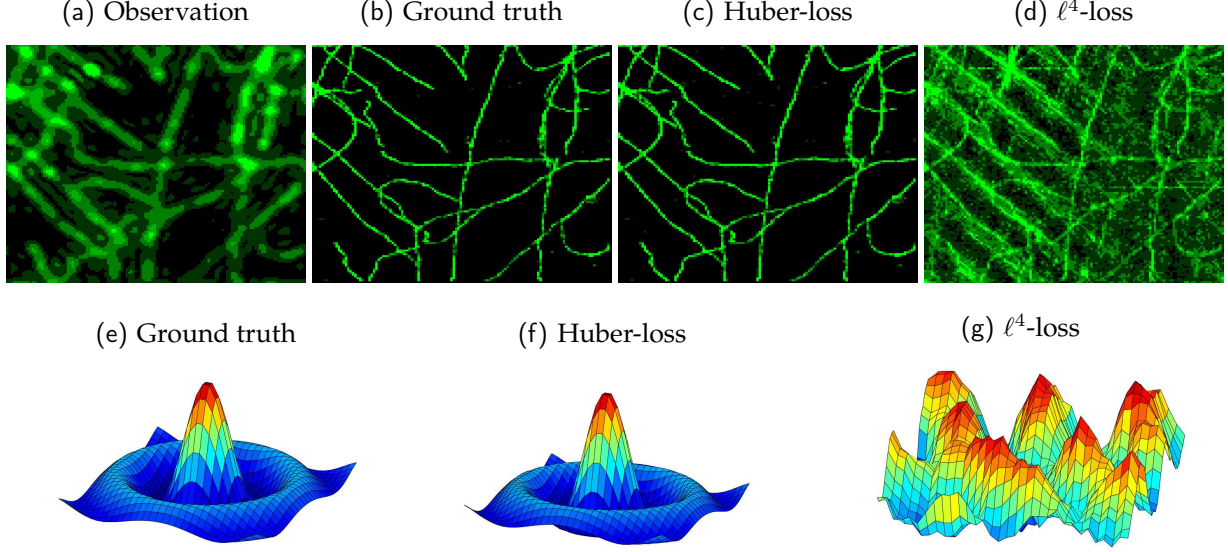


Figure 6: STORM imaging via solving MCS-BD. The first line shows (a) observed image, (b) ground truth, (c) recovered image by optimizing Huber-loss, and (d) by ℓ^4 -loss. The second line, (e) ground truth kernel, (f) recovered by optimizing Huber-loss, and (g) by ℓ^4 -loss.

4.2 Real experiment on 2D super-resolution microscopy imaging

As introduced in Section 1, stochastic optical reconstruction microscopy (STORM) is a new computation based imaging technique which breaks the resolution limits of optical fluorescence microscopy [BPS⁺06, HGM06, RBZ06]. The basic principle is using photoswitchable florescent probes to create multiple sparse frames of individual molecules to temporally separates the spatially overlapping low resolution image,

$$\underbrace{\mathbf{Y}_i}_{\text{frame}} = \underbrace{\mathbf{A}}_{\text{PSF}} \underbrace{[*]}_{\text{2D circular convolution}} \underbrace{\mathbf{X}_i}_{\text{sparse point sources}} + \underbrace{\mathbf{N}_i}_{\text{noise}}, \quad (16)$$

where $[*]$ denotes 2D circular convolution, \mathbf{A} is a 2D point spread function (PSF), $\{\mathbf{X}_i\}_{i=1}^p$ are sparse point-sources. The classical approaches solve the problem by fitting the blurred spots with Gaussian PSF using either maximum likelihood estimation or sparse recovery [HUK11, ZZE12, SS14]. However, these approaches suffer from limitations: (i) for the case when the cluster of spots overlap, it is often computationally expensive and results in bad estimation; (ii) for 3D imaging, the PSF exhibits aberration across the focus plane [SN06], making it almost impossible to directly estimate it due to defocus and unknown aberrations.

Therefore, given multiple frames $\{\mathbf{Y}_i\}_{i=1}^p$, in many cases we want to jointly estimate the PSF \mathbf{A} and point sources $\{\mathbf{X}_i\}_{i=1}^p$. Once $\{\mathbf{X}_i\}_{i=1}^p$ are recovered, we can obtain a high resolution image by aggregating all sparse point sources \mathbf{X}_i . We test our algorithms on this task, by using $p = 1000$ frames from Tubulin Conj-AL647 dataset obtained from SMLM challenge website¹⁷. The fluorescence wavelength is 690 nanometer (nm) and the imaging frequency is $f = 25\text{Hz}$. Each frame is of size 128×128 with 100 nm pixel resolution, and we solve the single-molecule localization problem on the same grid¹⁸. As demonstrated in Figure 6, optimizing Huber-loss using our two-stage method can near perfectly recover both the underlying Bessel PSF and point-sources $\{\mathbf{X}_i\}_{i=1}^p$, producing accurate high resolution image. In contrast, optimizing ℓ^4 -loss [LB18] fails to recover the PSF, resulting in some aliasing effects of the recovered high resolution image.

¹⁷Available at <http://bigwww.epfl.ch/smlm/datasets/index.html?p=tubulin-conjal647>.

¹⁸Here, we are estimating the point sources \mathbf{X}_i on the same pixel grid as the original image. To obtain even higher resolution than the result we obtain here, people are usually estimating the points sources on a finer grid. This results in a simultaneous sparse deconvolution and super-resolution problem, which could be an interesting problem for future research.

5 Discussion and Conclusion

In this section, we first discuss related work on provable nonconvex methods for blind deconvolution and dictionary learning. We then conclude by pointing out several promising directions for future research.

5.1 Relation to the literature

Aside from the multichannel sparse model we studied here, many other low-dimensional models for blind deconvolution problems have been considered and investigated in the literature, that we discuss the relationship below.

Blind deconvolution with subspace model Recently, there is a line of work studied the blind deconvolution problem with a single input $\mathbf{y} = \mathbf{a} \circledast \mathbf{x}$, where the unknown \mathbf{a} and \mathbf{x} either live in known low-dimensional subspaces, or are sparse in some known dictionaries [ARR14, Chi16, LS15, LLB16, KK17, AD18, Li18]. These results assumed that the subspaces/dictionaries are chosen at random, such that the problem exhibits no signed shift ambiguity and can be provably solved either by convex relaxation [ARR14, Chi16] or nonconvex optimization [LLSW18, MWCC17]. However, their application to real problem is limited by the assumption of random subspace/dictionary model which is often not satisfied in practice. In contrast, sparsity is a more natural assumption that appears in many signal processing [TBSR17], imaging [BPS⁺06, KT98, LWDF11] and neuroscience [GPAF03, ETS11, WLS⁺13, FZP17, PSG⁺16] applications.

Multichannel deconvolution via cross-correlation based methods The MCS-BD problem we considered here is also closely related to the multichannel blind deconvolution with finite impulse response (FIR) models [XLTK95, MDCM95, HB98, LCKL08, LKR18, LTR18]. These methods utilize the second-order statistics of the observation, resulting in problems of larger size than MCS-BD. They often solve the problem via least squares or spectral methods. In particular, (i) Lin et al. [LCKL08] proposed an ℓ^1 -regularized least-squares method based on convex relaxation. However, the convex method could suffer similar sparsity limitation as [WC16, Cos17], and it limits to two channels without theoretical guarantees. Lee et al. [LKR18] proposed an eigen approach for subspace model, and thus as discussed above it cannot directly handle our case with random sparse nonzero support.

Short-and-sparse deconvolution Another line of research related to this work is sparse blind deconvolution with short-and-sparse (SaS) model [ZLK⁺17, ZKW18, KLZW19, LQK⁺19]. They assume that there is a single measurement of the form $\mathbf{y} = \mathbf{a} \circledast \mathbf{x}$, that \mathbf{x} is sparse and the length of the kernel \mathbf{a} is much shorter than \mathbf{y} and \mathbf{x} . In particular, Zhang et al. [ZKW18] formulated the problem as an ℓ^4 -maximization problem over the sphere similar to [LB18], proving on a local region that every local minimizer is near a truncated signed shift of \mathbf{a} . Kuo et al. [KLZW19] studied a dropped quadratic simplification of bilinear Lasso objective [LQK⁺19], which provably obtains exact recovery for an incoherent kernel \mathbf{a} and sparse \mathbf{x} . However, as the kernel and measurements are not the same length in SaS, the SaS deconvolution is much harder than MCS-BD: the problem has spurious local minimizers such as shift-truncations, so that most of the results there can only show benign local geometry structure regardless of the choice of objectives. This is in contrast to the MCS-BD problem we considered here, which has benign global geometric structure: as \mathbf{y} and \mathbf{a} are of the same length, every local minimizer corresponds to a full shift of \mathbf{a} and there is no spurious local minimizer over the sphere [LB18]. On the other hand, despite the apparent similarity between the SaS model and MCS-BD, these problems are not equivalent: it might seem possible to reduce SaS to MCS-BD by dividing the single observation \mathbf{y} into p pieces; this apparent reduction fails due to boundary effects (e.g., shift-truncations on each piece).

Relation to dictionary learning It should be noted that the MCS-BD problem is closely related to the complete dictionary learning problem studied in [SQW16]. Indeed, if one writes

$$\underset{\text{data } Y}{[C_{y_1} \cdots C_{y_p}]} = C_a \cdot \underset{\text{data } X}{[C_{x_1} \cdots C_{x_p}]}$$

so that it reduces to the dictionary learning model $Y = C_a X$ with structured dictionary C_a . Thus, one may expect to directly recover¹⁹ one shift of a by optimizing

$$\min_q \|q^\top P Y\|_1 = \|q^\top P C_a X\|_1, \quad \text{s.t.} \quad \|q\| = 1.$$

However, our preliminary experiment suggests that this formulation has some stability issues and often requires more samples in comparison to our formulation (4). We left further investigations for future work.

It should be noted that our proof ideas of convergence of RGD from random initialization are similar to that of Bai et al. and Gilboa et al. [BJS18, GBW18] for dictionary learning. Although dictionary learning and MCS-BD are related, these results do not directly apply to the sparse blind deconvolution problem. First of all, these results only apply to orthogonal dictionaries, while in sparse blind deconvolution the dictionary (in other words, the circulant matrix) C_a is not orthogonal for generic unknown a . To deal with this issue, preconditioning is needed as shown in our work. Furthermore, as the authors in [BJS18] considered a nonsmooth ℓ^1 -loss, the non-Lipschitzness of subgradient of ℓ^1 causes tremendous difficulties in measure concentration and dealing with preconditioning matrix. In this work, we considered the Huber-loss, which can be viewed as a first-order smooth surrogate of ℓ^1 -loss. Thus, we can utilize the Lipschitz continuity of its gradient to ease the analysis but achieving similar performances of using ℓ^1 -loss in terms sample complexity. In comparison with the sample complexity for complete dictionary learning with $p \sim \mathcal{O}(n^9)$ ignoring the condition number, our result is much tighter $p \sim \mathcal{O}(n^5)$ here.

Moreover, it should also be noted that both results [BJS18, GBW18] only guarantees sublinear convergence of their methods. In this work, we show a stronger result, that the vanilla RGD converges linearly to the target solution. Finally, we noticed that there appeared a result similar to ours [SC19] after submission of our work, which considered a log cosh function with improved sample complexity $p \sim \mathcal{O}(n^{4.5})$.

Finding the sparsest vectors in a subspace As shown in [WC16], the problem formulation considered here for MCS-BD can be regarded as a variant of finding the sparsest vectors in a subspace [QSW14, QZL⁺20]. Prior to our result, similar ideas have led to new provable guarantees and efficient methods for several fundamental problems in signal processing and machine learning, such as complete dictionary learning [SQW16, SQW17] and robust subspace recovery [TV15, LM18, ZWR⁺18]. We hope the methodology developed here can be applied to other problems falling in this category.

5.2 Future directions

Finally, we close this paper by pointing out several interesting directions for future work.

Improving sample complexity Our result substantially improves upon [LB18]. However, there is still a large sample complexity *gap* between our theory and practice. From the degree of freedom perspective (e.g., [MDCM95]), a constant p is seemingly enough for solution uniqueness of MCS-BD. However, as the problem is highly nonconvex with unknown nonzero supports of the signals $\{x_i\}$, to have provable efficient methods, we conjecture that paying extra log factors $p \geq \Omega(\text{poly log}(n))$ is necessary for optimizing ℓ^1 and Huber losses, which is empirically confirmed by the phase transitions in Figure 5 and experiments on 2D super-resolution imaging. This is similar to recent results on provable efficient method for multichannel blind deconvolution, which considers a different FIR model [LTR18, LKR18]. On the other hand, we believe

¹⁹The intuition is that $\mathbb{E}[\|q^\top P Y\|_1] \propto \|q^\top P C_a\|_1$. Given $P C_a$ is near orthogonal, one may expect $q^\top P C_a$ is one sparse when q equals one preconditioned shift, which is the target solution.

our *far from tight* sample complexity $p \geq \Omega(\text{poly}(n))$ is due to the looseness in our analysis: (i) tiny gradient near the boundary of the set \mathcal{S}_ξ^{\pm} for measure concentration, and (ii) loose control of summations of dependent random variables. To seek improvement, as the iterates of RGD only visit a small measure of the sphere, it could be better to perform an iterative analysis instead of uniformly characterizing the function landscape over \mathcal{S}_ξ^{\pm} . Additionally, for tighter concentration of summation of dependent random variables, one might need to resort to more advanced probability tools such as decoupling [DIPG12, QZE17] and generic chaining [Tal14, D⁺15].

Huber vs. ℓ^1 loss and smooth vs. nonsmooth optimization Our choice of Huber loss rather than ℓ^1 -loss is to simplify theoretical analysis. Undoubtedly, ℓ^1 -loss is a more natural sparsity promoting function and performs better than Huber as demonstrated by our experiments. When ℓ^1 -loss is utilized, Figure 3 tends to suggest that the underlying kernel and signals can be exactly recovered even without LP rounding²⁰. However, on the theoretic side, the subgradient of ℓ^1 -loss is *non-Lipschitz* which introduces tremendous difficulty in controlling suprema of a random process and in perturbation analysis for preconditioning. Although recent work [BJS18, DZD⁺19] introduced a novel method of controlling suprema of *non-Lipschitz* random process, the difficulty of dealing with the preconditioning matrix in the subgradient remains very challenging. Similar to the ideas of [LZSV18, CCD⁺19], one possibility might be showing *weak convexity* and *sharpness* of the Lipschitz ℓ^1 -loss function, rather than proving the regularity condition for the non-Lipschitz subgradient. We leave analyzing ℓ^1 -loss as a promising future research direction.

Robustness in the presence of noise The current analysis focuses on the noiseless case. It is of interest to extend our result to the noisy case with measurements $\mathbf{y}_i = \mathbf{a} \otimes \mathbf{x}_i + \mathbf{n}_i, \forall i \in [p]$, where \mathbf{n}_i denotes the additive Gaussian noise. Note that in the noiseless case (i.e., $\mathbf{n}_i = 0$), $\mathbf{C}_{\mathbf{y}_i} \mathbf{q}$ is sparse when \mathbf{q} is the inverse of \mathbf{a} , motivating our approach (4). Therefore, in the noisy case, we expect $\mathbf{C}_{\mathbf{y}_i} \mathbf{q}$ to be close to a sparse vector in the Euclidean space, which may lead to the following approach: $\min_{\mathbf{q} \in \mathbb{S}^{n-1}, \mathbf{v}_i} \frac{1}{np} \sum_{i=1}^p \lambda H_\mu(\mathbf{v}_i) + \|\mathbf{v}_i - \mathbf{C}_{\mathbf{y}_i} \mathbf{P} \mathbf{q}\|^2$, where λ is the balancing factor. On the other hand, the recent work [DZD⁺19] on noisy robust subspace learning demonstrates that directly minimizing the ℓ^1 -loss over the sphere is robust to the additive noise, and achieves nearly optimal result in terms of the noise level. Motivated by this result, we also expect that both the formulation in (4) and the RGD in Section 3 are robust to the additive noise. Depending on the noise level and the parameter μ , the LP rounding step may not be required in the noisy case. We leave the full investigation as future work.

Solving MCS-BD with extra data structures In applications such as super-resolution microscopy imaging considered in Section 4.2, the data actually has more structures to be exploited. For example, the point sources $\{\mathbf{X}_i\}_{i=1}^p$ are often correlated that they share similar sparsity patterns, i.e., similar nonzero supports. Therefore, one may want to enforce joint sparsity to capture this structure (e.g., by the $\|\cdot\|_{1,2}$ norm). Analyzing this problem requires us to deal with probabilistic dependency across $\{\mathbf{X}_i\}_{i=1}^p$ [LB18]. On the other hand, we also want to solve the problem on a finer grid where the measurements are

$$\mathbf{Y}_i = \mathcal{D}[\mathbf{A} \boxtimes \mathbf{X}_i], \quad 1 \leq i \leq p$$

instead of Equation (16). Here $\mathcal{D}[\cdot]$ is a downsampling operator. We leave these MCS-BD with the super-resolution problems for future research.

Solving other nonconvex problems This work joins recent line of research on provable nonconvex optimization [JK⁺17, Sun, CLC18]. We believe the methodology developed here might be possible to be extended to other nonconvex bilinear problems. For instance, the blind gain and phase calibration problem [LLB16, LS18, LLB18] is closely related to the MCS-BD problem, as mentioned by [LB18]. It is also

²⁰As the preconditioning matrix \mathbf{P} introduces approximation error $\mathbf{R}\mathbf{Q}^{-1} \approx \mathbf{I}$ from (9) to (10), this is against our intuition in some sense.

of great interest to extend our approach for solving the so-called convolutional dictionary learning problem [CF17, GCW18], in which each measurement consists of a superposition of multiple circulant convolutions:

$$\mathbf{y}_i = \sum_{k=1}^K \mathbf{a}_k \otimes \mathbf{x}_{ik}, \quad 1 \leq i \leq p.$$

Given $\{\mathbf{y}_i\}_{i=1}^p$ we want to recover all the kernels $\{\mathbf{a}_k\}_{k=1}^K$ and sparse signals $\{\mathbf{x}_{ik}\}_{1 \leq k \leq K, 1 \leq i \leq p}$ simultaneously. We suspect our approach can be used to tackle this challenging problem and the number of samples will increase only proportionally to the number of kernels. We leave the full investigation as future work.

Acknowledgement

Part of this work is done when QQ, XL and ZZ were attending "Computational Imaging" workshop at ICERM Brown in Spring 2019. We would like to thank the National Science Foundation under Grant No. DMS-1439786 for the generous support of participating in this workshop. We would like to thank Shuyang Ling (NYU Shanghai), Carlos Fernandez-Granda (NYU Courant), Yuxin Chen (Princeton), Yuejie Chi (CMU), and Pengcheng Zhou (Columbia U.) for fruitful discussions. QQ also would like to acknowledge the support of Microsoft PhD fellowship, and Moore-Sloan foundation fellowship. XL would like to acknowledge the support by Grant CUHK14210617 from the Hong Kong Research Grants Council. ZZ was partly supported by NSF Grant 1704458.

References

- [AD18] Ali Ahmed and Laurent Demanet. Leveraging diversity and sparsity in blind deconvolution. *IEEE Transactions on Information Theory*, 64(6):3975–4000, 2018.
- [ADCY97] Shun-ichi Amari, Scott C Douglas, Andrzej Cichocki, and Howard H Yang. Multichannel blind deconvolution and equalization using the natural gradient. In *First IEEE Signal Processing Workshop on Signal Processing Advances in Wireless Communications*, pages 101–104. IEEE, 1997.
- [AMS09] P-A Absil, Robert Mahony, and Rodolphe Sepulchre. *Optimization algorithms on matrix manifolds*. Princeton University Press, 2009.
- [ARR14] Ali Ahmed, Benjamin Recht, and Justin Romberg. Blind deconvolution using convex programming. *IEEE Transactions on Information Theory*, 60(3):1711–1732, 2014.
- [BEL13] Hilton Bristow, Anders Eriksson, and Simon Lucey. Fast convolutional sparse coding. In *Proceedings of the IEEE Conference on Computer Vision and Pattern Recognition*, pages 391–398, 2013.
- [BF93] James V Burke and Michael C Ferris. Weak sharp minima in mathematical programming. *SIAM Journal on Control and Optimization*, 31(5):1340–1359, 1993.
- [Bha13] Rajendra Bhatia. *Matrix analysis*, volume 169. Springer Science & Business Media, 2013.
- [BJS18] Yu Bai, Qijia Jiang, and Ju Sun. Subgradient descent learns orthogonal dictionaries. *arXiv preprint arXiv:1810.10702*, 2018.
- [BPS⁺06] Eric Betzig, George H Patterson, Rachid Sougrat, O Wolf Lindwasser, Scott Olenych, Juan S Bonifacino, Michael W Davidson, Jennifer Lippincott-Schwartz, and Harald F Hess. Imaging intracellular fluorescent proteins at nanometer resolution. *Science*, 313(5793):1642–1645, 2006.
- [BXM03] Stephen Boyd, Lin Xiao, and Almir Mutapcic. Subgradient methods. *lecture notes of EE392o, Stanford University, Autumn Quarter*, 2004:2004–2005, 2003.
- [CC18] Yudong Chen and Yuejie Chi. Harnessing structures in big data via guaranteed low-rank matrix estimation: Recent theory and fast algorithms via convex and nonconvex optimization. *IEEE Signal Processing Magazine*, 35(4), 2018.
- [CCD⁺19] Vasileios Charisopoulos, Yudong Chen, Damek Davis, Mateo Díaz, Lijun Ding, and Dmitriy Drusvyatskiy. Low-rank matrix recovery with composite optimization: good conditioning and rapid convergence. *arXiv preprint arXiv:1904.10020*, 2019.
- [CCFM19] Yuxin Chen, Yuejie Chi, Jianqing Fan, and Cong Ma. Gradient descent with random initialization: fast global convergence for nonconvex phase retrieval. *Mathematical Programming*, 176(1-2):5–37, 2019.
- [CF17] Il Yong Chun and Jeffrey A Fessler. Convolutional dictionary learning: Acceleration and convergence. *IEEE Transactions on Image Processing*, 27(4):1697–1712, 2017.
- [Chi16] Yuejie Chi. Guaranteed blind sparse spikes deconvolution via lifting and convex optimization. *IEEE Journal of Selected Topics in Signal Processing*, 10(4):782–794, 2016.
- [CLC18] Yuejie Chi, Yue M Lu, and Yuxin Chen. Nonconvex optimization meets low-rank matrix factorization: An overview. *arXiv preprint arXiv:1809.09573*, 2018.
- [CLS15] Emmanuel J. Candès, Xiaodong Li, and Mahdi Soltanolkotabi. Phase retrieval via wirtinger flow: Theory and algorithms. *Information Theory, IEEE Transactions on*, 61(4):1985–2007, April 2015.
- [Cos17] Augustin Cosse. A note on the blind deconvolution of multiple sparse signals from unknown subspaces. In *Wavelets and Sparsity XVII*, volume 10394, page 103941N. International Society for Optics and Photonics, 2017.
- [CP86] Thomas F Coleman and Alex Pothen. The null space problem i. complexity. *SIAM Journal on Algebraic Discrete Methods*, 7(4):527–537, 1986.
- [D⁺15] Sjoerd Dirksen et al. Tail bounds via generic chaining. *Electronic Journal of Probability*, 20, 2015.
- [DDMP18] Damek Davis, Dmitriy Drusvyatskiy, Kellie J MacPhee, and Courtney Paquette. Subgradient methods for sharp weakly convex functions. *Journal of Optimization Theory and Applications*, 179(3):962–982, 2018.
- [DIPG12] Victor De la Pena and Evarist Giné. *Decoupling: from dependence to independence*. Springer Science & Business Media, 2012.

- [DZD⁺19] Tianyu Ding, Zhihui Zhu, Tianjiao Ding, Yunchen Yang, Daniel Robinson, Manolis Tsakiris, and Rene Vidal. Noisy dual principal component pursuit. In *International Conference on Machine Learning*, pages 1617–1625, 2019.
- [ETS11] Chaitanya Ekanadham, Daniel Tranchina, and Eero P Simoncelli. A blind sparse deconvolution method for neural spike identification. In *Advances in Neural Information Processing Systems*, pages 1440–1448, 2011.
- [FR13] Simon Foucart and Holger Rauhut. *A Mathematical Introduction to Compressive Sensing*. Springer, 2013.
- [FZP17] Johannes Friedrich, Pengcheng Zhou, and Liam Paninski. Fast online deconvolution of calcium imaging data. *PLoS computational biology*, 13(3):e1005423, 2017.
- [G⁺06] Robert M Gray et al. Toeplitz and circulant matrices: A review. *Foundations and Trends® in Communications and Information Theory*, 2(3):155–239, 2006.
- [GBW18] Dar Gilboa, Sam Buchanan, and John Wright. Efficient dictionary learning with gradient descent. *arXiv preprint arXiv:1809.10313*, 2018.
- [GBY08] Michael Grant, Stephen Boyd, and Yinyu Ye. Cvx: Matlab software for disciplined convex programming, 2008.
- [GCW18] Cristina Garcia-Cardona and Brendt Wohlberg. Convolutional dictionary learning: A comparative review and new algorithms. *IEEE Transactions on Computational Imaging*, 4(3):366–381, 2018.
- [Gof77] Jean-Louis Goffin. On convergence rates of subgradient optimization methods. *Mathematical programming*, 13(1):329–347, 1977.
- [GPAF03] Darren R Gitelman, William D Penny, John Ashburner, and Karl J Friston. Modeling regional and psychophysiology interactions in fmri: the importance of hemodynamic deconvolution. *Neuroimage*, 19(1):200–207, 2003.
- [GWB⁺17] Suriya Gunasekar, Blake E Woodworth, Srinadh Bhojanapalli, Behnam Neyshabur, and Nati Srebro. Implicit regularization in matrix factorization. In *Advances in Neural Information Processing Systems*, pages 6151–6159, 2017.
- [HB98] Gopal Harikumar and Yoram Bresler. Fir perfect signal reconstruction from multiple convolutions: minimum deconvolver orders. *IEEE Transactions on Signal Processing*, 46(1):215–218, 1998.
- [HGM06] Samuel T Hess, Thanu PK Girirajan, and Michael D Mason. Ultra-high resolution imaging by fluorescence photoactivation localization microscopy. *Biophysical journal*, 91(11):4258–4272, 2006.
- [Hub92] Peter J Huber. Robust estimation of a location parameter. In *Breakthroughs in statistics*, pages 492–518. Springer, 1992.
- [HUK11] Seamus J Holden, Stephan Uphoff, and Achillefs N Kapanidis. Daostorm: an algorithm for high-density super-resolution microscopy. *Nature methods*, 8(4):279, 2011.
- [JK⁺17] Prateek Jain, Purushottam Kar, et al. Non-convex optimization for machine learning. *Foundations and Trends® in Machine Learning*, 10(3-4):142–336, 2017.
- [KK17] Michael Kech and Felix Krahmer. Optimal injectivity conditions for bilinear inverse problems with applications to identifiability of deconvolution problems. *SIAM Journal on Applied Algebra and Geometry*, 1(1):20–37, 2017.
- [KLZW19] Han-Wen Kuo, Yenson Lau, Yuqian Zhang, and John Wright. Geometry and symmetry in short-and-sparse deconvolution. *arXiv preprint arXiv:1901.00256*, 2019.
- [KMR14] Felix Krahmer, Shahar Mendelson, and Holger Rauhut. Suprema of chaos processes and the restricted isometry property. *Communications on Pure and Applied Mathematics*, 67(11):1877–1904, 2014.
- [KT98] Kjetil F Kaaresen and Tofinn Taxt. Multichannel blind deconvolution of seismic signals. *Geophysics*, 63(6):2093–2107, 1998.
- [LB18] Yanjun Li and Yoram Bresler. Global geometry of multichannel sparse blind deconvolution on the sphere. *arXiv preprint arXiv:1805.10437*, 2018.
- [LCKL08] Yuanqing Lin, Jingdong Chen, Youngmoo Kim, and Daniel D Lee. Blind channel identification for speech dereverberation using l1-norm sparse learning. In *Advances in Neural Information Processing Systems*, pages 921–928, 2008.

- [Li18] Yanjun Li. *Bilinear inverse problems with sparsity: optimal identifiability conditions and efficient recovery*. PhD thesis, University of Illinois at Urbana-Champaign, 2018.
- [LKR18] Kiryung Lee, Felix Krahmer, and Justin Romberg. Spectral methods for passive imaging: Nonasymptotic performance and robustness. *SIAM Journal on Imaging Sciences*, 11(3):2110–2164, 2018.
- [LLB16] Yanjun Li, Kiryung Lee, and Yoram Bresler. Identifiability in blind deconvolution with subspace or sparsity constraints. *IEEE Transactions on Information Theory*, 62(7):4266–4275, 2016.
- [LLB17] Yanjun Li, Kiryung Lee, and Yoram Bresler. Identifiability in bilinear inverse problems with applications to subspace or sparsity-constrained blind gain and phase calibration. *IEEE Transactions on Information Theory*, 63(2):822–842, 2017.
- [LLB18] Yanjun Li, Kiryung Lee, and Yoram Bresler. Blind gain and phase calibration via sparse spectral methods. *IEEE Transactions on Information Theory*, 65(5):3097–3123, 2018.
- [LLSW18] Xiaodong Li, Shuyang Ling, Thomas Strohmer, and Ke Wei. Rapid, robust, and reliable blind deconvolution via nonconvex optimization. *Applied and Computational Harmonic Analysis*, 2018.
- [LM18] Gilad Lerman and Tyler Maunu. An overview of robust subspace recovery. *Proceedings of the IEEE*, 106(8):1380–1410, 2018.
- [LQK⁺19] Yenson Lau, Qing Qu, Han-Wen Kuo, Pengcheng Zhou, Yuqian Zhang, and John Wright. Short-and-sparse deconvolution – a geometric approach. *Preprint*, 2019.
- [LS15] Shuyang Ling and Thomas Strohmer. Self-calibration and biconvex compressive sensing. *Inverse Problems*, 31(11):115002, 2015.
- [LS18] Shuyang Ling and Thomas Strohmer. Self-calibration and bilinear inverse problems via linear least squares. *SIAM Journal on Imaging Sciences*, 11(1):252–292, 2018.
- [LTR18] Kiryung Lee, Ning Tian, and Justin Romberg. Fast and guaranteed blind multichannel deconvolution under a bilinear system model. *IEEE Transactions on Information Theory*, 64(7):4792–4818, 2018.
- [LWDF11] Anat Levin, Yair Weiss, Fredo Durand, and William T Freeman. Understanding blind deconvolution algorithms. *IEEE Transactions on Pattern Analysis and Machine Intelligence*, 33(12):2354–2367, 2011.
- [LZSL19] Xiao Li, Zhihui Zhu, Anthony Man-Cho So, and Jason D Lee. Incremental methods for weakly convex optimization. *arXiv preprint arXiv.org:1907.11687*, 2019.
- [LZSV18] Xiao Li, Zhihui Zhu, Anthony Man-Cho So, and Rene Vidal. Nonconvex robust low-rank matrix recovery. *arXiv preprint arXiv:1809.09237*, 2018.
- [MDCM95] Eric Moulines, Pierre Duhamel, J-F Cardoso, and Sylvie Mayrargue. Subspace methods for the blind identification of multichannel fir filters. *IEEE Transactions on signal processing*, 43(2):516–525, 1995.
- [MWCC17] Cong Ma, Kaizheng Wang, Yuejie Chi, and Yuxin Chen. Implicit regularization in nonconvex statistical estimation: Gradient descent converges linearly for phase retrieval, matrix completion and blind deconvolution. *arXiv preprint arXiv:1711.10467*, 2017.
- [Nat95] Balas Kausik Natarajan. Sparse approximate solutions to linear systems. *SIAM journal on computing*, 24(2):227–234, 1995.
- [NFTLR15] Kenji Nose-Filho, André K Takahata, Renato Lopes, and João MT Romano. A fast algorithm for sparse multichannel blind deconvolution. *Geophysics*, 81(1):V7–V16, 2015.
- [NTSS17] Behnam Neyshabur, Ryota Tomioka, Ruslan Salakhutdinov, and Nathan Srebro. Geometry of optimization and implicit regularization in deep learning. *arXiv preprint arXiv:1705.03071*, 2017.
- [PSG⁺16] Eftychios A Pnevmatikakis, Daniel Soudry, Yuanjun Gao, Timothy A Machado, Josh Merel, David Pfau, Thomas Reardon, Yu Mu, Clay Lacefield, Weijian Yang, et al. Simultaneous denoising, deconvolution, and demixing of calcium imaging data. *Neuron*, 89(2):285–299, 2016.
- [QSW14] Qing Qu, Ju Sun, and John Wright. Finding a sparse vector in a subspace: Linear sparsity using alternating directions. In *Advances in Neural Information Processing Systems*, pages 3401–3409, 2014.
- [QZEW17] Qing Qu, Yuqian Zhang, Yonina Eldar, and John Wright. Convolutional phase retrieval. In *Advances in Neural Information Processing Systems*, pages 6086–6096, 2017.
- [QZL⁺20] Qing Qu, Zhihui Zhu, Xiao Li, Manolis C. Tsakiris, John Wright, and RenÁI Vidal. Finding the sparsest vectors in a subspace: Theory, algorithms, and applications, 2020.

- [RBZ06] Michael J Rust, Mark Bates, and Xiaowei Zhuang. Sub-diffraction-limit imaging by stochastic optical reconstruction microscopy (storm). *Nature methods*, 3(10):793, 2006.
- [RPD⁺15] Audrey Repetti, Mai Quyen Pham, Laurent Duval, Emilie Chouzenoux, and Jean-Christophe Pesquet. Euclid in a taxicab: Sparse blind deconvolution with smoothed ℓ_1/ℓ_2 regularization. *IEEE signal processing letters*, 22(5):539–543, 2015.
- [SC19] Laixi Shi and Yuejie Chi. Manifold gradient descent solves multi-channel sparse blind deconvolution provably and efficiently, 2019.
- [SCL⁺15] Huajun She, Rong-Rong Chen, Dong Liang, Yuchou Chang, and Leslie Ying. Image reconstruction from phased-array data based on multichannel blind deconvolution. *Magnetic resonance imaging*, 33(9):1106–1113, 2015.
- [SM12] Filip Sroubek and Peyman Milanfar. Robust multichannel blind deconvolution via fast alternating minimization. *IEEE Transactions on Image processing*, 21(4):1687–1700, 2012.
- [SN06] Pinaki Sarder and Arye Nehorai. Deconvolution methods for 3-d fluorescence microscopy images. *IEEE Signal Processing Magazine*, 23(3):32–45, 2006.
- [SQW16] Ju Sun, Qing Qu, and John Wright. Complete dictionary recovery over the sphere i: Overview and the geometric picture. *IEEE Transactions on Information Theory*, 63(2):853–884, 2016.
- [SQW17] Ju Sun, Qing Qu, and John Wright. Complete dictionary recovery over the sphere ii: Recovery by riemannian trust-region method. *IEEE Transactions on Information Theory*, 63(2):885–914, 2017.
- [SS14] Alex Small and Shane Stahlheber. Fluorophore localization algorithms for super-resolution microscopy. *Nature methods*, 11(3):267, 2014.
- [Sun] Ju Sun. Provable nonconvex methods/algorithms. <https://sunju.org/research/nonconvex/>.
- [Tal14] Michel Talagrand. *Upper and lower bounds for stochastic processes: modern methods and classical problems*, volume 60. Springer Science & Business Media, 2014.
- [TBSR17] Ning Tian, Sung-Hoon Byun, Karim Sabra, and Justin Romberg. Multichannel myopic deconvolution in underwater acoustic channels via low-rank recovery. *The Journal of the Acoustical Society of America*, 141(5):3337–3348, 2017.
- [TV15] Manolis C Tsakiris and René Vidal. Dual principal component pursuit. In *Proceedings of the IEEE International Conference on Computer Vision Workshops*, pages 10–18, 2015.
- [WC16] Liming Wang and Yuejie Chi. Blind deconvolution from multiple sparse inputs. *IEEE Signal Processing Letters*, 23(10):1384–1388, 2016.
- [WLS⁺13] Guo-Rong Wu, Wei Liao, Sebastiano Stramaglia, Ju-Rong Ding, Huaifu Chen, and Daniele Marinazzo. A blind deconvolution approach to recover effective connectivity brain networks from resting state fmri data. *Medical image analysis*, 17(3):365–374, 2013.
- [XLTK95] Guanghan Xu, Hui Liu, Lang Tong, and Thomas Kailath. A least-squares approach to blind channel identification. *IEEE Transactions on signal processing*, 43(12):2982–2993, 1995.
- [ZKW18] Yuqian Zhang, Han-wen Kuo, and John Wright. Structured local minima in sparse blind deconvolution. In S. Bengio, H. Wallach, H. Larochelle, K. Grauman, N. Cesa-Bianchi, and R. Garnett, editors, *Advances in Neural Information Processing Systems 31*, pages 2328–2337. Curran Associates, Inc., 2018.
- [ZLK⁺17] Yuqian Zhang, Yenson Lau, Han-Wen Kuo, Sky Cheung, Abhay Pasupathy, and John Wright. On the global geometry of sphere-constrained sparse blind deconvolution. In *Computer Vision and Pattern Recognition (CVPR), 2017 IEEE Conference on*, pages 4381–4389. IEEE, 2017.
- [ZWR⁺18] Zhihui Zhu, Yifan Wang, Daniel Robinson, Daniel Naiman, Rene Vidal, and Manolis Tsakiris. Dual principal component pursuit: Improved analysis and efficient algorithms. In *Advances in Neural Information Processing Systems*, pages 2171–2181, 2018.
- [ZWZ13] Haichao Zhang, David Wipf, and Yanning Zhang. Multi-image blind deblurring using a coupled adaptive sparse prior. In *Proceedings of the IEEE Conference on Computer Vision and Pattern Recognition*, pages 1051–1058, 2013.
- [ZYL⁺19] Yuexiang Zhai, Zitong Yang, Zhenyu Liao, John Wright, and Yi Ma. Complete dictionary learning via ℓ^4 -norm maximization over the orthogonal group. *arXiv preprint arXiv:1906.02435*, 2019.
- [ZZEH12] Lei Zhu, Wei Zhang, Daniel Elnatan, and Bo Huang. Faster storm using compressed sensing. *Nature methods*, 9(7):721, 2012.

Appendices

The appendices are organized as follows. In Appendix A we introduce the basic notations and problem reductions that are used throughout the main draft and the appendix. We list the basic technical tools and results in Appendix B. In Appendix C we describe and prove the main geometric properties of the optimization landscape for Huber loss. In Appendix D, we provide global convergence analysis for the propose Riemannian gradient descent methods for optimizing the Huber loss, and the subgradient methods for solving LP rounding. All the technical geometric analysis are postponed to Appendix E, Appendix F, Appendix G, and Appendix H. Finally, in Appendix I we describe the proposed optimization algorithms in full details for all ℓ^1 , Huber, and ℓ^4 losses.

A Basic Notations and Problem Reductions

Throughout this paper, all vectors/matrices are written in bold font \mathbf{a}/\mathbf{A} ; indexed values are written as a_i, A_{ij} . We use \mathbf{v}_{-i} to denote a subvector of \mathbf{v} without the i -th entry. Zeros or ones vectors are defined as $\mathbf{0}_m$ or $\mathbf{1}_m$ with m denoting its length, and i -th canonical basis vector defined as \mathbf{e}_i . We use \mathbb{S}^{n-1} to denote an n -dimensional unit sphere in the Euclidean space \mathbb{R}^n . We use $\mathbf{z}^{(k)}$ to denote an optimization variable \mathbf{z} at k -th iteration. We let $[m] = \{1, 2, \dots, m\}$. Let $\mathbf{F}_n \in \mathbb{C}^{n \times n}$ denote a unnormalized $n \times n$ DFT matrix, with $\|\mathbf{F}_n\| = \sqrt{n}$, and $\mathbf{F}_n^{-1} = n^{-1} \mathbf{F}_n^*$. In many cases, we just use \mathbf{F} to denote the DFT matrix. We define $\text{sign}(\cdot)$ as

$$\text{sign}(z) = \begin{cases} z/|z|, & z \neq 0 \\ 0, & z = 0 \end{cases}$$

Some basic operators. We use \mathcal{P}_v and \mathcal{P}_{v^\perp} to denote projections onto v and its orthogonal complement, respectively. We let $\mathcal{P}_{\mathbb{S}^{n-1}}$ to be the ℓ^2 -normalization operator. To sum up, we have

$$\mathcal{P}_{v^\perp} \mathbf{u} = \mathbf{u} - \frac{\mathbf{v}\mathbf{v}^\top}{\|\mathbf{v}\|^2} \mathbf{u}, \quad \mathcal{P}_v \mathbf{u} = \frac{\mathbf{v}\mathbf{v}^\top}{\|\mathbf{v}\|^2} \mathbf{u}, \quad \mathcal{P}_{\mathbb{S}^{n-1}} \mathbf{v} = \frac{\mathbf{v}}{\|\mathbf{v}\|}.$$

Circular convolution and circulant matrices. The convolution operator \circledast is *circular* with modulo- m : $(\mathbf{a} \circledast \mathbf{x})_i = \sum_{j=0}^{m-1} a_j x_{i-j}$, and we use \boxtimes to specify the *circular* convolution in 2D. For a vector $\mathbf{v} \in \mathbb{R}^m$, let $s_\ell[\mathbf{v}]$ denote the cyclic shift of \mathbf{v} with length ℓ . Thus, we can introduce the circulant matrix $\mathbf{C}_v \in \mathbb{R}^{m \times m}$ generated through $\mathbf{v} \in \mathbb{R}^m$,

$$\mathbf{C}_v = \begin{bmatrix} v_1 & v_m & \cdots & v_3 & v_2 \\ v_2 & v_1 & v_m & & \\ \vdots & v_2 & v_1 & \ddots & \vdots \\ v_{m-1} & & \ddots & \ddots & v_m \\ v_m & v_{m-1} & \cdots & v_2 & v_1 \end{bmatrix} = [s_0[\mathbf{v}] \quad s_1[\mathbf{v}] \quad \cdots \quad s_{m-1}[\mathbf{v}]]. \quad (17)$$

Now the circulant convolution can also be written in a simpler matrix-vector product form. For instance, for any $\mathbf{u} \in \mathbb{R}^m$ and $\mathbf{v} \in \mathbb{R}^m$,

$$\mathbf{u} \circledast \mathbf{v} = \mathbf{C}_u \cdot \mathbf{v} = \mathbf{C}_v \cdot \mathbf{u}.$$

In addition, the correlation between \mathbf{u} and \mathbf{v} can be also written in a similar form of convolution operator which reverses one vector before convolution. Let $\check{\mathbf{v}}$ denote a *cyclic reversal* of $\mathbf{v} \in \mathbb{R}^m$, i.e., $\check{\mathbf{v}} = [v_1, v_m, v_{m-1}, \dots, v_2]^\top$, and define two correlation matrices $\mathbf{C}_v^* \mathbf{e}_j = s_j[\mathbf{v}]$ and $\check{\mathbf{C}}_v \mathbf{e}_j = s_{-j}[\mathbf{v}]$. The two operators satisfy

$$\mathbf{C}_v^* \mathbf{u} = \check{\mathbf{v}} \circledast \mathbf{u}, \quad \check{\mathbf{C}}_v \mathbf{u} = \mathbf{v} \circledast \check{\mathbf{u}}.$$

Notation for several distributions. We use *i.i.d.* to denote *identically and independently distributed* random variables, and we introduce abbreviations for other distributions as follows.

- we use $\mathcal{N}(\mu, \sigma^2)$ to denote Gaussian distribution with mean μ and variance σ^2 ;
- we use $\mathcal{U}(\mathbb{S}^{n-1})$ to denote the uniform distribution over the sphere \mathbb{S}^{n-1} ;
- we use $\mathcal{B}(\theta)$ to denote the Bernoulli distribution with parameter θ controlling the nonzero probability;
- we use $\mathcal{BG}(\theta)$ to denote Bernoulli-Gaussian distribution, i.e., if $u \sim \mathcal{BG}(\theta)$, then $u = b \cdot g$ with $b \sim \mathcal{B}(\theta)$ and $g \sim \mathcal{N}(0, 1)$;
- we use $\mathcal{BR}(\theta)$ to denote Bernoulli-Rademacher distribution, i.e., if $u \sim \mathcal{BR}(\theta)$, then $u = b \cdot r$ with $b \sim \mathcal{B}(\theta)$ and r follows Rademacher distribution.

B Basic Tools

Lemma B.1 (Moments of the Gaussian Random Variable) *If $X \sim \mathcal{N}(0, \sigma_X^2)$, then it holds for all integer $m \geq 1$ that*

$$\mathbb{E}[|X|^m] = \sigma_X^m (m-1)!! \left[\sqrt{\frac{2}{\pi}} \mathbb{1}_{m=2k+1} + \mathbb{1}_{m=2k} \right] \leq \sigma_X^m (m-1)!!, \quad k = \lfloor m/2 \rfloor.$$

Lemma B.2 (sub-Gaussian Random Variables) *Let X be a centered σ^2 sub-Gaussian random variable, such that*

$$\mathbb{P}(|X| \geq t) \leq 2 \exp\left(-\frac{t^2}{2\sigma^2}\right),$$

then for any integer $p \geq 1$, we have

$$\mathbb{E}[|X|^p] \leq (2\sigma^2)^{p/2} p\Gamma(p/2).$$

In particular, we have

$$\|X\|_{L^p} = (\mathbb{E}[|X|^p])^{1/p} \leq \sigma e^{1/e} \sqrt{p}, \quad p \geq 2,$$

and $\mathbb{E}[|X|] \leq \sigma\sqrt{2\pi}$.

Lemma B.3 (Moment-Control Bernstein's Inequality for Random Variables [FR13]) *Let X_1, \dots, X_N be i.i.d. real-valued random variables. Suppose that there exist some positive numbers R and σ_X^2 such that*

$$\mathbb{E}[|X_k|^m] \leq \frac{m!}{2} \sigma_X^2 R^{m-2}, \quad \text{for all integers } m \geq 2.$$

Let $S \doteq \frac{1}{N} \sum_{k=1}^N X_k$, then for all $t > 0$, it holds that

$$\mathbb{P}[|S - \mathbb{E}[S]| \geq t] \leq 2 \exp\left(-\frac{Nt^2}{2\sigma_X^2 + 2Rt}\right).$$

Lemma B.4 (Gaussian Concentration Inequality) *Let $\mathbf{g} \in \mathbb{R}^n$ be a standard Gaussian random variable $\mathbf{g} \sim \mathcal{N}(\mathbf{0}, \mathbf{I})$, and let $f : \mathbb{R}^n \mapsto \mathbb{R}$ denote an L -Lipschitz function. Then for all $t > 0$,*

$$\mathbb{P}(|f(\mathbf{g}) - \mathbb{E}[f(\mathbf{g})]| \geq t) \leq 2 \exp\left(-\frac{t^2}{2L^2}\right).$$

Lemma B.5 (Lemma VII.1, [SQW17]) Let $\mathbf{M} \in \mathbb{R}^{n_1 \times n_2}$ with $\mathbf{M} \sim \mathcal{BG}(\theta)$ and $\theta \in (0, 1/3)$. For a given set $\mathcal{I} \subseteq [n_2]$ with $|\mathcal{I}| \leq \frac{9}{8}\theta n_2$, whenever $n_2 \geq \frac{C}{\theta^2} n_1 \log\left(\frac{n_1}{\theta}\right)$, it holds

$$\|\mathbf{v}^\top \mathbf{M}_{\mathcal{I}^c}\|_1 - \|\mathbf{v}^\top \mathbf{M}_{\mathcal{I}}\|_1 \geq \frac{n_2}{6} \sqrt{\frac{2}{\pi}} \theta \|\mathbf{v}\|$$

for all $\mathbf{v} \in \mathbb{R}^{n_1}$, with probability at least $1 - cn_2^{-6}$.

Lemma B.6 (Derivates of $h_\mu(z)$) The first two derivatives of $h_\mu(z)$ are

$$\nabla h_\mu(z) = \begin{cases} \text{sign}(z) & |z| \geq \mu \\ z/\mu & |z| < \mu \end{cases}, \quad \nabla^2 h_\mu(z) = \begin{cases} 0 & |z| > \mu \\ 1/\mu & |z| < \mu \end{cases}. \quad (18)$$

Whenever necessary, we define $\nabla^2 h_\mu(\mu) = 0$, and write the “second derivative” as $\nabla^2 \bar{h}_\mu(\mu)$ instead. Moreover for all z, z' ,

$$|\nabla h_\mu(z) - \nabla h_\mu(z')| \leq \frac{1}{\mu} |z - z'|. \quad (19)$$

Lemma B.7 Let $X \sim \mathcal{N}(0, \sigma_x^2)$ and $Y \sim \mathcal{N}(0, \sigma_y^2)$ and $Z \sim \mathcal{N}(0, \sigma_z^2)$ be independent random variables. Then we have

$$\mathbb{E}[X \mathbb{1}_{X+Y \geq \mu}] = \frac{\sigma_x^2}{\sqrt{2\pi} \sqrt{\sigma_x^2 + \sigma_y^2}} \exp\left(-\frac{\mu^2}{2(\sigma_x^2 + \sigma_y^2)}\right), \quad (20)$$

$$\mathbb{E}[XY \mathbb{1}_{|X+Y| \leq \mu}] = -\sqrt{\frac{2}{\pi}} \frac{\mu \sigma_x^2 \sigma_y^2}{(\sigma_x^2 + \sigma_y^2)^{3/2}} \exp\left(-\frac{\mu^2}{2(\sigma_x^2 + \sigma_y^2)}\right), \quad (21)$$

$$\mathbb{E}[|X| \mathbb{1}_{|X| > \mu}] = \sqrt{\frac{2}{\pi}} \sigma_x \exp\left(-\frac{\mu^2}{2\sigma_x^2}\right), \quad (22)$$

$$\mathbb{E}[XY \mathbb{1}_{|X+Y+Z| < \mu}] = -\sqrt{\frac{2}{\pi}} \mu \exp\left(-\frac{\mu^2}{2(\sigma_x^2 + \sigma_y^2 + \sigma_z^2)}\right) \frac{\sigma_x^2 \sigma_y^2}{(\sigma_x^2 + \sigma_y^2 + \sigma_z^2)^{3/2}}, \quad (23)$$

$$\mathbb{E}[X^2 \mathbb{1}_{|X| < \mu}] = -\sqrt{\frac{2}{\pi}} \sigma_x \mu \exp\left(-\frac{\mu^2}{2\sigma_x^2}\right) + \sigma_x^2 \mathbb{P}[|X| < \mu], \quad (24)$$

$$\mathbb{E}[X^2 \mathbb{1}_{|X+Y| < \mu}] = -\sqrt{\frac{2}{\pi}} \mu \frac{\sigma_x^4}{(\sigma_x^2 + \sigma_y^2)^{3/2}} \exp\left(-\frac{\mu^2}{2(\sigma_x^2 + \sigma_y^2)}\right) + \sigma_x^2 \mathbb{P}[|X+Y| < \mu]. \quad (25)$$

Proof Direct calculations. ■

Lemma B.8 (Calculus for Function of Matrices, Chapter X of [Bha13]) Let $\mathcal{S}^{n \times n}$ be the set of symmetric matrices of size $n \times n$. We define a map $f : \mathcal{S}^{n \times n} \mapsto \mathcal{S}^{n \times n}$ as

$$f(\mathbf{A}) = \mathbf{U} f(\mathbf{\Lambda}) \mathbf{U}^*,$$

where $\mathbf{A} \in \mathcal{S}^{n \times n}$ has the eigen-decomposition $\mathbf{A} = \mathbf{U} \mathbf{\Lambda} \mathbf{U}^*$. The map f is called (Fréchet) differentiable at \mathbf{A} if there exists a linear transformation on $\mathcal{S}^{n \times n}$ such that for all $\mathbf{\Delta}$

$$\|f(\mathbf{A} + \mathbf{\Delta}) - f(\mathbf{A}) - \mathbf{D}f(\mathbf{A})[\mathbf{\Delta}]\| = o(\|\mathbf{\Delta}\|).$$

The linear operator $\mathbf{D}f(\mathbf{A})$ is called the derivative of f at \mathbf{A} , and $\mathbf{D}f(\mathbf{A})[\mathbf{\Delta}]$ is the directional derivative of f along $\mathbf{\Delta}$. If f is differentiable at \mathbf{A} , then

$$\mathbf{D}f(\mathbf{A})[\mathbf{\Delta}] = \left. \frac{d}{dt} f(\mathbf{A} + t\mathbf{\Delta}) \right|_{t=0}.$$

We denote the operator norm of the derivative $Df(\mathbf{A})$ as

$$\|Df(\mathbf{A})\| \doteq \sup_{\|\Delta\|=1} \|Df(\mathbf{A})[\Delta]\|.$$

Lemma B.9 (Mean Value Theorem for Function of Matrices) *Let f be a differentiable map from a convex subset \mathcal{U} of a Banach space \mathcal{X} into the Banach space \mathcal{Y} . Let $\mathbf{A}, \mathbf{B} \in \mathcal{U}$, and let \mathcal{L} be the line segment joining them. Then*

$$\|f(\mathbf{B}) - f(\mathbf{A})\| \leq \|\mathbf{B} - \mathbf{A}\| \sup_{U \in \mathcal{L}} \|Df(U)\|.$$

Lemma B.10 (Theorem VII.2.3 of [Bha13]) *Let \mathbf{A} and \mathbf{B} be operators whose spectra are contained in the open right half-plane and open left half-plane, respectively. Then the solution of the equation $\mathbf{A}\mathbf{X} - \mathbf{X}\mathbf{B} = \mathbf{Y}$ can be expressed as*

$$\mathbf{X} = \int_0^\infty e^{-t\mathbf{A}} \mathbf{Y} e^{t\mathbf{B}} dt$$

Lemma B.11 *Let $f(\mathbf{A}) = \mathbf{A}^{-1/2}$, defined the set of all $n \times n$ positive definite matrices $\mathcal{S}_+^{n \times n}$, then we have*

$$\|Df(\mathbf{A})\| \leq \frac{1}{\sigma_{\min}^2(\mathbf{A})},$$

where $\sigma_{\min}(\mathbf{A})$ is the smallest singular value of \mathbf{A} .

Proof To bound the operator norm $\|Df(\mathbf{A})\|$, we introduce an auxiliary function

$$g(\mathbf{A}) = \mathbf{A}^{-2}, \quad f(\mathbf{A}) = g^{-1}(\mathbf{A}),$$

such that f and g are the inverse function to each other. Whenever $g(f(\mathbf{A})) \neq 0$ (which is true for our case $\mathbf{A} > \mathbf{0}$), this gives

$$Df(\mathbf{A}) = [Dg(f(\mathbf{A}))]^{-1} = \left[Dg(\mathbf{A}^{-1/2}) \right]^{-1}. \quad (26)$$

This suggests that we can estimate $Df(\mathbf{A})$ via estimating $Dg(\mathbf{A})$ of its inverse function g . Let

$$g = h(w(\mathbf{A})), \quad h(\mathbf{A}) = \mathbf{A}^{-1}, \quad w(\mathbf{A}) = \mathbf{A}^2,$$

such that their directional derivatives have simple form

$$Dh(\mathbf{A})[\Delta] = -\mathbf{A}^{-1}\Delta\mathbf{A}^{-1}, \quad Dw(\mathbf{A})[\Delta] = \Delta\mathbf{A} + \mathbf{A}\Delta.$$

By using chain rule, simple calculation gives

$$\begin{aligned} Dg(\mathbf{A})[\Delta] &= Dh(w(\mathbf{A})) [Dw(\mathbf{A})[\Delta]], \\ &= -(\mathbf{A}^{-2}\Delta\mathbf{A}^{-1} + \mathbf{A}^{-1}\Delta\mathbf{A}^{-2}). \end{aligned}$$

Now by (26), the directional derivative

$$\mathbf{Z} \doteq Df(\mathbf{A})[\Delta]$$

satisfies

$$\mathbf{A}\mathbf{Z}\mathbf{A}^{1/2} + \mathbf{A}^{1/2}\mathbf{Z}\mathbf{A} = -\Delta.$$

Since $\mathbf{A} > \mathbf{0}$, we write the eigen decomposition as $\mathbf{A} = \mathbf{U}\mathbf{\Lambda}\mathbf{U}^*$, with \mathbf{U} orthogonal and $\mathbf{\Lambda} > 0$ diagonal. Let $\tilde{\mathbf{Z}} = \mathbf{U}^* \mathbf{Z} \mathbf{U}$ and $\tilde{\mathbf{\Delta}} = \mathbf{U}^* \mathbf{\Delta} \mathbf{U}$, then the equation above gives

$$\mathbf{\Lambda}^{1/2} \tilde{\mathbf{Z}} - \tilde{\mathbf{Z}} \left(-\mathbf{\Lambda}^{1/2} \right) = -\mathbf{\Lambda}^{-1/2} \tilde{\mathbf{\Delta}} \mathbf{\Lambda}^{-1/2},$$

which is the Sylvester equation []. Since $\mathbf{\Lambda}^{1/2}$ and $-\mathbf{\Lambda}^{1/2}$ do not have common eigenvalues, Lemma B.10 gives

$$\text{D}f(\mathbf{A})[\mathbf{\Delta}] = \mathbf{U} \left[\int_0^\infty e^{-\mathbf{\Lambda}^{1/2} \tau} \left(-\mathbf{\Lambda}^{-1/2} \tilde{\mathbf{\Delta}} \mathbf{\Lambda}^{-1/2} \right) e^{-\mathbf{\Lambda}^{1/2} \tau} d\tau \right] \mathbf{U}^*.$$

Thus, by Lemma B.8 we know that

$$\begin{aligned} \|\text{D}f(\mathbf{A})\| &= \sup_{\|\mathbf{\Delta}\|=1} \|\text{D}f(\mathbf{A})[\mathbf{\Delta}]\| \\ &\leq \int_0^\infty \left\| e^{-\mathbf{\Lambda}^{1/2} \tau} \left(-\mathbf{\Lambda}^{-1/2} \tilde{\mathbf{\Delta}} \mathbf{\Lambda}^{-1/2} \right) e^{-\mathbf{\Lambda}^{1/2} \tau} \right\| d\tau \\ &\leq \left\| \mathbf{\Lambda}^{-1/2} \tilde{\mathbf{\Delta}} \mathbf{\Lambda}^{-1/2} \right\| \int_0^\infty e^{-\sigma_{\min} \tau} d\tau \leq \frac{1}{\sigma_{\min}^2(\mathbf{A})}. \end{aligned}$$

■

Lemma B.12 (Matrix Perturbation Bound) Suppose $\mathbf{A} > \mathbf{0}$. Then for any symmetric perturbation matrix $\mathbf{\Delta}$ with $\|\mathbf{\Delta}\| \leq \frac{1}{2}\sigma_{\min}(\mathbf{A})$, it holds that

$$\left\| (\mathbf{A} + \mathbf{\Delta})^{-1/2} - \mathbf{A}^{-1/2} \right\| \leq \frac{4 \|\mathbf{\Delta}\|}{\sigma_{\min}^2(\mathbf{A})},$$

where $\sigma_{\min}(\mathbf{A})$ denotes the minimum singular value of \mathbf{A} .

Proof Let us denote $f(\mathbf{A}) = \mathbf{A}^{-1/2}$. Given a symmetric perturbation matrix $\mathbf{\Delta}$, by mean value theorem, we have

$$\begin{aligned} \left\| (\mathbf{A} + \mathbf{\Delta})^{-1/2} - \mathbf{A}^{-1/2} \right\| &= \left\| \int_0^1 \text{D}f(\mathbf{A} + t\mathbf{\Delta})[\mathbf{\Delta}] dt \right\| \\ &\leq \left(\sup_{t \in [0,1]} \|\text{D}f(\mathbf{A} + t\mathbf{\Delta})\| \right) \cdot \|\mathbf{\Delta}\|. \end{aligned}$$

Thus, by Lemma B.11 and by using the fact that $\|\mathbf{\Delta}\| \leq \frac{1}{2}\sigma_{\min}(\mathbf{A})$, we have

$$\left\| (\mathbf{A} + \mathbf{\Delta})^{-1/2} - \mathbf{A}^{-1/2} \right\| \leq \left(\sup_{t \in [0,1]} \frac{1}{\sigma_{\min}^2(\mathbf{A} + t\mathbf{\Delta})} \right) \|\mathbf{\Delta}\| \leq \frac{4 \|\mathbf{\Delta}\|}{\sigma_{\min}^2(\mathbf{A})},$$

as desired. ■

C Geometry: Main Results

In this part of the appendix, we prove our main geometric result stated in Section 3.1. Namely, we show the objective introduced in (9)

$$\min_{\mathbf{q}} f(\mathbf{q}) := \frac{1}{np} \sum_{i=1}^p H_{\mu}(C_{x_i} R \mathbf{Q}^{-1} \mathbf{q}), \quad \text{s.t.} \quad \|\mathbf{q}\| = 1 \quad (27)$$

with

$$\mathbf{R} = \mathbf{C}_a \left(\frac{1}{\theta np} \sum_{i=1}^p \mathbf{C}_{\mathbf{y}_i}^\top \mathbf{C}_{\mathbf{y}_i} \right)^{-1/2}, \quad \mathbf{Q} = \mathbf{C}_a (\mathbf{C}_a^\top \mathbf{C}_a)^{-1/2},$$

have benign first-order geometric structure. Namely, we prove that the function satisfies the regularity condition in Proposition C.1 and implicit regularization in Proposition C.2 properties over every one of the sets

$$\mathcal{S}_\xi^{i\pm} := \left\{ \mathbf{q} \in \mathbb{S}^{n-1} \mid \frac{|q_i|}{\|\mathbf{q}_{-i}\|_\infty} \geq \sqrt{1+\xi}, q_i \geq 0 \right\}, \quad \xi \in (0, \infty),$$

and we also show that the gradient is bounded all over the sphere (Proposition C.3). These geometric properties enable efficient optimization via vanilla Riemannian gradient descent methods. In Appendix D, we will leverage on these properties for proving convergence of our proposed optimization methods.

As aforementioned in Section 3.1, the basic idea of our analysis is first reducing (27) to a simpler objective

$$\min_{\mathbf{q}} \tilde{f}(\mathbf{q}) = \frac{1}{np} \sum_{i=1}^p H_\mu(\mathbf{C}_{x_i} \mathbf{q}), \quad \text{s.t.} \quad \|\mathbf{q}\| = 1. \quad (28)$$

by using the fact that $\mathbf{R} \approx \mathbf{Q}$ and assuming $\mathbf{R}\mathbf{Q}^{-1} = \mathbf{I}$. In Appendix E and Appendix F, we show the geometric properties hold in population for $\tilde{f}(\mathbf{q})$. We turn these results into non-asymptotic version via concentration analysis in Appendix G. Finally, we prove these results for $f(\mathbf{q})$ in (27) via a perturbation analysis in Appendix H.

First, we show that regularity condition of the Riemannian gradient of $f(\mathbf{q})$ over the set $\mathcal{S}_\xi^{i\pm}$ as follows.

Proposition C.1 (Regularity condition) Suppose $\theta \geq \frac{1}{n}$ and $\mu \leq c_0 \min \left\{ \theta, \frac{1}{\sqrt{n}} \right\}$. There exists some numerical constant $\gamma \in (0, 1)$, when the sample complexity

$$p \geq C \max \left\{ n, \frac{\kappa^8}{\theta \mu^2 \sigma_{\min}^2} \log^4 n \right\} \xi^{-2} \theta^{-2} n^4 \log \left(\frac{\theta n}{\mu} \right),$$

with probability at least $1 - n^{-c_1} - c_2 np^{-c_3 n \theta}$ over the randomness of $\{\mathbf{x}_i\}_{i=1}^p$, we have

$$\langle \text{grad } f(\mathbf{q}), q_i \mathbf{q} - \mathbf{e}_i \rangle \geq c_4 \theta (1 - \theta) q_i \|\mathbf{q} - \mathbf{e}_i\|, \quad \sqrt{1 - q_i^2} \in [\mu, \gamma], \quad (29)$$

$$\langle \text{grad } f(\mathbf{q}), q_i \mathbf{q} - \mathbf{e}_i \rangle \geq c_4 \theta (1 - \theta) q_i n^{-1} \|\mathbf{q} - \mathbf{e}_i\|, \quad \sqrt{1 - q_i^2} \in \left[\gamma, \sqrt{\frac{n-1}{n}} \right], \quad (30)$$

holds for any $\mathbf{q} \in \mathcal{S}_\xi^{i+}$ and each index $i \in [n]$. Here, c_0, c_1, c_2, c_3, c_4 , and C are positive numerical constants.

Proof Without loss of generality, it is enough to consider the case $i = n$. For all $\mathbf{q} \in \mathcal{S}_\xi^{n+}$, we have

$$\begin{aligned} & \langle \text{grad } f(\mathbf{q}), q_n \mathbf{q} - \mathbf{e}_n \rangle \\ &= \left\langle \text{grad } f(\mathbf{q}) - \text{grad } \tilde{f}(\mathbf{q}) + \text{grad } \tilde{f}(\mathbf{q}) - \text{grad } \mathbb{E} [\tilde{f}(\mathbf{q})] + \text{grad } \mathbb{E} [\tilde{f}(\mathbf{q})], q_n \mathbf{q} - \mathbf{e}_n \right\rangle \\ &\geq \left\langle \text{grad } \mathbb{E} [\tilde{f}(\mathbf{q})], q_n \mathbf{q} - \mathbf{e}_n \right\rangle - \left| \left\langle \text{grad } f(\mathbf{q}) - \text{grad } \tilde{f}(\mathbf{q}), q_n \mathbf{q} - \mathbf{e}_n \right\rangle \right| \\ &\quad - \left| \left\langle \text{grad } \tilde{f}(\mathbf{q}) - \text{grad } \mathbb{E} [\tilde{f}(\mathbf{q})], q_n \mathbf{q} - \mathbf{e}_n \right\rangle \right|. \end{aligned}$$

From Proposition E.1, when $\theta \geq \frac{1}{n}$ and $\mu \leq c_0 \min \left\{ \theta, \frac{1}{\sqrt{n}} \right\}$, we know that in the worst case scenario,

$$\left\langle \text{grad } \mathbb{E} [\tilde{f}(\mathbf{q})], q_n \mathbf{q} - \mathbf{e}_n \right\rangle \geq c_1 \theta (1 - \theta) \xi n^{-3/2} \|\mathbf{q}_{-n}\|$$

holds for all $\mathbf{q} \in \mathcal{S}_\xi^{n+}$. On the other hand, by Corollary G.2, when $p \geq C_1 \theta^{-2} \xi^{-2} n^5 \log\left(\frac{\theta n}{\mu}\right)$, we have

$$\begin{aligned} \left| \left\langle \text{grad } \tilde{f}(\mathbf{q}) - \text{grad } \mathbb{E}[\tilde{f}(\mathbf{q})], q_n \mathbf{q} - \mathbf{e}_n \right\rangle \right| &\leq \left\| \text{grad } \tilde{f}(\mathbf{q}) - \text{grad } \mathbb{E}[\tilde{f}(\mathbf{q})] \right\| \|q_n \mathbf{q} - \mathbf{e}_n\| \\ &\leq \frac{c_1}{3} \theta (1 - \theta) \xi n^{-3/2} \|q_n \mathbf{q} - \mathbf{e}_n\| \end{aligned}$$

holds for all $\mathbf{q} \in \mathcal{S}_\xi^{n+}$ with probability at least $1 - np^{-c_2 \theta n} - n \exp(-c_3 n^2)$. Moreover, from Proposition H.1, we know that when $p \geq C \frac{\kappa^8 n^4}{\mu^2 \theta^3 \sigma_{\min}^2 \xi^2} \log^4 n \log\left(\frac{\theta n}{\mu}\right)$

$$\begin{aligned} \left| \left\langle \text{grad } f(\mathbf{q}) - \text{grad } \tilde{f}(\mathbf{q}), q_n \mathbf{q} - \mathbf{e}_n \right\rangle \right| &\leq \|q_n \mathbf{q} - \mathbf{e}_n\| \cdot \left\| \text{grad } f(\mathbf{q}) - \text{grad } \tilde{f}(\mathbf{q}) \right\| \\ &\leq \frac{c_1}{3} \theta (1 - \theta) \xi n^{-3/2} \|q_n \mathbf{q} - \mathbf{e}_n\| \end{aligned}$$

holds for all $\mathbf{q} \in \mathcal{S}_\xi^{n+}$ with probability at least $1 - c_4 p^{-c_5 n \theta} - n^{-c_6} - n e^{-c_7 \theta n p}$. By combining all the bounds above, we obtain the desired result. \blacksquare

Second, we show that the Riemannian gradient of $f(\mathbf{q})$ also satisfies implicit regularization over $\mathcal{S}_\xi^{i\pm}$, such that iterates of the RGD method stays within one of the sets $\mathcal{S}_\xi^{i\pm}$ for sufficiently small stepsizes.

Proposition C.2 (Implicit Regularization) Suppose $\theta \geq \frac{1}{n}$ and $\mu \leq \frac{c_0}{\sqrt{n}}$. For any index $i \in [n]$, when the sample

$$p \geq C \max \left\{ n, \frac{\kappa^8}{\theta \mu^2 \sigma_{\min}^2} \log^4 n \right\} \xi^{-2} \theta^{-2} n^4 \log\left(\frac{\theta n}{\mu}\right),$$

with probability at least $1 - n^{-c_1} - c_2 n p^{-c_3 n \theta}$ over the randomness of $\{\mathbf{x}_i\}_{i=1}^p$, we have

$$\left\langle \text{grad } f(\mathbf{q}), \frac{1}{q_j} \mathbf{e}_j - \frac{1}{q_i} \mathbf{e}_i \right\rangle \geq c_4 \frac{\theta(1 - \theta)}{n} \frac{\xi}{1 + \xi}, \quad (31)$$

holds for all $\mathbf{q} \in \mathcal{S}_\xi^{i+}$ and any q_j such that $j \neq i$ and $q_j^2 \geq \frac{1}{3} q_i^2$. Here, c_0, c_1, c_2, c_3, c_4 , and C are positive numerical constants.

Proof Without loss of generality, it is enough to consider the case $i = n$. For all $\mathbf{q} \in \mathcal{S}_\xi^{n+}$, we have

$$\begin{aligned} &\left\langle \text{grad } f(\mathbf{q}), \frac{1}{q_j} \mathbf{e}_j - \frac{1}{q_n} \mathbf{e}_n \right\rangle \\ &= \left\langle \text{grad } f(\mathbf{q}) - \text{grad } \tilde{f}(\mathbf{q}) + \text{grad } \tilde{f}(\mathbf{q}) - \text{grad } \mathbb{E}[\tilde{f}(\mathbf{q})] + \text{grad } \mathbb{E}[\tilde{f}(\mathbf{q})], \frac{1}{q_j} \mathbf{e}_j - \frac{1}{q_n} \mathbf{e}_n \right\rangle \\ &\geq \left\langle \text{grad } \mathbb{E}[\tilde{f}(\mathbf{q})], \frac{1}{q_j} \mathbf{e}_j - \frac{1}{q_n} \mathbf{e}_n \right\rangle - \left| \left\langle \text{grad } f(\mathbf{q}) - \text{grad } \tilde{f}(\mathbf{q}), \frac{1}{q_j} \mathbf{e}_j - \frac{1}{q_n} \mathbf{e}_n \right\rangle \right| \\ &\quad - \left| \left\langle \text{grad } \tilde{f}(\mathbf{q}) - \text{grad } \mathbb{E}[\tilde{f}(\mathbf{q})], \frac{1}{q_j} \mathbf{e}_j - \frac{1}{q_n} \mathbf{e}_n \right\rangle \right|. \end{aligned}$$

From Proposition F.1, when $\theta \geq \frac{1}{n}$ and $\mu \leq \frac{c_0}{\sqrt{n}}$, we know that

$$\left\langle \text{grad } \mathbb{E}[\tilde{f}(\mathbf{q})], \frac{1}{q_j} \mathbf{e}_j - \frac{1}{q_n} \mathbf{e}_n \right\rangle \geq \frac{\theta(1 - \theta)}{4n} \frac{\xi}{1 + \xi}$$

holds for all $\mathbf{q} \in \mathcal{S}_\xi^{n+}$ and any q_j such that $q_j^2 \geq \frac{1}{3}q_i^2$. On the other hand, by Corollary G.2, when $p \geq C_1\theta^{-2}\xi^{-2}n^5 \log\left(\frac{\theta n}{\mu}\right)$, we have

$$\begin{aligned} \left| \left\langle \text{grad } \tilde{f}(\mathbf{q}) - \text{grad } \mathbb{E}[\tilde{f}(\mathbf{q})], \frac{1}{q_j}\mathbf{e}_j - \frac{1}{q_n}\mathbf{e}_n \right\rangle \right| &\leq \left\| \text{grad } \tilde{f}(\mathbf{q}) - \text{grad } \mathbb{E}[\tilde{f}(\mathbf{q})] \right\| \cdot \left\| \frac{1}{q_j}\mathbf{e}_j - \frac{1}{q_n}\mathbf{e}_n \right\| \\ &\leq \frac{\theta(1-\theta)}{12n} \frac{\xi}{1+\xi} \end{aligned}$$

holds for all $\mathbf{q} \in \mathcal{S}_\xi^{n+}$ with probability at least $1 - np^{-c_2\theta n} - n \exp(-c_3n^2)$. For the last inequality, we used the fact that

$$\left\| \frac{1}{q_j}\mathbf{e}_j - \frac{1}{q_n}\mathbf{e}_n \right\| = \sqrt{\frac{1}{q_j^2} + \frac{1}{q_n^2}} \leq 2\sqrt{n}.$$

Moreover, from Proposition H.1, we know that when $p \geq C \frac{\kappa^8 n^4}{\mu^2 \theta^3 \sigma_{\min}^2 \xi^2} \log^4 n \log\left(\frac{\theta n}{\mu}\right)$

$$\begin{aligned} \left| \left\langle \text{grad } f(\mathbf{q}) - \text{grad } \tilde{f}(\mathbf{q}), q_n \mathbf{q} - \mathbf{e}_n \right\rangle \right| &\leq \left\| \text{grad } f(\mathbf{q}) - \text{grad } \tilde{f}(\mathbf{q}) \right\| \cdot \left\| \frac{1}{q_j}\mathbf{e}_j - \frac{1}{q_n}\mathbf{e}_n \right\| \\ &\leq \frac{\theta(1-\theta)}{12n} \frac{\xi}{1+\xi} \end{aligned}$$

holds for all $\mathbf{q} \in \mathcal{S}_\xi^{n+}$ with probability at least $1 - c_4 p^{-c_5 n \theta} - n^{-c_6} - n e^{-c_7 \theta n p}$. By combining all the bounds above, we obtain the desired result. \blacksquare

Finally, we prove that the Riemannian gradient of $f(\mathbf{q})$ are uniformly bounded over the sphere.

Proposition C.3 (Bounded gradient) Suppose $\theta \geq \frac{1}{n}$ and $\mu \leq \frac{c_0}{\sqrt{n}}$. For any index $i \in [n]$, when the sample

$$p \geq C \max \left\{ n, \frac{\kappa^8}{\theta \mu^2 \sigma_{\min}^2} \log^4 n \right\} \theta^{-2} n \log \left(\frac{\theta n}{\mu} \right),$$

with probability at least $1 - n^{-c_1} - c_2 n p^{-c_3 n \theta}$ over the randomness of $\{\mathbf{x}_i\}_{i=1}^p$, we have

$$|\langle \text{grad } f(\mathbf{q}), \mathbf{e}_i \rangle| \leq 2, \tag{32}$$

$$\|\text{grad } f(\mathbf{q})\| \leq 2\sqrt{\theta n}. \tag{33}$$

holds for all $\mathbf{q} \in \mathbb{S}^{n-1}$ and any index $i \in [n]$. Here, c_0, c_1, c_2, c_3 and C are positive numerical constants.

Proof For any index $i \in [n]$, we have

$$\begin{aligned} \sup_{\mathbf{q} \in \mathbb{S}^{n-1}} |\langle \text{grad } f(\mathbf{q}), \mathbf{e}_i \rangle| &\leq \sup_{\mathbf{q} \in \mathbb{S}^{n-1}} \left| \langle \text{grad } \tilde{f}(\mathbf{q}), \mathbf{e}_i \rangle \right| + \sup_{\mathbf{q} \in \mathbb{S}^{n-1}} \left| \langle \text{grad } f(\mathbf{q}) - \text{grad } \tilde{f}(\mathbf{q}), \mathbf{e}_i \rangle \right| \\ &\leq \sup_{\mathbf{q} \in \mathbb{S}^{n-1}} \left| \langle \text{grad } \tilde{f}(\mathbf{q}), \mathbf{e}_i \rangle \right| + \left\| \text{grad } f(\mathbf{q}) - \text{grad } \tilde{f}(\mathbf{q}) \right\|. \end{aligned}$$

By Corollary G.3, when $p \geq C_1 n \log\left(\frac{\theta n}{\mu}\right)$, we have

$$\sup_{\mathbf{q} \in \mathbb{S}^{n-1}} \left| \langle \text{grad } \tilde{f}(\mathbf{q}), \mathbf{e}_i \rangle \right| \leq \frac{3}{2}$$

holds for any index $i \in [n]$ with probability at least $1 - np^{-c_1\theta n} - n \exp(-c_2 p)$. On the other hand, Proposition H.1 implies that, when $p \geq C_2 \frac{\kappa^8 n}{\mu^2 \theta \sigma_{\min}^2} \log^4 n \log\left(\frac{\theta n}{\mu}\right)$, we have

$$\left\| \text{grad } f(\mathbf{q}) - \text{grad } \tilde{f}(\mathbf{q}) \right\| \leq \frac{1}{2},$$

holds with probability at least $1 - c_3 p^{-c_4 n \theta} - n^{-c_5} - n e^{-c_6 \theta n p}$. Combining the bounds above gives (32). The bound (33) can be proved in a similar fashion. ■

D Convergence Analysis

In this section, we prove the convergence result of proposed two-stage optimization method for Huber-loss stated in Section 3.2. Firstly, we prove that the vanilla RGD converges to an approximate solution in polynomial steps with linear rate. Second, we show linear convergence of subgradient method to the target solution, which solves Phase-2 LP rounding problem.

Our analysis leverages on the geometric properties of the optimization landscape showed in Appendix C. Namely, our following proofs are based on the results in Proposition C.1, Proposition C.2, and Proposition C.3 (i.e., (29), (30), (32), and (33)) holding for the rest of this section.

D.1 Proof of linear convergence for vanilla RGD

First, assuming the geometric properties in Appendix C hold, we show that starting from a random initialization, optimizing

$$\min_{\mathbf{q}} f(\mathbf{q}) = \frac{1}{np} \sum_{i=1}^p H_{\mu}(C_{x_i} R \mathbf{Q}^{-1} \mathbf{q}), \quad \text{s.t. } \mathbf{q} \in \mathbb{S}^{n-1} \quad (34)$$

via vanilla RGD in (13)

$$\mathbf{q}^{(k+1)} = \mathcal{P}_{\mathbb{S}^{n-1}} \left(\mathbf{q}^{(k)} - \tau \cdot \text{grad } f(\mathbf{q}^{(k)}) \right)$$

recovers an approximate solution with linear rate.

Theorem D.1 (Linear convergence of RGD) *Given an initialization $\mathbf{q}^{(0)} \sim \mathcal{U}(\mathbb{S}^{n-1})$ uniform random drawn from the sphere, choose a stepsize*

$$\tau = c \min \left\{ \frac{1}{n^{5/2}}, \frac{\mu}{n} \right\},$$

then the vanilla gradient descent method for (5) produces a solution

$$\left\| \mathbf{q}^{(k)} - \mathbf{e}_i \right\| \leq 2\mu$$

for some $i \in [n]$, whenever

$$k \geq K := \frac{C}{\theta} \max \left\{ n^4, \frac{n^{5/2}}{\mu} \right\} \log \left(\frac{1}{\mu} \right).$$

Proof [Proof of Theorem D.1]

Initialization and iterate stays within the region. First, from Lemma D.3, we know that when $\xi = \frac{1}{5 \log n}$, with probability at least $1/2$, our random initialization $\mathbf{q}^{(0)}$ falls into one of the sets $\{\mathcal{S}_\xi^{1+}, \mathcal{S}_\xi^{1-}, \dots, \mathcal{S}_\xi^{n+}, \mathcal{S}_\xi^{n-}\}$. Without loss of generality, we assume that $\mathbf{q}^{(0)} \in \mathcal{S}_\xi^{n+}$.

Once $\mathbf{q}^{(0)}$ initialized within the region \mathcal{S}_ξ^{n+} , from Lemma D.4, whenever the stepsize $\tau \leq c_0/\sqrt{n}$, we know that our gradient descent stays within the region \mathcal{S}_ξ^{n+} when the stepsize $\tau \leq c_1/\sqrt{n}$ for some $c_1 > 0$. Based on this, to complete the proof, we now proceed by proving the following results.

Linear convergence until reaching $\|\mathbf{q} - \mathbf{e}_n\| \leq \mu$. From Proposition C.1, there exists some numerical constant $\gamma \in (\mu, 1)$, such that the regularity condition

$$\langle \text{grad } f(\mathbf{q}), q_n \mathbf{q} - \mathbf{e}_n \rangle \geq \underbrace{c_2 \theta (1 - \theta) n^{-3/2}}_{\alpha_1} \cdot \|\mathbf{q} - \mathbf{e}_n\|, \quad \sqrt{1 - q_n^2} \in \left[\gamma, \sqrt{\frac{n-1}{n}} \right], \quad (35)$$

$$\langle \text{grad } f(\mathbf{q}), q_n \mathbf{q} - \mathbf{e}_n \rangle \geq \underbrace{c'_2 \theta (1 - \theta)}_{\alpha_2} \cdot \|\mathbf{q} - \mathbf{e}_n\|, \quad \sqrt{1 - q_n^2} \in [\mu, \gamma], \quad (36)$$

holds w.h.p. for all $\mathbf{q} \in \mathcal{S}_\xi^{n+}$. As $\alpha_2 \geq \alpha_1$, the regularity condition holds for all \mathbf{q} with $\alpha = \alpha_1$. Select a stepsize τ such that $\tau \leq \gamma \frac{\alpha_1}{2\sqrt{2\theta n}}$. By Lemma D.5 and the regularity condition (35), we have

$$\left\| \mathbf{q}^{(k)} - \mathbf{e}_n \right\|^2 - \frac{\gamma^2}{2} \leq (1 - \tau \alpha_1)^k \left[\left\| \mathbf{q}^{(0)} - \mathbf{e}_n \right\|^2 - \frac{\gamma^2}{2} \right] \leq 2(1 - \tau \alpha_1)^k,$$

where the last inequality utilizes the fact that $\|\mathbf{q}^{(0)} - \mathbf{e}_n\|^2 \leq 2$. This further implies that

$$1 - q_n^2 \leq \left\| \mathbf{q}^{(k)} - \mathbf{e}_n \right\|^2 \leq \frac{\gamma^2}{2} + 2(1 - \tau \alpha_1)^k \leq \gamma^2,$$

when

$$2(1 - \tau \alpha_1)^k \leq \frac{\gamma^2}{2} \implies k \geq K_1 := \frac{\log(\gamma^2/4)}{\log(1 - \tau \alpha_1)}.$$

This implies that $\sqrt{1 - q_n^2} \leq \gamma$ for $\forall k \geq K_1$. Thus, from (36), we know that the regularity condition holds with $\alpha = \alpha_2$. Choose stepsize $\tau \leq \frac{\mu \alpha_2}{2\sqrt{2\theta n}}$, apply Lemma D.5 again with $\alpha = \alpha_2$, for all $k \geq 1$, we have

$$\left\| \mathbf{q}^{(K_1+k)} - \mathbf{e}_n \right\|^2 - \frac{\mu^2}{2} \leq (1 - \tau \alpha_2)^k \left(\left\| \mathbf{q}^{(0)} - \mathbf{e}_n \right\|^2 - \frac{\mu^2}{2} \right) \leq (\gamma^2 - \mu^2)(1 - \tau \alpha_2)^k.$$

This further implies that

$$\left\| \mathbf{q}^{(K_1+k)} - \mathbf{e}_n \right\|^2 \leq \frac{\mu^2}{2} + \left(\gamma^2 - \frac{\mu^2}{2} \right) (1 - \tau \alpha_2)^k \leq \mu^2$$

whenever

$$\left(\gamma^2 - \frac{\mu^2}{2} \right) (1 - \tau \alpha_2)^k \leq \frac{\mu^2}{2} \implies k \geq K_2 := \frac{\log(\mu^2 / (2\gamma^2 - \mu^2))}{\log(1 - \tau \alpha_2)}.$$

Therefore, combining the results above, by using the fact that $\alpha_1 = c_2 \theta (1 - \theta) n^{-3/2}$ and $\alpha_2 = c'_2 \theta (1 - \theta)$, we have $\|\mathbf{q}^{(k)} - \mathbf{e}_n\| \leq \mu$ whenever

$$\tau \leq \min \left\{ \frac{\gamma \alpha_1}{2\sqrt{2\theta n}}, \frac{\mu \alpha_2}{2\sqrt{2\theta n}} \right\} = C \min \left\{ \frac{1}{n^{5/2}}, \frac{\mu}{n} \right\}$$

and $k \geq K := K_1 + K_2$ with

$$\begin{aligned} K &= \frac{\log(4/\gamma^2)}{\log((1-\tau\alpha_1)^{-1})} + \frac{\log((2\gamma^2 - \mu^2)/\mu^2)}{\log((1-\tau\alpha_2)^{-1})} \\ &\leq \frac{c_3}{\tau\alpha_1} + \frac{c_4}{\tau\alpha_2} \log\left(\frac{1}{\mu}\right) \leq \frac{c_5}{\theta} \max\left\{n^4, \frac{n^{5/2}}{\mu}\right\} \log\left(\frac{1}{\mu}\right), \end{aligned}$$

where we used the fact that $\log^{-1}((1-x)^{-1}) \leq 2/x$ for small x .

No jump away from an approximate solution e_n . Finally, we show that once our iterate reaches the region

$$\mathcal{S} := \{\mathbf{q} \in \mathbb{S}^{n-1} \mid \|\mathbf{q} - \mathbf{e}_n\| \leq 2\mu\},$$

it will stay within the region \mathcal{S} , such that our final iterates will always stay close to an approximate solution e_n . Towards this end, suppose $\mathbf{q}^{(k)} \in \mathcal{S}$. Therefore two possibilities: (i) $\mu \leq \|\mathbf{q}^{(k)} - \mathbf{e}_n\| \leq 2\mu$ (ii) $\|\mathbf{q}^{(k)} - \mathbf{e}_n\| \leq \mu$. If the case (i) holds, then our argument above implies that $\|\mathbf{q}^{(k+1)} - \mathbf{e}_n\| \leq \|\mathbf{q}^{(k)} - \mathbf{e}_n\| \leq 2\mu$. Otherwise $\|\mathbf{q}^{(k)} - \mathbf{e}_n\| \leq \mu$, for which we have

$$\begin{aligned} \|\mathbf{q}^{(k+1)} - \mathbf{e}_n\| &\leq \|\mathbf{q}^{(k)} - \tau \operatorname{grad} f(\mathbf{q}) - \mathbf{e}_n\| \\ &\leq \|\mathbf{q}^{(k)} - \mathbf{e}_n\| + \tau \|\operatorname{grad} f(\mathbf{q})\| \leq \mu + 2\tau\sqrt{\theta n} \leq 2\mu, \end{aligned}$$

where we used the fact that $\tau \leq \frac{\mu}{\sqrt{\theta n}}$. Thus, by induction, we have $\mathbf{q}^{(k')} \in \mathcal{S}$ for all future iterates $k' = k+1, k+2, \dots$. This completes the proof. \blacksquare

Lemma D.2 For any $\mathbf{q} \in \mathcal{S}_\xi^{n+}$, we have

$$1 - q_n^2 \leq \|\mathbf{q} - \mathbf{e}_n\|^2 \leq 2(1 - q_n^2) \leq 2.$$

Proof We have

$$1 - q_n^2 \leq \|\mathbf{q} - \mathbf{e}_n\|^2 = \|\mathbf{q}_{-n}\|^2 + (1 - q_n)^2 \|\mathbf{e}_n\|^2 = 2(1 - q_n) = 2\frac{1 - q_n^2}{1 + q_n} \leq 2(1 - q_n^2)$$

as desired. \blacksquare

Lemma D.3 (Random initialization falls into good region) Let $\mathbf{q}^{(0)} \sim \mathcal{U}(\mathbb{S}^{n-1})$ be uniformly random generated from the unit sphere \mathbb{S}^{n-1} . When $\xi = \frac{1}{5 \log n}$, then with probability at least $1/2$, $\mathbf{q}^{(0)}$ belongs to one of the $2n$ sets $\{\mathcal{S}_\xi^{1+}, \mathcal{S}_\xi^{1-}, \dots, \mathcal{S}_\xi^{n+}, \mathcal{S}_\xi^{n-}\}$. The set $\mathbf{q}^{(0)}$ belongs to is uniformly at random.

Proof We refer the readers to Lemma 3.9 of [BJS18] and Theorem 1 of [GBW18] for detailed proofs. \blacksquare

Lemma D.4 (Stay within the region \mathcal{S}_ξ^{n+}) Suppose $\mathbf{q}^{(0)} \in \mathcal{S}_\xi^{n+}$ with $\xi \leq 1$. There exists some constant $c > 0$, such that when the stepsize satisfies $\tau \leq \frac{c}{\sqrt{n}}$, our Riemannian gradient iterate $\mathbf{q}^{(k)} = \mathcal{P}_{\mathbb{S}^{n-1}}(\mathbf{q}^{(k-1)} - \tau \cdot \operatorname{grad} f(\mathbf{q}^{(k-1)}))$ satisfies $\mathbf{q}^{(k)} \in \mathcal{S}_\xi^{n+}$ for all $k \geq 1$.

Proof We prove this by induction. For any $k \geq 1$, suppose $\mathbf{q}^{(k)} \in \mathcal{S}_\xi^{n+}$. For convenience, let $\mathbf{g}^{(k)} = \operatorname{grad} f(\mathbf{q}^{(k)})$. Then, for any $j \neq k$, we have

$$\left(\frac{q_n^{(k+1)}}{q_j^{(k+1)}}\right)^2 = \left(\frac{q_n^{(k)} - \tau g_n^{(k)}}{q_j^{(k)} - \tau g_j^{(k)}}\right)^2.$$

We proceed by considering the following two cases.

Case (i): $\left|q_n^{(k)}/q_j^{(k)}\right| \geq \sqrt{3}$. In this case, we have

$$\left(\frac{q_n^{(k+1)}}{q_j^{(k+1)}}\right)^2 = \left(\frac{q_n^{(k)} - \tau g_n^{(k)}}{q_j^{(k)} - \tau g_j^{(k)}}\right)^2 \geq \left(\frac{1 - \tau \cdot g_n^{(k)}/q_n^{(k)}}{q_j^{(k)}/q_n^{(k)} - \tau g_j^{(k)}/q_n^{(k)}}\right)^2 \geq \left(\frac{1 - 2\tau\sqrt{n}}{1/\sqrt{3} + 2\tau\sqrt{n}}\right)^2 \geq 2,$$

where the second inequality utilizes (32) and the fact $q_n^{(k)} \geq \frac{1}{\sqrt{n}}$, and the last inequality follows when $\tau \leq \frac{\sqrt{3}-\sqrt{2}}{2(\sqrt{6}+\sqrt{3})} \frac{1}{\sqrt{n}}$.

Case (ii): $\left|q_n^{(k)}/q_j^{(k)}\right| \leq \sqrt{3}$. Proposition C.1 and Proposition C.2 implies that

$$\frac{g_j^{(k)}}{q_j^{(k)}} \geq 0, \quad \frac{g_j^{(k)}}{q_j^{(k)}} - \frac{g_n^{(k)}}{q_n^{(k)}} \geq 0. \quad (37)$$

By noting that $\left|q_j^{(k)}\right| \geq \left|q_n^{(k)}\right|/\sqrt{3} \geq 1/\sqrt{3n}$ and $\left|g_j^{(k)}\right| \leq 2$, we have

$$\tau \leq \frac{1}{2\sqrt{3n}} \leq \frac{q_j^{(k)}}{g_j^{(k)}} \implies \tau \cdot \frac{g_j^{(k)}}{q_j^{(k)}} \leq 1. \quad (38)$$

Thus, we have

$$\begin{aligned} \left(\frac{q_n^{(k+1)}}{q_j^{(k+1)}}\right)^2 &= \left(\frac{q_n^{(k)}}{q_j^{(k)}}\right)^2 \left(1 + \tau \cdot \frac{g_j^{(k)}/q_j^{(k)} - g_n^{(k)}/q_n^{(k)}}{1 - \tau g_j^{(k)}/q_j^{(k)}}\right)^2 \\ &\geq \left(\frac{q_n^{(k)}}{q_j^{(k)}}\right)^2 \left(1 + \tau \cdot \left(\frac{g_j^{(k)}}{q_j^{(k)}} - \frac{g_n^{(k)}}{q_n^{(k)}}\right)\right)^2 \geq \left(\frac{q_n^{(k)}}{q_j^{(k)}}\right)^2 \left(1 + \tau \cdot \frac{\theta(1-\theta)}{4n} \frac{\xi}{1+\xi}\right)^2. \end{aligned}$$

The first inequality follows from (37) and (38), and the second inequality directly follows from Proposition C.2. Therefore, when $\xi \leq 1$, this implies that $\mathbf{q}^{(k+1)} \in \mathcal{S}_\xi^{n+}$. By induction, this holds for all $k \geq 1$. ■

In the following, we show that the iterates get closer to \mathbf{e}_n .

Lemma D.5 (Iterate contraction) For any $\mathbf{q} \in \mathcal{S}_\xi^{n+}$, assuming the following regularity condition

$$\langle \text{grad } f(\mathbf{q}), q_i \mathbf{q} - \mathbf{e}_n \rangle \geq \alpha \|\mathbf{q} - \mathbf{e}_n\| \quad (39)$$

holds for a parameter $\alpha > 0$. Then if $\mathbf{q}^{(k)} \in \mathcal{S}_\xi^{n+}$ and the stepsize $\tau \leq c \frac{\alpha}{\theta n}$, the iterate $\mathbf{q}^{(k+1)} = \mathcal{P}_{\mathbb{S}^{n-1}}(\mathbf{q} - \tau \cdot \text{grad } f(\mathbf{q}))$ satisfies

$$\left\|\mathbf{q}^{(k+1)} - \mathbf{e}_n\right\|^2 - \left(\frac{2\tau\theta n}{\alpha}\right)^2 \leq (1 - \tau\alpha) \left[\left\|\mathbf{q}^{(k)} - \mathbf{e}_n\right\|^2 - \left(\frac{2\tau\theta n}{\alpha}\right)^2 \right].$$

Proof First, note that

$$\begin{aligned} \left\|\mathbf{q}^{(k+1)} - \mathbf{e}_n\right\|^2 &= \left\|\mathcal{P}_{\mathbb{S}^{n-1}}\left(\mathbf{q}^{(k)} - \tau \cdot \text{grad } f(\mathbf{q}^{(k)})\right) - \mathcal{P}_{\mathbb{S}^{n-1}}(\mathbf{e}_n)\right\|^2 \\ &\leq \left\|\mathbf{q}^{(k)} - \tau \cdot \text{grad } f(\mathbf{q}^{(k)}) - \mathbf{e}_n\right\|^2 \\ &= \left\|\mathbf{q}^{(k)} - \mathbf{e}_n\right\|^2 - 2\tau \cdot \langle \text{grad } f(\mathbf{q}^{(k)}), \mathbf{q}^{(k)} - \mathbf{e}_n \rangle + \tau^2 \left\|\text{grad } f(\mathbf{q}^{(k)})\right\|^2 \\ &\leq \left\|\mathbf{q}^{(k)} - \mathbf{e}_n\right\|^2 - 2\tau\alpha \left\|\mathbf{q}^{(k)} - \mathbf{e}_n\right\| + 4\tau^2\theta n, \end{aligned}$$

where the first inequality utilizes the fact that $\mathcal{P}_{\mathbb{S}^{n-1}}(\cdot)$ is 1-Lipschitz continuous, and the last line follows from (39) and (33) in Proposition C.3. We now subtract both sides by $\left(\frac{2\tau\theta n}{\alpha}\right)^2$,

$$\begin{aligned} \left\| \mathbf{q}^{(k+1)} - \mathbf{e}_n \right\|^2 - \left(\frac{2\tau\theta n}{\alpha} \right)^2 &\leq \left\| \mathbf{q}^{(k)} - \mathbf{e}_n \right\|^2 - \left(\frac{2\tau\theta n}{\alpha} \right)^2 - 2\tau\alpha \left(\left\| \mathbf{q}^{(k)} - \mathbf{e}_n \right\| - \frac{2\tau\theta n}{\alpha} \right) \\ &= \left[1 - 2\tau\alpha \left(\left\| \mathbf{q}^{(k)} - \mathbf{e}_n \right\| + \frac{2\tau\theta n}{\alpha} \right)^{-1} \right] \left[\left\| \mathbf{q}^{(k)} - \mathbf{e}_n \right\|^2 - \left(\frac{2\tau\theta n}{\alpha} \right)^2 \right] \\ &\leq (1 - \tau\alpha) \left[\left\| \mathbf{q}^{(k)} - \mathbf{e}_n \right\|^2 - \left(\frac{2\tau\theta n}{\alpha} \right)^2 \right], \end{aligned}$$

where the last inequality follows because

$$\left\| \mathbf{q}^{(k)} - \mathbf{e}_n \right\|^2 \leq 2, \quad \tau \leq \left(1 - \frac{1}{\sqrt{2}} \right) \frac{\alpha}{\theta n},$$

such that

$$\left\| \mathbf{q} - \mathbf{e}_n \right\| + \frac{2\tau\theta n}{\alpha} \leq 2.$$

This completes the proof. ■

D.2 Proof of exact recovery via LP rounding

To obtain exact solutions, we use the approximate solution \mathbf{q}_\star from Phase-1 gradient descent method as a warm start $\mathbf{r} = \mathbf{q}_\star$, and consider solving a *convex* Phase-2 LP rounding problem introduced in (14)

$$\min_{\mathbf{q}} \zeta(\mathbf{q}) := \frac{1}{np} \sum_{i=1}^p \left\| \mathbf{C}_{\mathbf{x}_i} \mathbf{R} \mathbf{Q}^{-1} \mathbf{q} \right\|_1, \quad \text{s.t.} \quad \langle \mathbf{r}, \mathbf{q} \rangle = 1.$$

In the following, we show the function is sharp around [BF93, LZSL19] the target solution, so that projected subgradient descent methods converge linearly to the truth with geometrically decreasing stepsizes.

D.2.1 Sharpness of the objective function.

Proposition D.6 Suppose $\theta \in \left(\frac{1}{n}, \frac{1}{3} \right)$ and \mathbf{r} satisfies

$$\frac{\left\| \mathbf{r}_{-n} \right\|}{r_n} \leq \frac{1}{20}. \quad (40)$$

Whenever $p \geq C \frac{\kappa^8}{\theta \sigma_{\min}^2(\mathbf{C}_a)} \log^3 n$, with probability at least $1 - p^{-c_1 n \theta} - n^{-c_2}$, the function $\zeta(\mathbf{q})$ is sharp in a sense that

$$\zeta(\mathbf{q}) - \zeta \left((\mathbf{R} \mathbf{Q}^{-1})^{-1} \frac{\mathbf{e}_n}{\tilde{r}_n} \right) \geq \frac{1}{50} \sqrt{\frac{2}{\pi}} \theta \left\| \mathbf{q} - (\mathbf{R} \mathbf{Q}^{-1})^{-1} \frac{\mathbf{e}_n}{\tilde{r}_n} \right\| \quad (41)$$

for any feasible \mathbf{q} with $\langle \mathbf{r}, \mathbf{q} \rangle = 1$. Here, $\tilde{\mathbf{r}} = (\mathbf{R} \mathbf{Q}^{-1})^{-\top} \mathbf{r}$.

Proof Let us denote $\tilde{\mathbf{q}} = \mathbf{R} \mathbf{Q}^{-1} \mathbf{q}$. Then we can rewrite our original problem as

$$\min_{\tilde{\mathbf{q}}} \tilde{\zeta}(\tilde{\mathbf{q}}) = \frac{1}{np} \sum_{i=1}^p \left\| \mathbf{C}_{\mathbf{x}_i} \tilde{\mathbf{q}} \right\|_1 \quad \text{s.t.} \quad \langle \tilde{\mathbf{r}}, \tilde{\mathbf{q}} \rangle = 1,$$

which is reduced to the orthogonal problem in (42) of Lemma D.7. To utilize the result in Lemma D.7, we first prove that $\tilde{\mathbf{r}}$ satisfies (43) if \mathbf{r} satisfies (40). Towards that end, note that

$$\tilde{\mathbf{r}} = (\mathbf{R}\mathbf{Q}^{-1})^{-\top} \mathbf{r} = \mathbf{r} + \left((\mathbf{R}\mathbf{Q}^{-1})^{-\top} - \mathbf{I} \right) \mathbf{r}.$$

By Lemma H.4, we know that, for any $\delta \in (0, 1)$, whenever $p \geq C \frac{\kappa^8}{\theta \delta^2 \sigma_{\min}^2(\mathbf{C}_a)} \log^3 n$,

$$\left\| \left((\mathbf{R}\mathbf{Q}^{-1})^{-\top} - \mathbf{I} \right) \mathbf{r} \right\| \leq \left\| (\mathbf{R}\mathbf{Q}^{-1})^{-1} - \mathbf{I} \right\| \|\mathbf{r}\| \leq 2\delta \|\mathbf{r}\|$$

holds with probability at least $1 - p^{-c_1 n \theta} - n^{-c_2}$. This further implies that

$$\tilde{r}_n \geq r_n - 2\delta \|\mathbf{r}\|, \quad \|\tilde{\mathbf{r}}_{-n}\| \leq \|\mathbf{r}_{-n}\| + 2\delta \|\mathbf{r}\|.$$

Therefore, by choose δ sufficiently small, we have

$$\frac{\|\tilde{\mathbf{r}}_{-n}\|}{\tilde{r}_n} \leq \frac{\|\mathbf{r}_{-n}\| + 2\delta \|\mathbf{r}\|}{r_n - 2\delta \|\mathbf{r}\|} = \frac{\|\mathbf{r}_{-n}\|/r_n + 2\delta \sqrt{1 + (\|\mathbf{r}_{-n}\|/r_n)^2}}{1 - 2\delta \sqrt{1 + (\|\mathbf{r}_{-n}\|/r_n)^2}} \leq \frac{1}{10},$$

where the last inequality follows from (40). Therefore, by Lemma D.7, we obtain

$$\begin{aligned} \zeta(\mathbf{q}) - \zeta\left((\mathbf{R}\mathbf{Q}^{-1})^{-1} \frac{\mathbf{e}_n}{\tilde{r}_n}\right) &= \tilde{\zeta}(\mathbf{q}) - \tilde{\zeta}\left(\frac{\mathbf{e}_n}{\tilde{r}_n}\right) \\ &\geq \frac{1}{25} \sqrt{\frac{2}{\pi}} \theta \left\| \tilde{\mathbf{q}} - \frac{\mathbf{e}_n}{\tilde{r}_n} \right\| \\ &= \frac{1}{25} \sqrt{\frac{2}{\pi}} \theta \left\| (\mathbf{R}\mathbf{Q}^{-1}) \cdot \left(\mathbf{q} - (\mathbf{R}\mathbf{Q}^{-1})^{-1} \frac{\mathbf{e}_n}{\tilde{r}_n} \right) \right\| \\ &\geq \frac{1}{25} \sqrt{\frac{2}{\pi}} \theta \cdot \sigma_{\min}(\mathbf{R}\mathbf{Q}^{-1}) \cdot \left\| \mathbf{q} - (\mathbf{R}\mathbf{Q}^{-1})^{-1} \frac{\mathbf{e}_n}{\tilde{r}_n} \right\| \end{aligned}$$

By Lemma H.4, we know that $\left\| (\mathbf{R}\mathbf{Q}^{-1})^{-1} \right\| \leq 1 + 2\delta$, so that

$$\sigma_{\min}(\mathbf{R}\mathbf{Q}^{-1}) = \left\| (\mathbf{R}\mathbf{Q}^{-1})^{-1} \right\|^{-1} \geq \frac{1}{1 + 2\delta}.$$

Thus, this further implies that

$$\zeta(\mathbf{q}) - \zeta\left((\mathbf{R}\mathbf{Q}^{-1})^{-1} \frac{\mathbf{e}_n}{\tilde{r}_n}\right) \geq \frac{1}{25} \sqrt{\frac{2}{\pi}} \frac{\theta}{1 + 2\delta} \cdot \left\| \mathbf{q} - (\mathbf{R}\mathbf{Q}^{-1})^{-1} \frac{\mathbf{e}_n}{\tilde{r}_n} \right\|,$$

as desired. ■

Lemma D.7 (Sharpness for the orthogonal case) *Consider the following problem*

$$\min_{\mathbf{q}} \tilde{\zeta}(\mathbf{q}) := \frac{1}{np} \sum_{i=1}^p \|C_{\mathbf{x}_i} \mathbf{q}\|_1 \quad \text{s.t.} \quad \langle \mathbf{r}, \mathbf{q} \rangle = 1, \quad (42)$$

with $\mathbf{r} \in \mathbb{S}^{n-1}$ satisfying

$$\frac{\|\mathbf{r}_{-n}\|}{r_n} \leq \frac{1}{10}, \quad r_n > 0. \quad (43)$$

Whenever $p \geq \frac{C}{\theta^2} n \log\left(\frac{n}{\theta}\right)$, with probability at least $1 - c_1 n p^{-6} - c_2 n e^{-c_3 \theta^2 p}$, the function $\tilde{\zeta}(\mathbf{q})$ is sharp in a sense that

$$\tilde{\zeta}(\mathbf{q}) - \tilde{\zeta}\left(\frac{\mathbf{e}_n}{r_n}\right) \geq \frac{1}{25} \sqrt{\frac{2}{\pi}} \theta \left\| \mathbf{q} - \frac{\mathbf{e}_n}{r_n} \right\|$$

for any feasible \mathbf{q} with $\langle \mathbf{r}, \mathbf{q} \rangle = 1$.

Proof Observing that $\langle \mathbf{r}, \mathbf{q} \rangle = \mathbf{r}_{-n}^\top \mathbf{q}_{-n} + r_n q_n = 1$, we have

$$\|\mathbf{r}_{-n}\| \|\mathbf{q}_{-n}\| \geq \mathbf{r}_{-n}^\top \mathbf{q}_{-n} = r_n \left(\frac{1}{r_n} - q_n \right) \geq r_n \left(\frac{1}{r_n} - |q_n| \right).$$

This further implies that

$$\frac{1}{r_n} - |q_n| \leq \frac{\|\mathbf{r}_{-n}\|}{r_n} \|\mathbf{q}_{-n}\|. \quad (44)$$

Second, we have

$$\left\| \mathbf{q} - \frac{\mathbf{e}_n}{r_n} \right\| = \sqrt{\left(\frac{1}{r_n} - q_n \right)^2 + \|\mathbf{q}_{-n}\|^2} \leq \sqrt{1 + \left(\frac{\|\mathbf{r}_{-n}\|}{r_n} \right)^2} \|\mathbf{q}_{-n}\|,$$

which implies that

$$\left(1 + \left(\frac{\|\mathbf{r}_{-n}\|}{r_n} \right)^2 \right)^{-1/2} \left\| \mathbf{q} - \frac{\mathbf{e}_n}{r_n} \right\| \leq \|\mathbf{q}_{-n}\|. \quad (45)$$

We now proceed by considering the following two cases.

Case i: $|q_n| \geq \frac{1}{r_n}$. In this case, we have

$$\begin{aligned} \tilde{\zeta}(\mathbf{q}) - \tilde{\zeta}\left(\frac{\mathbf{e}_n}{r_n}\right) &\geq \frac{1}{6} \sqrt{\frac{2}{\pi}} \theta \|\mathbf{q}_{-n}\| \geq \frac{1}{6} \sqrt{\frac{2}{\pi}} \theta \left(1 + \left(\frac{\|\mathbf{r}_{-n}\|}{r_n} \right)^2 \right)^{-1/2} \left\| \mathbf{q} - \frac{\mathbf{e}_n}{r_n} \right\| \\ &\geq \frac{5}{33} \sqrt{\frac{2}{\pi}} \theta \left\| \mathbf{q} - \frac{\mathbf{e}_n}{r_n} \right\|, \end{aligned}$$

where the first inequality follows by (46), the second inequality follows by (45), and the last inequality follows because $\frac{\|\mathbf{r}_{-n}\|}{r_n} \leq \frac{1}{10}$.

Case ii: $|q_n| \leq \frac{1}{r_n}$. In this case, we have

$$\begin{aligned} \tilde{\zeta}(\mathbf{q}) - \tilde{\zeta}\left(\frac{\mathbf{e}_n}{r_n}\right) &\geq \frac{1}{6} \sqrt{\frac{2}{\pi}} \theta \|\mathbf{q}_{-n}\| - \frac{5}{4} \sqrt{\frac{2}{\pi}} \theta \left(\frac{1}{r_n} - |q_n| \right) \\ &\geq \theta \left(\frac{1}{6} \sqrt{\frac{2}{\pi}} - \frac{5}{4} \sqrt{\frac{2}{\pi}} \frac{\|\mathbf{r}_{-n}\|}{r_n} \right) \|\mathbf{q}_{-n}\| \\ &\geq \theta \left(\frac{1}{6} \sqrt{\frac{2}{\pi}} - \frac{5}{4} \sqrt{\frac{2}{\pi}} \frac{\|\mathbf{r}_{-n}\|}{r_n} \right) \left(1 + \left(\frac{\|\mathbf{r}_{-n}\|}{r_n} \right)^2 \right)^{-1/2} \left\| \mathbf{q} - \frac{\mathbf{e}_n}{r_n} \right\| \\ &\geq \frac{\theta}{25} \sqrt{\frac{2}{\pi}} \left\| \mathbf{q} - \frac{\mathbf{e}_n}{r_n} \right\|, \end{aligned}$$

where the first inequality follows by (46), the second inequality follows from (44), the third inequality follows from (45), and the last one follows because $\frac{\|\mathbf{r}_{-n}\|}{r_n} \leq \frac{1}{10}$.

Combining the results in both cases, we obtain the desired result. \blacksquare

Lemma D.8 Suppose $\theta \in (\frac{1}{n}, \frac{1}{3})$. Whenever $p \geq \frac{C}{\theta^2} n \log(\frac{n}{\theta})$, we have

$$\tilde{\zeta}(\mathbf{q}) - \tilde{\zeta}\left(\frac{\mathbf{e}_n}{r_n}\right) \geq \begin{cases} \frac{1}{6}\sqrt{\frac{2}{\pi}}\theta \|\mathbf{q}_{-n}\|, & \text{if } |q_n| - \frac{1}{r_n} \geq 0, \\ \frac{1}{6}\sqrt{\frac{2}{\pi}}\theta \|\bar{\mathbf{q}}\| - \frac{5}{4}\sqrt{\frac{2}{\pi}}\theta \left(\frac{1}{r_n} - |q_n|\right), & \text{if } |q_n| - \frac{1}{r_n} < 0, \end{cases} \quad (46)$$

holds with probability at least $1 - c_1 np^{-6} - c_2 ne^{-c_3 \theta^2 p}$.

Proof For each $j \in [n]$, let us define an index set $\mathcal{I}_j := \{i \in [p] : (s_j[\tilde{\mathbf{x}}_i])_n \neq 0\}$, and let us define events

$$\mathcal{E} := \bigcap_{j=0}^{n-1} \mathcal{E}_j, \quad \mathcal{E}_j := \left\{ |\mathcal{I}_j| \leq \frac{9}{8}\theta p \right\}, \quad (0 \leq j \leq n-1).$$

By Hoeffding's inequality and a union bound, we know that

$$\mathbb{P}(\mathcal{E}^c) \leq \sum_{j=0}^{n-1} \mathbb{P}(\mathcal{E}_j^c) \leq n \exp(-p\theta^2/2).$$

Based on this, we have

$$\begin{aligned} & \tilde{\zeta}(\mathbf{q}) - \tilde{\zeta}\left(\frac{\mathbf{e}_n}{r_n}\right) \\ &= \frac{1}{np} \sum_{i=1}^p \|\mathbf{C}_{\mathbf{x}_i} \mathbf{q}\|_1 - \frac{1}{np} \frac{1}{r_n} \sum_{i=1}^p \|\mathbf{x}_i\|_1 \\ &= \frac{1}{np} \sum_{i=1}^p \sum_{j=0}^{n-1} |\langle s_j[\tilde{\mathbf{x}}_i], \mathbf{q} \rangle| - \frac{1}{np} \frac{1}{r_n} \sum_{i=1}^p \|\mathbf{x}_i\|_1 \\ &\geq \frac{1}{np} \left(|q_n| - \frac{1}{r_n} \right) \sum_{i=1}^p \|\mathbf{x}_i\|_1 + \frac{1}{np} \sum_{j=0}^{n-1} \left(\sum_{i \in \mathcal{I}_j^c} |\langle (s_j[\tilde{\mathbf{x}}_i])_{-n}, \mathbf{q}_{-n} \rangle| - \sum_{i \in \mathcal{I}_j} |\langle (s_j[\tilde{\mathbf{x}}_i])_{-n}, \mathbf{q}_{-n} \rangle| \right) \\ &= \frac{1}{np} \left(|q_n| - \frac{1}{r_n} \right) \sum_{i=1}^p \|\mathbf{x}_i\|_1 + \frac{1}{np} \sum_{j=0}^{n-1} \left(\|\mathbf{q}_{-n}^\top \mathbf{M}_{\mathcal{I}_j^c}^j\|_1 - \|\mathbf{q}_{-n}^\top \mathbf{M}_{\mathcal{I}_j}^j\|_1 \right), \end{aligned}$$

where we denote $\mathbf{M}^j = [(s_j[\tilde{\mathbf{x}}_1])_{-n} \quad (s_j[\tilde{\mathbf{x}}_2])_{-n} \quad \cdots \quad (s_j[\tilde{\mathbf{x}}_p])_{-n}]$, and $\mathbf{M}_{\mathcal{I}}^j$ denote a submatrix of \mathbf{M}^j with columns indexed by \mathcal{I} . Conditioned on the event \mathcal{E} , by Lemma B.5 and a union bound, whenever $p \geq \frac{C}{\theta^2} n \log(\frac{n}{\theta})$, we have

$$\|\mathbf{q}_{-n}^\top \mathbf{M}_{\mathcal{I}_j^c}^j\|_1 - \|\mathbf{q}_{-n}^\top \mathbf{M}_{\mathcal{I}_j}^j\|_1 \geq \frac{p}{6} \sqrt{\frac{2}{\pi}} \theta \|\mathbf{q}_{-n}\|, \quad \forall \mathbf{q}_{-n} \in \mathbb{R}^{n-1}, \quad (0 \leq j \leq n-1)$$

with probability at least $1 - cnp^{-6}$. On the other hand, by Gaussian concentration inequality, we have

$$\mathbb{P}\left(\frac{1}{np} \sum_{i=1}^p \|\mathbf{x}_i\|_1 \geq \frac{5}{4} \sqrt{\frac{2}{\pi}} \theta\right) \leq \exp\left(-\frac{\theta^2 p}{64\pi}\right).$$

Therefore, combining all the results above, we have

$$\tilde{\zeta}(\mathbf{q}) - \tilde{\zeta}\left(\frac{\mathbf{e}_n}{r_n}\right) \geq \begin{cases} \frac{1}{6}\sqrt{\frac{2}{\pi}}\theta \|\mathbf{q}_{-n}\|, & \text{if } |q_n| - \frac{1}{r_n} \geq 0, \\ \frac{1}{6}\sqrt{\frac{2}{\pi}}\theta \|\tilde{\mathbf{q}}\| - \frac{5}{4}\sqrt{\frac{2}{\pi}}\theta \left(\frac{1}{r_n} - |q_n|\right), & \text{if } |q_n| - \frac{1}{r_n} < 0, \end{cases}$$

as desired. ■

D.3 Linear convergence for projection subgradient descent for rounding

Now based on the sharpness condition, we are ready to show that the projected subgradient descent method

$$\mathbf{q}^{(k+1)} = \mathbf{q}^{(k)} - \tau^{(k)} \mathcal{P}_{\mathbf{r}^\perp} \mathbf{g}^{(k)}, \quad \mathbf{g}^{(k)} = \sum_{i=1}^p (\mathbf{R}\mathbf{Q}^{-1})^\top \mathbf{C}_{\mathbf{x}_i}^\top \text{sign}\left(\mathbf{C}_{\mathbf{x}_i} \mathbf{R}\mathbf{Q}^{-1} \mathbf{q}^{(k)}\right).$$

on $\zeta(\mathbf{q})$ converges linearly to the target solution up to a scaling factor. For convenience, let us first define the distance between the iterate and the target solution

$$d^{(k)} := \|\mathbf{s}^{(k)}\|, \quad \mathbf{s}^{(k)} := \mathbf{q}^{(k)} - (\mathbf{R}\mathbf{Q}^{-1})^{-1} \frac{\mathbf{e}_n}{\tilde{r}_n},$$

and several parameters

$$\alpha := \frac{1}{50}\sqrt{\frac{2}{\pi}}\theta, \quad \beta := 36 \log(np).$$

We show the following result.

Proposition D.9 Suppose $\theta \in (\frac{1}{n}, \frac{1}{3})$ and \mathbf{r} satisfies

$$\frac{\|\mathbf{r}_{-n}\|}{r_n} \leq \frac{1}{20}, \quad r_n > 0, \quad \|\mathbf{r}\| = 1. \quad (47)$$

Let $\mathbf{q}^{(k)}$ be the sequence generated by the projected subgradient method (cf. [Algorithm 3](#)) with initialization $\mathbf{q}^{(0)} = \mathbf{r}$ and geometrically decreasing step size

$$\tau^{(k)} = \eta^k \tau^{(0)}, \quad \tau^{(0)} = \frac{16}{25} \frac{\alpha}{\beta^2}, \quad \sqrt{1 - \frac{\alpha^2}{2\beta^2}} \leq \eta < 1 \quad (48)$$

Whenever $p \geq C \frac{\kappa^8}{\theta \sigma_{\min}^2(\mathbf{C}_a)} \log^3 n$, with probability at least $1 - p^{-c_1 n \theta} - n^{-c_2}$, the sequence $\{\mathbf{q}^{(k)}\}_{k \geq 0}$ satisfies

$$\left\| \mathbf{q}^{(k)} - (\mathbf{R}\mathbf{Q}^{-1})^{-1} \frac{\mathbf{e}_n}{\tilde{r}_n} \right\| \leq \frac{2}{5} \eta^k, \quad (49)$$

for all iteration $k = 0, 1, 2, \dots$.

Proof Given the initialization $\mathbf{q}^{(0)} = \mathbf{r}$, we have

$$\begin{aligned} d^{(0)} &= \left\| \mathbf{r} - (\mathbf{R}\mathbf{Q}^{-1})^{-1} \frac{\mathbf{e}_n}{\tilde{r}_n} \right\| \leq \|(\mathbf{R}\mathbf{Q}^{-1})^{-1}\| \left\| \tilde{\mathbf{r}} - \frac{\mathbf{e}_n}{\tilde{r}_n} \right\| \\ &\leq \frac{10}{9} \cdot \left(\|\tilde{\mathbf{r}}_{-n}\|^2 + \left(\tilde{r}_n - \frac{1}{\tilde{r}_n} \right)^2 \right)^{1/2}, \end{aligned}$$

where the last inequality we used Lemma H.4. From the argument in Proposition D.6, we know that (47) implies $\|\tilde{r}_{-n}\|/\tilde{r}_n \leq 1/10$. By the fact that $\|\tilde{r}\| \leq 10/9$, we have

$$\|\tilde{r}_{-n}\| \leq \frac{1}{9}, \quad \left| \tilde{r}_n - \frac{1}{\tilde{r}_n} \right| \leq \left| \frac{8}{9} - \frac{9}{8} \right| \leq \frac{1}{4} \implies d^{(0)} \leq \frac{2}{5}. \quad (50)$$

On the other hand, notice that

$$\begin{aligned} \left(d^{(k+1)}\right)^2 &= \left\| \mathbf{q}^{(k)} - \tau^{(k)} \mathcal{P}_{\mathbf{r}^\perp} \mathbf{g}^{(k)} - (\mathbf{RQ}^{-1})^{-1} \frac{\mathbf{e}_n}{\tilde{r}_n} \right\|^2 \\ &= \left(d^{(k)}\right)^2 - 2\tau^{(k)} \left\langle \mathbf{s}^{(k)}, \mathcal{P}_{\mathbf{r}^\perp} \mathbf{g}^{(k)} \right\rangle + \left(\tau^{(k)}\right)^2 \left\| \mathcal{P}_{\mathbf{r}^\perp} \mathbf{g}^{(k)} \right\|^2 \end{aligned}$$

By Lemma D.10, we know that when $p \geq C \frac{\kappa^8}{\theta \sigma_{\min}^2(\mathbf{C}_a)} \log^3 n$, for any $k = 1, 2, \dots$,

$$\left\| \mathcal{P}_{\mathbf{r}^\perp} \mathbf{g}^{(k)} \right\|^2 \leq 36 \log(np) = \beta$$

holds with probability at least $1 - p^{-c_1 n^\theta} - n^{-c_2}$. On the other hand, by the sharpness property of the function in Proposition D.6, for any $k = 1, 2, \dots$,

$$\begin{aligned} \left\langle \mathbf{s}^{(k)}, \mathcal{P}_{\mathbf{r}^\perp} \mathbf{g}^{(k)} \right\rangle &= \left\langle \mathbf{s}^{(k)}, \mathbf{g}^{(k)} \right\rangle \geq \zeta(\mathbf{q}^{(k)}) - \zeta\left((\mathbf{RQ}^{-1})^{-1} \frac{\mathbf{e}_n}{\tilde{r}_n}\right) \\ &\geq \frac{1}{50} \sqrt{\frac{2}{\pi}} \theta \left\| \mathbf{q}^{(k)} - (\mathbf{RQ}^{-1})^{-1} \frac{\mathbf{e}_n}{\tilde{r}_n} \right\| = \alpha \cdot d^{(k)}, \end{aligned}$$

where the first equality follows from the fact that $\langle \mathbf{r}, \mathbf{s}^{(k)} \rangle = 0$ so that $\mathcal{P}_{\mathbf{r}^\perp} \mathbf{s}^{(k)} = \mathbf{s}^{(k)}$, the first inequality follows from the fact that $\zeta(\mathbf{q})$ is convex, and the second inequality utilizes the sharpness of the function in Proposition D.6 given the condition (47). Thus, we have

$$\left(d^{(k+1)}\right)^2 \leq \left(d^{(k)}\right)^2 - 2\alpha \cdot \tau^{(k)} \cdot d^{(k)} + \beta^2 \cdot \left(\tau^{(k)}\right)^2.$$

Now we proceed to prove (49) by induction. It is clear that (49) holds for $\mathbf{q}^{(0)}$. Suppose $\mathbf{q}^{(k)}$ satisfies (49), i.e., $d^{(k)} \leq \eta^k d^{(0)}$ for some $k \geq 1$. The quadratic term of $d^{(k)}$ on the right hand side of the inequality above will obtain its maximum at $\frac{2}{5}\eta^k$ due to the definition of $\tau^{(0)}$ and $d^{(0)} \leq \frac{2}{5}$ as shown in (50). This, together with $\tau^{(k)} = \eta \tau^{(k-1)}$, it gives

$$\begin{aligned} \left(d^{(k+1)}\right)^2 &\leq \frac{4}{25} \eta^{2k} - \frac{4}{5} \alpha \cdot \eta^{2k} \tau^{(0)} + \beta^2 \cdot \eta^{2k} \left(\tau^{(0)}\right)^2 \\ &= \frac{4}{25} \eta^{2k} \cdot \left[1 - 5\alpha \tau^{(0)} + \frac{25}{4} \beta^2 \left(\tau^{(0)}\right)^2 \right] \leq \eta^{2k+2} \cdot \left(d^{(0)}\right)^2 \end{aligned}$$

where the last inequality follows from (48), where

$$1 - 5\alpha \tau^{(0)} + \frac{25}{4} \beta^2 \left(\tau^{(0)}\right)^2 \leq 1 - \alpha \tau^{(0)} \leq 1 - \frac{\alpha^2}{2\beta^2} \leq \eta^2 < 1.$$

This completes the proof. ■

Lemma D.10 Suppose $\theta \in (\frac{1}{n}, \frac{1}{3})$. Whenever $p \geq C \frac{\kappa^8}{\theta \sigma_{\min}^2(\mathbf{C}_a)} \log^3 n$, we have

$$\rho := \sup_{\mathbf{q}: \mathbf{q}^\top \mathbf{r} = 1} \frac{1}{np} \left\| \mathcal{P}_{\mathbf{r}^\perp} \sum_{i=1}^p (\mathbf{RQ}^{-1})^\top \mathbf{C}_{\mathbf{x}_i}^\top \text{sign}(\mathbf{C}_{\mathbf{x}_i} \mathbf{RQ}^{-1} \mathbf{q}) \right\| \leq 6\sqrt{\log(np)} \quad (51)$$

holds with probability at least $1 - p^{-c_1 n^\theta} - n^{-c_2}$.

Proof We have

$$\rho \leq \frac{1}{np} \|RQ^{-1}\| \sum_{i=1}^p \left(\|C_{x_i}\| \sup_{q: q^\top r=1} \|\text{sign}(C_{x_i} RQ^{-1} q)\| \right).$$

Since the $\text{sign}(\cdot)$ function is bounded by 1, we have

$$\rho \leq \frac{1}{np} \|RQ^{-1}\| \cdot \left(\sum_{i=1}^p \|F x_i\|_\infty \right) \cdot \sqrt{n},$$

where we used the fact that $\|C_{x_i}\| = \|F x_i\|_\infty$. As $x_i \sim_{i.i.d.} \mathcal{BG}(\theta)$, let $x_i = b_i \odot g_i$ with $b_i \sim \mathcal{B}(\theta)$ and $g_i \sim \mathcal{N}(\mathbf{0}, \mathbf{I})$. Then we have

$$\|C_{x_i}\| = \|F x_i\|_\infty = \max_{1 \leq j \leq n} |(f_j \odot b_i)^* g_i|.$$

By Gaussian concentration inequality in Lemma B.4 and a union bound, we have

$$\mathbb{P} \left(\max_{1 \leq i \leq p} \|F x_i\| \geq t \right) \leq (np) \cdot \exp \left(-\frac{t^2}{2n} \right).$$

Choose $t = 4\sqrt{n \log(np)}$, then we have

$$\max_{1 \leq i \leq p} \|F x_i\| \leq 4\sqrt{n \log(np)},$$

with probability at least $1 - (np)^{-7}$. On the other hand, by Lemma H.4, we know that whenever $p \geq C \frac{\kappa^8}{\theta \sigma_{\min}^2(C_a)} \log^3 n$, we have

$$\|RQ^{-1}\| \leq \frac{3}{2},$$

holds with probability at least $1 - p^{-c_1 n \theta} - n^{-c_2}$. Combining all the results above, we obtain

$$\rho \leq \frac{1}{np} \cdot \frac{3}{2} \cdot \left(4p\sqrt{n \log(np)} \right) \cdot \sqrt{n} = 6\sqrt{\log(np)},$$

as desired. ■

E Regularity Condition in Population

Here, we show that the reduced objective introduced in (28)

$$\min_q \tilde{f}(q) = \frac{1}{np} \sum_{i=1}^p H_\mu(C_{x_i} q), \quad \text{s.t.} \quad \|q\| = 1.$$

satisfies the regularity condition in population ($p \rightarrow +\infty$) on the set

$$\mathcal{S}_\xi^{i\pm} := \left\{ q \in \mathbb{S}^{n-1} \mid \frac{|q_i|}{\|q_{-i}\|_\infty} \geq \sqrt{1+\xi}, q_i \geq 0 \right\},$$

for every $i \in [n]$ and $\xi > 0$.

Proposition E.1 *Whenever $\theta \in (\frac{1}{n}, c_0)$ and $\mu \leq c_1 \min \left\{ \theta, \frac{1}{\sqrt{n}} \right\}$, we have*

$$\left\langle \mathbb{E} \left[\text{grad } \tilde{f}(q) \right], q_i q - e_i \right\rangle \geq c_2 \theta (1 - \theta) q_i \|q_{-i}\|, \quad \sqrt{1 - q_i^2} \in [\mu, c_3] \quad (52)$$

$$\left\langle \mathbb{E} \left[\text{grad } \tilde{f}(q) \right], q_i q - e_i \right\rangle \geq c_2 \theta (1 - \theta) q_i n^{-1} \|q_{-i}\|, \quad \sqrt{1 - q_i^2} \in \left[c_3, \sqrt{\frac{n-1}{n}} \right], \quad (53)$$

hold for any $q \in \mathcal{S}_\xi^{i\pm}$ and each $i \in [n]$.

Remarks. For proving this result, we first introduce some basic notations. We use \mathcal{I} to denote the generic support set of $\mathbf{q} \in \mathbb{S}^{n-1}$ of i.i.d. $\mathcal{B}(\theta)$ law. Since the landscape is symmetric for each $i \in [n]$, without loss of generality, it is enough to consider the case when $i = n$. We reparameterize $\mathbf{q} \in \mathbb{S}^{n-1}$ by

$$\mathbf{q}(\mathbf{w}) : \mathbf{w} \mapsto \left[\frac{\mathbf{w}}{\sqrt{1 - \|\mathbf{w}\|^2}} \right], \quad (54)$$

where $\mathbf{w} \in \mathbb{R}^{n-1}$ with $\|\mathbf{w}\| \leq \sqrt{\frac{n-1}{n}}$. We write

$$\mathbf{q}_{\mathcal{I}} = \begin{bmatrix} \mathbf{w}_{\mathcal{I}} \\ q_n \mathbb{1}_{n \in \mathcal{I}} \end{bmatrix},$$

where we use \mathcal{I} to denote the support set of \mathbf{w} of i.i.d. $\mathcal{B}(\theta)$ law.

Proof We denote

$$g(\mathbf{w}) = h_{\mu} \left(\mathbf{w}^{\top} \mathbf{x}_{-n} + x_n \sqrt{1 - \|\mathbf{w}\|^2} \right) \quad (55)$$

Note that if \mathbf{e}_n is a local minimizer of $\mathbb{E} [\tilde{f}(\mathbf{q})]$, then $\mathbb{E} [g(\mathbf{w})]$ has a corresponding local minimum at $\mathbf{0}$. Since $g(\cdot)$ satisfies chain rule when computing its gradient, we have

$$\begin{aligned} \langle \mathbb{E} [\nabla g(\mathbf{w})], \mathbf{w} - \mathbf{0} \rangle &= \left\langle \begin{bmatrix} \mathbf{I}_{n-1} & \frac{-\mathbf{w}}{\sqrt{1 - \|\mathbf{w}\|^2}} \end{bmatrix} \nabla \mathbb{E} [\tilde{f}(\mathbf{q})], \mathbf{w} \right\rangle \\ &= \left\langle \mathbb{E} [\nabla \tilde{f}(\mathbf{q})], \mathbf{q} - \frac{1}{q_n} \mathbf{e}_n \right\rangle = \frac{1}{q_n} \left\langle \mathbb{E} [\text{grad } \tilde{f}(\mathbf{q})], q_n \mathbf{q} - \mathbf{e}_n \right\rangle, \end{aligned}$$

which gives

$$\left\langle \mathbb{E} [\text{grad } \tilde{f}(\mathbf{q})], q_n \mathbf{q} - \mathbf{e}_n \right\rangle = q_n \langle \mathbb{E} [\nabla g(\mathbf{w})], \mathbf{w} \rangle. \quad (56)$$

Thus, the above relationship implies that we can work on the “unconstrained” function $g(\mathbf{w})$ and establish the following: for any $\mathbf{q}(\mathbf{w}) \in \mathcal{S}_{\xi}^{n+}$ with $\xi > 0$, or equivalently,

$$\|\mathbf{w}\|^2 + (1 + \xi) \|\mathbf{w}\|_{\infty}^2 \leq 1,$$

the following holds

$$\langle \nabla \mathbb{E} [g(\mathbf{w})], \mathbf{w} - \mathbf{0} \rangle \gtrsim \|\mathbf{w}\|.$$

When $\|\mathbf{w}\| \in [c_0 \mu, c_1]$, Lemma E.4 implies that

$$\mathbf{w}^{\top} \nabla \mathbb{E} [g(\mathbf{w})] \geq c_2 \theta (1 - \theta) \|\mathbf{w}\|.$$

By Lemma E.5, we know that when $c_1 \leq \|\mathbf{w}\| \leq \sqrt{\frac{n-1}{n}}$,

$$\mathbf{w}^{\top} \nabla^2 \mathbb{E} [g(\mathbf{w})] \mathbf{w} \leq -c_3 \theta (1 - \theta) \|\mathbf{w}\|^2,$$

which implies concavity of $g(\mathbf{w})$ along the \mathbf{w} direction. Let us denote $\mathbf{v} = \mathbf{w} / \|\mathbf{w}\|$, then the directional concavity implies that

$$t \mathbf{v}^{\top} \nabla \mathbb{E} [g(t \mathbf{v})] \geq (t' \mathbf{v})^{\top} \nabla \mathbb{E} [g(t' \mathbf{v})] + c_4 \theta (1 - \theta) (t' - t),$$

for any $t, t' \in \left[c_1, \sqrt{\frac{n-1}{n}} \right]$. Choose $t' = \frac{\|\mathbf{w}\|}{\sqrt{\|\mathbf{w}\|^2 + \|\mathbf{w}\|_\infty^2}}$ and $t = \|\mathbf{w}\|$, by Lemma E.3, we know that

$$\mathbf{w}^\top \nabla \mathbb{E}[g(\mathbf{w})] \geq c_4 \theta (1 - \theta) \|\mathbf{w}\| \left(\frac{1}{\sqrt{\|\mathbf{w}\|^2 + \|\mathbf{w}\|_\infty^2}} - 1 \right).$$

The function

$$h_{\mathbf{v}}(t) \doteq \frac{\|t\mathbf{v}\|}{\sqrt{\|t\mathbf{v}\|^2 + \|t\mathbf{v}\|_\infty^2}} - \|t\mathbf{v}\| = \frac{1}{\sqrt{1 + \|\mathbf{v}\|_\infty^2}} - t$$

is obviously monotonically decreasing w.r.t. t . Since $\mathbf{q} \in \mathcal{S}_\xi^{n+}$, we have

$$\|t\mathbf{v}\|^2 + (1 + \xi) \|t\mathbf{v}\|_\infty^2 \leq 1 \implies t \leq \frac{1}{\sqrt{1 + (1 + \xi) \|\mathbf{v}\|_\infty^2}}.$$

Therefore, we can uniformly lower bound $h_{\mathbf{v}}(t)$ by

$$h_{\mathbf{v}}(t) \geq \frac{1}{\sqrt{1 + \|\mathbf{v}\|_\infty^2}} - \frac{1}{\sqrt{1 + (1 + \xi) \|\mathbf{v}\|_\infty^2}} \geq \xi \|\mathbf{v}\|_\infty^2 \geq \xi n^{-1}$$

Therefore, we have

$$\mathbf{w}^\top \nabla \mathbb{E}[g(\mathbf{w})] \geq c_4 \xi \theta (1 - \theta) n^{-1} \|\mathbf{w}\|,$$

when $\|\mathbf{w}\| \in \left[c_1, \sqrt{\frac{n-1}{n}} \right]$. Combining the bounds above, we obtain the desired results. \blacksquare

Lemma E.2 Suppose $\mathbf{g} \in \mathcal{N}(\mathbf{0}, \mathbf{I}_n)$, we have

$$\mathbf{w}^\top \nabla \mathbb{E}[g(\mathbf{w})] = \frac{1}{\mu} \mathbb{E}_{\mathcal{I}} \left[\left(\|\mathbf{q}_{\mathcal{I}}\|^2 - \mathbb{1}_{n \in \mathcal{I}} \right) \mathbb{P}(|\mathbf{q}_{\mathcal{I}}^\top \mathbf{g}| \leq \mu) \right]. \quad (57)$$

Proof In particular, exchange of gradient and expectation operator can again be justified. By simple calculation, we obtain that

$$\nabla g(\mathbf{w}) = \nabla h_\mu(\mathbf{q}^\top \mathbf{x}) \left(\mathbf{x}_{-n} - \frac{x_n}{q_n} \mathbf{w} \right) = \begin{cases} \frac{\mathbf{q}^\top \mathbf{x}}{\mu} \left(\mathbf{x}_{-n} - \frac{x_n}{q_n} \mathbf{w} \right), & |\mathbf{q}^\top \mathbf{x}| \leq \mu \\ \text{sign}(\mathbf{q}^\top \mathbf{x}) \left(\mathbf{x}_{-n} - \frac{x_n}{q_n} \mathbf{w} \right), & |\mathbf{q}^\top \mathbf{x}| > \mu. \end{cases} \quad (58)$$

Thus, we obtain

$$\begin{aligned} & \mathbf{w}^\top \nabla \mathbb{E}[g(\mathbf{w})] \\ &= \mathbb{E} \left[\text{sign}(\mathbf{q}^\top \mathbf{x}) \left(\mathbf{w}^\top \mathbf{x}_{-n} - \frac{x_n}{q_n} \|\mathbf{w}\|^2 \right) \mathbb{1}_{|\mathbf{q}^\top \mathbf{x}| \geq \mu} \right] + \mathbb{E} \left[\frac{\mathbf{q}^\top \mathbf{x}}{\mu} \left(\mathbf{w}^\top \mathbf{x}_{-n} - \frac{x_n}{q_n} \|\mathbf{w}\|^2 \right) \mathbb{1}_{|\mathbf{q}^\top \mathbf{x}| \leq \mu} \right] \\ &= \mathbb{E} \left[\text{sign}(\mathbf{q}^\top \mathbf{x}) \left(\mathbf{q}^\top \mathbf{x} - \frac{x_n}{q_n} \right) \mathbb{1}_{|\mathbf{q}^\top \mathbf{x}| \geq \mu} \right] + \frac{1}{\mu} \mathbb{E} \left[(\mathbf{q}^\top \mathbf{x}) \left(\mathbf{q}^\top \mathbf{x} - \frac{x_n}{q_n} \right) \mathbb{1}_{|\mathbf{q}^\top \mathbf{x}| \leq \mu} \right], \end{aligned}$$

where we used the fact that

$$\mathbf{w}^\top \mathbf{x}_{-n} - \frac{x_n}{q_n} \|\mathbf{w}\|^2 = \mathbf{w}^\top \mathbf{x}_{-n} + q_n x_n - x_n \frac{\|\mathbf{w}\|^2 + q_n^2}{q_n} = \mathbf{q}^\top \mathbf{x} - \frac{x_n}{q_n}.$$

Let $Z = X + Y$, with

$$X = \mathbf{w}^\top \mathbf{x}_{-n} \sim \mathcal{N}(\mathbf{0}, \|\mathbf{w}_{\mathcal{I}}\|^2), \quad Y = q_n x_n \sim \mathcal{N}(0, q_n^2 \mathbb{1}_{n \in \mathcal{I}}), \quad Z \sim \mathcal{N}(\mathbf{0}, \|\mathbf{q}_{\mathcal{I}}\|^2). \quad (59)$$

This gives

$$\begin{aligned} \mathbf{w}^\top \nabla \mathbb{E}[g(\mathbf{w})] &= \mathbb{E}[|\mathbf{q}^\top \mathbf{x}| \mathbb{1}_{|\mathbf{q}^\top \mathbf{x}| \geq \mu}] - \frac{1}{q_n} \mathbb{E}[\text{sign}(\mathbf{q}^\top \mathbf{x}) x_n \mathbb{1}_{|\mathbf{q}^\top \mathbf{x}| \geq \mu}] \\ &\quad + \frac{1}{\mu} \mathbb{E}[(\mathbf{q}^\top \mathbf{x})^2 \mathbb{1}_{|\mathbf{q}^\top \mathbf{x}| \leq \mu}] - \frac{1}{q_n \mu} \mathbb{E}[x_n (\mathbf{w}^\top \mathbf{x}_{-n}) \mathbb{1}_{|\mathbf{q}^\top \mathbf{x}| \leq \mu}] - \frac{1}{\mu} \mathbb{E}[x_n^2 \mathbb{1}_{|\mathbf{q}^\top \mathbf{x}| \leq \mu}] \\ &= \mathbb{E}[|Z| \mathbb{1}_{|Z| \geq \mu}] - \frac{1}{q_n^2} \mathbb{E}[\text{sign}(X + Y) Y \mathbb{1}_{|X+Y| \geq \mu}] + \frac{1}{\mu} \mathbb{E}[Z^2 \mathbb{1}_{|Z| \leq \mu}] \\ &\quad - \frac{1}{\mu q_n^2} \mathbb{E}[XY \mathbb{1}_{|X+Y| \leq \mu}] - \frac{1}{\mu q_n^2} \mathbb{E}[Y^2 \mathbb{1}_{|X+Y| \leq \mu}]. \end{aligned}$$

Now by Lemma B.7, we have

$$\begin{aligned} \mathbb{E}[|Z| \mathbb{1}_{|Z| \geq \mu}] &= \sqrt{\frac{2}{\pi}} \mathbb{E}_{\mathcal{I}} \left[\|\mathbf{q}_{\mathcal{I}}\| \exp\left(-\frac{\mu^2}{2 \|\mathbf{q}_{\mathcal{I}}\|^2}\right) \right] \\ \mathbb{E}[\text{sign}(X + Y) Y \mathbb{1}_{|X+Y| \geq \mu}] &= q_n^2 \sqrt{\frac{2}{\pi}} \mathbb{E} \left[\frac{\mathbb{1}_{n \in \mathcal{I}}}{\|\mathbf{q}_{\mathcal{I}}\|} \exp\left(-\frac{\mu^2}{2 \|\mathbf{q}_{\mathcal{I}}\|^2}\right) \right] \\ \mathbb{E}[Z^2 \mathbb{1}_{|Z| \leq \mu}] &= -\mu \sqrt{\frac{2}{\pi}} \mathbb{E}_{\mathcal{I}} \left[\|\mathbf{q}_{\mathcal{I}}\| \exp\left(-\frac{\mu^2}{2 \|\mathbf{q}_{\mathcal{I}}\|^2}\right) \right] + \mathbb{E}_{\mathcal{I}} [\|\mathbf{q}_{\mathcal{I}}\|^2 \mathbb{P}(|\mathbf{q}_{\mathcal{I}}^\top \mathbf{g}| \leq \mu)] \\ \mathbb{E}[XY \mathbb{1}_{|X+Y| \leq \mu}] &= -\mu q_n^2 \sqrt{\frac{2}{\pi}} \mathbb{E}_{\mathcal{I}} \left[\frac{\mathbb{1}_{n \in \mathcal{I}} \|\mathbf{w}_{\mathcal{I}}\|^2}{\|\mathbf{q}_{\mathcal{I}}\|^3} \exp\left(-\frac{\mu^2}{2 \|\mathbf{q}_{\mathcal{I}}\|^2}\right) \right] \\ \mathbb{E}[Y^2 \mathbb{1}_{|X+Y| \leq \mu}] &= -\mu q_n^4 \sqrt{\frac{2}{\pi}} \mathbb{E}_{\mathcal{I}} \left[\frac{\mathbb{1}_{n \in \mathcal{I}}}{\|\mathbf{q}_{\mathcal{I}}\|^3} \exp\left(-\frac{\mu^2}{2 \|\mathbf{q}_{\mathcal{I}}\|^2}\right) \right] + q_n^2 \mathbb{E}_{\mathcal{I}} [\mathbb{1}_{n \in \mathcal{I}} \mathbb{P}(|\mathbf{q}_{\mathcal{I}}^\top \mathbf{g}| \leq \mu)] \end{aligned}$$

Putting the above calculations together and simplify, we obtain the desired result in (57). ■

Lemma E.3 When for any $\mathbf{w} \in \mathbb{R}^{n-1}$ satisfies $\|\mathbf{w}\|^2 + \|\mathbf{w}\|_\infty^2 \leq 1$, we have

$$\mathbf{w}^\top \nabla \mathbb{E}[g(\mathbf{w})] \geq 0.$$

Proof From Lemma E.2, we know that

$$\begin{aligned}
& \mu \cdot \mathbf{w}^\top \nabla \mathbb{E}[g(\mathbf{w})] \\
&= \mathbb{E}_{\mathcal{I}} \left[\left(\|\mathbf{q}_{\mathcal{I}}\|^2 - \mathbb{1}_{n \in \mathcal{I}} \right) \mathbb{P}(|\mathbf{q}_{\mathcal{I}}^\top \mathbf{g}| \leq \mu) \right] \\
&= \mathbb{E}_{\mathcal{J}} \left[(1 - \theta) \|\mathbf{w}_{\mathcal{J}}\|^2 \mathbb{P}(|\mathbf{g}_{-n}^\top \mathbf{w}_{\mathcal{J}}| \leq \mu) - \theta \|\mathbf{w}_{\mathcal{J}^c}\|^2 \mathbb{P}(|\mathbf{g}_{-n}^\top \mathbf{w}_{\mathcal{J}} + q_n g_n| \leq \mu) \right] \\
&= \mathbb{E}_{\mathcal{J}} \left[\int_{-\mu}^{\mu} \left(\frac{1 - \theta}{\sqrt{2\pi}} \frac{\|\mathbf{w}_{\mathcal{J}}\|^2}{\|\mathbf{w}_{\mathcal{J}}\|} \exp\left(-\frac{t^2}{2\|\mathbf{w}_{\mathcal{J}}\|^2}\right) - \frac{\theta}{\sqrt{2\pi}} \frac{\|\mathbf{w}_{\mathcal{J}^c}\|^2}{\sqrt{1 - \|\mathbf{w}_{\mathcal{J}^c}\|^2}} \exp\left(\frac{-t^2}{2 - 2\|\mathbf{w}_{\mathcal{J}^c}\|^2}\right) \right) dt \right] \\
&= \frac{1 - \theta}{\sqrt{2\pi}} \sum_{i=1}^{n-1} \int_{-\mu}^{\mu} \mathbb{E}_{\mathcal{J}} \left[\frac{w_i^2 \mathbb{1}_{i \in \mathcal{J}}}{\sqrt{w_i^2 \mathbb{1}_{i \in \mathcal{J}} + \|\mathbf{w}_{\mathcal{J} \setminus \{i\}}\|^2}} \exp\left(-\frac{t^2}{2w_i^2 \mathbb{1}_{i \in \mathcal{J}} + 2\|\mathbf{w}_{\mathcal{J} \setminus \{i\}}\|^2}\right) \right] dt \\
&\quad - \frac{\theta}{\sqrt{2\pi}} \sum_{i=1}^{n-1} \int_{-\mu}^{\mu} \mathbb{E}_{\mathcal{J}} \left[\frac{w_i^2 \mathbb{1}_{i \notin \mathcal{J}}}{\sqrt{1 - w_i^2 \mathbb{1}_{i \notin \mathcal{J}} - \|\mathbf{w}_{\mathcal{J}^c \setminus \{i\}}\|^2}} \exp\left(-\frac{t^2}{2 - 2w_i^2 \mathbb{1}_{i \notin \mathcal{J}} - 2\|\mathbf{w}_{\mathcal{J}^c \setminus \{i\}}\|^2}\right) \right] dt \\
&= \frac{(1 - \theta)\theta}{\sqrt{2\pi}} \sum_{i=1}^{n-1} \int_{-\mu}^{\mu} \mathbb{E}_{\mathcal{J}} \left[\frac{w_i^2}{\sqrt{w_i^2 + \|\mathbf{w}_{\mathcal{J} \setminus \{i\}}\|^2}} \exp\left(-\frac{t^2}{2w_i^2 + 2\|\mathbf{w}_{\mathcal{J} \setminus \{i\}}\|^2}\right) \right] dt \\
&\quad - \frac{(1 - \theta)\theta}{\sqrt{2\pi}} \sum_{i=1}^{n-1} \int_{-\mu}^{\mu} \mathbb{E}_{\mathcal{J}} \left[\frac{w_i^2}{\sqrt{1 - \|\mathbf{w}\|^2 + \|\mathbf{w}_{\mathcal{J} \setminus \{i\}}\|^2}} \exp\left(-\frac{t^2}{2 - 2\|\mathbf{w}\|^2 + 2\|\mathbf{w}_{\mathcal{J} \setminus \{i\}}\|^2}\right) \right] dt \\
&= (1 - \theta)\theta \sum_{i=1}^{n-1} w_i^2 \mathbb{E}_{\mathcal{J}} [\mathbb{P}(|Z_{i1}| \leq \mu) - \mathbb{P}(|Z_{i2}| \leq \mu)], \tag{60}
\end{aligned}$$

where

$$Z_{i1} \sim \mathcal{N}\left(0, w_i^2 + \|\mathbf{w}_{\mathcal{J} \setminus \{i\}}\|^2\right), \quad Z_{i2} \sim \mathcal{N}\left(0, 1 - \|\mathbf{w}\|^2 + \|\mathbf{w}_{\mathcal{J} \setminus \{i\}}\|^2\right). \tag{61}$$

Since we have $1 - \|\mathbf{w}\|^2 \geq \|\mathbf{w}\|_{\infty}^2 \geq w_i^2$, the variance of Z_{i2}^2 is larger than that of Z_{i1}^2 . Therefore, we have $\mathbb{P}(|Z_{i1}| \leq \mu) \geq \mathbb{P}(|Z_{i2}| \leq \mu)$ for each $i = 1, \dots, n - 1$. Hence, we obtain

$$\mathbf{w}^\top \nabla \mathbb{E}[g(\mathbf{w})] = \frac{1}{\mu} \theta (1 - \theta) \sum_{i=1}^{n-1} w_i^2 \mathbb{E}_{\mathcal{J}} [\mathbb{P}(|Z_{i1}| \leq \mu) - \mathbb{P}(|Z_{i2}| \leq \mu)] \geq 0.$$

■

Lemma E.4 For any \mathbf{w} with $c_0 \mu \leq \|\mathbf{w}\| \leq c_1$, we have

$$\mathbf{w}^\top \nabla \mathbb{E}[g(\mathbf{w})] \geq c\theta(1 - \theta) \|\mathbf{w}\|$$

Proof Recall from (60), we have

$$\mathbf{w}^\top \nabla \mathbb{E}[g(\mathbf{w})] = \frac{1}{\mu} (1 - \theta)\theta \sum_{i=1}^{n-1} w_i^2 \mathbb{E}_{\mathcal{J}} [\mathbb{P}(|Z_{i1}| \leq \mu) - \mathbb{P}(|Z_{i2}| \leq \mu)],$$

where Z_{i1} and Z_{i2} are defined the same as (61). Let us denote

$$Z_1 \sim \mathcal{N}\left(0, \|\mathbf{w}\|^2\right), \quad Z_2 \sim \mathcal{N}\left(0, 1 - \|\mathbf{w}\|^2\right).$$

Since we have $\|\mathbf{w}\|^2 \geq w_i^2 + \|\mathbf{w}_{\mathcal{J} \setminus \{i\}}\|^2$, the variance of Z_1 is larger than that of Z_{i1} . Therefore, we have $\mathbb{P}(|Z_{i1}| \leq \mu) \geq \mathbb{P}(|Z_1| \leq \mu)$ for each $i = 1, \dots, n-1$. By a similar argument, we have $\mathbb{P}(|Z_{i2}| \leq \mu) \leq \mathbb{P}(|Z_2| \leq \mu)$ for each $i = 1, \dots, n-1$. Thus, we obtain

$$\begin{aligned}
& \mathbb{P}(|Z_{i1}| \leq \mu) - \mathbb{P}(|Z_{i2}| \leq \mu) \\
& \geq \mathbb{P}(|Z_1| \leq \mu) - \mathbb{P}(|Z_2| \leq \mu) \\
& = \sqrt{\frac{2}{\pi}} \frac{1}{\|\mathbf{w}\|} \int_0^\mu \exp\left(-\frac{t^2}{2\|\mathbf{w}\|^2}\right) dt - \sqrt{\frac{2}{\pi}} \frac{1}{\sqrt{1-\|\mathbf{w}\|^2}} \int_0^\mu \exp\left(-\frac{t^2}{2-2\|\mathbf{w}\|^2}\right) dt \\
& \geq \sqrt{\frac{2}{\pi}} \left[\frac{1}{\|\mathbf{w}\|} \int_0^\mu \left(1 - \frac{t^2}{2\|\mathbf{w}\|^2}\right) dt - \frac{\mu}{\sqrt{1-\|\mathbf{w}\|^2}} \right] \\
& = \sqrt{\frac{2}{\pi}} \left[\frac{1}{\|\mathbf{w}\|} \left(\mu - \frac{1}{6} \frac{\mu^3}{\|\mathbf{w}\|^2}\right) - \frac{\mu}{\sqrt{1-\|\mathbf{w}\|^2}} \right] \\
& \geq \mu \sqrt{\frac{2}{\pi}} \left(\frac{1}{\|\mathbf{w}\|} - 2 \frac{1}{\sqrt{1-\|\mathbf{w}\|^2}} \right) \geq \frac{\mu}{2\sqrt{2\pi}} \frac{1}{\|\mathbf{w}\|}
\end{aligned} \tag{62}$$

where we used the fact that $\mu/\sqrt{3} \leq \|\mathbf{w}\| \leq 1/\sqrt{17}$ for the last two inequalities. Plugging (62) back into (60) gives

$$\begin{aligned}
\mathbf{w}^\top \nabla \mathbb{E}[g(\mathbf{w})] &= \frac{1}{\mu} (1-\theta) \theta \sum_{i=1}^{n-1} w_i^2 \mathbb{E}_{\mathcal{J}} [\mathbb{P}(|Z_{i1}| \leq \mu) - \mathbb{P}(|Z_{i2}| \leq \mu)] \\
&\geq \frac{(1-\theta) \theta}{2\sqrt{2\pi} \|\mathbf{w}\|} \sum_{i=1}^{n-1} w_i^2 = \frac{1}{2\sqrt{2\pi}} (1-\theta) \theta \|\mathbf{w}\|,
\end{aligned}$$

as desired. ■

Lemma E.5 When $\mu \leq c_0 \min\left\{\frac{1}{\sqrt{n}}, \theta\right\}$ and $\theta \in (\frac{1}{n}, c_1)$, we have

$$\mathbf{w}^\top \nabla^2 \mathbb{E}[g(\mathbf{w})] \mathbf{w} \leq -c_2 \theta (1-\theta) \|\mathbf{w}\|^2$$

for all \mathbf{w} with $c_3 \leq \|\mathbf{w}\| \leq \sqrt{\frac{n-1}{n}}$. Here, c_0, c_1, c_2 , and c_3 are some numerical constants.

Proof Since the expectation and derivative are exchangeable, we have

$$\mathbf{w}^\top \nabla^2 \mathbb{E}[g(\mathbf{w})] \mathbf{w} = \mathbf{w}^\top \mathbb{E}[\nabla^2 g(\mathbf{w})] \mathbf{w}.$$

From (58), we obtain

$$\mathbf{w}^\top \nabla^2 g(\mathbf{w}) \mathbf{w} = \begin{cases} \frac{1}{\mu} \left[(\mathbf{q}^\top \mathbf{x})^2 - \frac{x_n}{q_n} (\mathbf{q}^\top \mathbf{x}) - \frac{x_n}{q_n^3} (\mathbf{x}_{-n}^\top \mathbf{w}) \right], & |\mathbf{q}^\top \mathbf{x}| \leq \mu \\ -\frac{x_n}{q_n^3} \|\mathbf{w}\|^2 \text{sign}(\mathbf{q}^\top \mathbf{x}), & |\mathbf{q}^\top \mathbf{x}| \geq \mu. \end{cases}$$

Thus, we have

$$\begin{aligned}
\mathbb{E}[\mathbf{w}^\top \nabla^2 g(\mathbf{w}) \mathbf{w} \mathbb{1}_{|\mathbf{q}^\top \mathbf{x}| \geq \mu}] &= -\frac{\|\mathbf{w}\|^2}{q_n^4} \mathbb{E}[q_n x_n \text{sign}(\mathbf{q}^\top \mathbf{x}) \mathbb{1}_{|\mathbf{q}^\top \mathbf{x}| \geq \mu}] \\
&= -\sqrt{\frac{2}{\pi}} \frac{\|\mathbf{w}\|^2}{q_n^2} \mathbb{E}_{\mathcal{I}} \left[\frac{\mathbb{1}_{n \in \mathcal{I}}}{\|\mathbf{q}_{\mathcal{I}}\|} \exp\left(-\frac{\mu^2}{2\|\mathbf{q}_{\mathcal{I}}\|^2}\right) \right]
\end{aligned}$$

and

$$\begin{aligned}
& \mathbb{E} [\mathbf{w}^\top \nabla^2 g(\mathbf{w}) \mathbf{w} \mathbb{1}_{|\mathbf{q}^\top \mathbf{x}| \leq \mu}] \\
&= \frac{1}{\mu} \mathbb{E} [(\mathbf{q}^\top \mathbf{x})^2 \mathbb{1}_{|\mathbf{q}^\top \mathbf{x}| \leq \mu}] - \frac{1}{\mu} \mathbb{E} \left[\frac{x_n}{q_n} (\mathbf{q}^\top \mathbf{x}) \mathbb{1}_{|\mathbf{q}^\top \mathbf{x}| \leq \mu} \right] - \frac{1}{\mu} \mathbb{E} \left[\frac{x_n}{q_n^3} (\mathbf{x}_{-n}^\top \mathbf{w}) \mathbb{1}_{|\mathbf{q}^\top \mathbf{x}| \leq \mu} \right] \\
&= \frac{1}{\mu} \mathbb{E} [Z^2 \mathbb{1}_{|Z| \leq \mu}] - \frac{1}{\mu q_n^2} \mathbb{E} [Y^2 \mathbb{1}_{|X+Y| \leq \mu}] - \frac{1}{\mu} \left(\frac{1}{q_n^2} + \frac{1}{q_n^4} \right) \mathbb{E} [XY \mathbb{1}_{|X+Y| \leq \mu}],
\end{aligned}$$

where X , Y and $Z = X + Y$ are defined the same as (59). Similar to Lemma E.2, by using Lemma B.7, we obtain

$$\begin{aligned}
& \mathbb{E} [\mathbf{w}^\top \nabla^2 g(\mathbf{w}) \mathbf{w} \mathbb{1}_{|\mathbf{q}^\top \mathbf{x}| \leq \mu}] \\
&= -\sqrt{\frac{2}{\pi}} \mathbb{E}_{\mathcal{I}} \left[\|\mathbf{q}_{\mathcal{I}}\| \exp \left(-\frac{\mu^2}{2 \|\mathbf{q}_{\mathcal{I}}\|^2} \right) \right] + \frac{1}{\mu} \mathbb{E} \left[(\|\mathbf{q}_{\mathcal{I}}\|^2 - \mathbb{1}_{n \in \mathcal{I}}) \mathbb{P} (|\mathbf{q}_{\mathcal{I}}^\top \mathbf{g}| \leq \mu) \right] \\
&+ \sqrt{\frac{2}{\pi}} \mathbb{E}_{\mathcal{I}} \left[\frac{q_n^2 \mathbb{1}_{n \in \mathcal{I}}}{\|\mathbf{q}_{\mathcal{I}}\|^3} \exp \left(-\frac{\mu^2}{2 \|\mathbf{q}_{\mathcal{I}}\|^2} \right) \right] + \sqrt{\frac{2}{\pi}} \left(1 + \frac{1}{q_n^2} \right) \mathbb{E}_{\mathcal{I}} \left[\frac{\|\mathbf{w}_{\mathcal{J}}\|^2 \mathbb{1}_{n \in \mathcal{I}}}{\|\mathbf{q}_{\mathcal{I}}\|^3} \exp \left(-\frac{\mu^2}{2 \|\mathbf{q}_{\mathcal{I}}\|^2} \right) \right].
\end{aligned}$$

Combining the results above and using integral by parts, we obtain

$$\begin{aligned}
& \mathbf{w}^\top \nabla^2 \mathbb{E} [g(\mathbf{w})] \mathbf{w} \\
&= -\sqrt{\frac{2}{\pi}} \mathbb{E}_{\mathcal{I}} \left[\frac{\mathbb{1}_{n \in \mathcal{I}}}{\|\mathbf{q}_{\mathcal{I}}\|^3} \exp \left(-\frac{\mu^2}{2 \|\mathbf{q}_{\mathcal{I}}\|^2} \right) \right] + 2\sqrt{\frac{2}{\pi}} \mathbb{E}_{\mathcal{I}} \left[\frac{\mathbb{1}_{n \in \mathcal{I}}}{\|\mathbf{q}_{\mathcal{I}}\|} \exp \left(-\frac{\mu^2}{2 \|\mathbf{q}_{\mathcal{I}}\|^2} \right) \right] \\
&- \sqrt{\frac{2}{\pi}} \mathbb{E}_{\mathcal{I}} \left[\|\mathbf{q}_{\mathcal{I}}\| \exp \left(-\frac{\mu^2}{2 \|\mathbf{q}_{\mathcal{I}}\|^2} \right) \right] + \frac{1}{\mu} \mathbb{E} \left[(\|\mathbf{q}_{\mathcal{I}}\|^2 - \mathbb{1}_{n \in \mathcal{I}}) \mathbb{P} (|\mathbf{q}_{\mathcal{I}}^\top \mathbf{g}| \leq \mu) \right] \\
&= -\sqrt{\frac{2}{\pi}} \mathbb{E}_{\mathcal{I}} \left[\frac{\|\mathbf{w}_{\mathcal{J}^c}\|^2 \mathbb{1}_{n \in \mathcal{I}}}{\|\mathbf{q}_{\mathcal{I}}\|^3} \exp \left(-\frac{\mu^2}{2 \|\mathbf{q}_{\mathcal{I}}\|^2} \right) \right] \\
&+ \sqrt{\frac{2}{\pi}} \mathbb{E}_{\mathcal{I}} \left[\frac{\mathbb{1}_{n \in \mathcal{I}}}{\|\mathbf{q}_{\mathcal{I}}\|} \left(\exp \left(-\frac{\mu^2}{2 \|\mathbf{q}_{\mathcal{I}}\|^2} \right) - \frac{\|\mathbf{q}_{\mathcal{I}}\|}{\mu} \int_0^{\mu/\|\mathbf{q}_{\mathcal{I}}\|} \exp(-t^2/2) dt \right) \right] \\
&- \sqrt{\frac{2}{\pi}} \mathbb{E}_{\mathcal{I}} \left[\|\mathbf{q}_{\mathcal{I}}\| \left(\exp \left(-\frac{\mu^2}{2 \|\mathbf{q}_{\mathcal{I}}\|^2} \right) - \frac{\|\mathbf{q}_{\mathcal{I}}\|}{\mu} \int_0^{\mu/\|\mathbf{q}_{\mathcal{I}}\|} \exp(-t^2/2) dt \right) \right] \\
&= -\sqrt{\frac{2}{\pi}} \mathbb{E}_{\mathcal{I}} \left[\|\mathbf{w}_{\mathcal{J}^c}\|^2 \frac{\mathbb{1}_{n \in \mathcal{I}}}{\|\mathbf{q}_{\mathcal{I}}\|^3} \exp \left(-\frac{\mu^2}{2 \|\mathbf{q}_{\mathcal{I}}\|^2} \right) \right] - \frac{1}{\mu} \sqrt{\frac{2}{\pi}} \mathbb{E}_{\mathcal{I}} \left[\mathbb{1}_{n \in \mathcal{I}} \int_0^{\mu/\|\mathbf{q}_{\mathcal{I}}\|} t^2 \exp(-t^2/2) dt \right] \\
&+ \frac{1}{\mu} \sqrt{\frac{2}{\pi}} \mathbb{E}_{\mathcal{I}} \left[\|\mathbf{q}_{\mathcal{I}}\|^2 \int_0^{\mu/\|\mathbf{q}_{\mathcal{I}}\|} t^2 \exp(-t^2/2) dt \right] \\
&\leq -\sqrt{\frac{2}{\pi}} \mathbb{E}_{\mathcal{I}} \left[\|\mathbf{w}_{\mathcal{J}^c}\|^2 \frac{\mathbb{1}_{n \in \mathcal{I}}}{\|\mathbf{q}_{\mathcal{I}}\|^3} \exp \left(-\frac{\mu^2}{2 \|\mathbf{q}_{\mathcal{I}}\|^2} \right) \right] + \frac{1}{\mu} \sqrt{\frac{2}{\pi}} \int_0^\mu t^2 \mathbb{E}_{\mathcal{I}} \left[\frac{1}{\|\mathbf{q}_{\mathcal{I}}\|} \exp \left(-\frac{t^2}{2 \|\mathbf{q}_{\mathcal{I}}\|^2} \right) \right] dt.
\end{aligned}$$

First, when $\sqrt{\frac{n-1}{n}} \geq \|\mathbf{w}\| \geq c_0$, we have

$$\begin{aligned}
& \mathbb{E}_{\mathcal{I}} \left[\|\mathbf{w}_{\mathcal{J}^c}\|^2 \frac{\mathbb{1}_{n \in \mathcal{I}}}{\|\mathbf{q}_{\mathcal{I}}\|^3} \exp \left(-\frac{\mu^2}{2\|\mathbf{q}_{\mathcal{I}}\|^2} \right) \right] \\
&= \theta \mathbb{E}_{\mathcal{J}} \left[\|\mathbf{w}_{\mathcal{J}^c}\|^2 \frac{1}{(q_n^2 + \|\mathbf{w}_{\mathcal{J}}\|^2)^{3/2}} \exp \left(-\frac{\mu^2}{2(q_n^2 + \|\mathbf{w}_{\mathcal{J}}\|^2)} \right) \right] \\
&\geq \theta \mathbb{E}_{\mathcal{J}} \left[\|\mathbf{w}_{\mathcal{J}^c}\|^2 \exp \left(-\frac{\mu^2}{2q_n^2 + 2\|\mathbf{w}_{\mathcal{J}}\|^2} \right) \right] \\
&\geq \theta \mathbb{E}_{\mathcal{J}} \left[\|\mathbf{w}_{\mathcal{J}^c}\|^2 \exp \left(-\frac{\mu^2}{2q_n^2} \right) \right] \geq c_1 \theta (1 - \theta) \|\mathbf{w}\|^2.
\end{aligned}$$

Second, notice that the function

$$h(x) = x^{-1} \exp \left(-\frac{t^2}{2x^2} \right), \quad x \in [0, 1]$$

reaches the maximum when $x = t$. Thus, we have

$$\frac{1}{\mu} \sqrt{\frac{2}{\pi}} \int_0^\mu t^2 \mathbb{E}_{\mathcal{I}} \left[\frac{1}{\|\mathbf{q}_{\mathcal{I}}\|} \exp \left(-\frac{t^2}{2\|\mathbf{q}_{\mathcal{I}}\|^2} \right) \right] dt \leq \frac{1}{\mu} \sqrt{\frac{2}{\pi}} \int_0^\mu t \exp \left(-\frac{1}{2} \right) dt \leq \frac{1}{\sqrt{2\pi}} e^{-1/2} \mu.$$

Therefore, when $\mu \leq \frac{1}{n} \leq \theta$, we have

$$\mathbf{w}^\top \nabla^2 \mathbb{E}[g(\mathbf{w})] \mathbf{w} \leq -c_2 \theta (1 - \theta) \|\mathbf{w}\|^2$$

for any $\sqrt{\frac{n-1}{n}} \geq \|\mathbf{w}\| \geq c_0$. ■

F Implicit Regularization in Population

Under the same settings of Appendix E, we show that the simplified function $\tilde{f}(\mathbf{q})$ satisfies the following implicit regularization property over $\mathbf{q} \in \mathcal{S}_\xi^{i\pm}$ for each $i \in [n]$.

Proposition F.1 Suppose $\theta \geq \frac{1}{n}$. Given any index $i \in [n]$, when $\mu \leq \frac{1}{\sqrt{3n}}$, we have

$$\left\langle \text{grad } \mathbb{E}[\tilde{f}(\mathbf{q})], \frac{1}{q_j} \mathbf{e}_j - \frac{1}{q_i} \mathbf{e}_i \right\rangle \geq \frac{\theta(1-\theta)}{4n} \frac{\xi}{1+\xi},$$

holds for all $\mathbf{q} \in \mathcal{S}_\xi^{i\pm}$ and any q_j such that $j \neq i$ and $q_j^2 \geq \frac{1}{3} q_i^2$

Proof Without loss of generality, let us consider the case $i = n$. For any $j \neq n$, we have

$$\begin{aligned}
& \left\langle \text{grad } \mathbb{E}[\tilde{f}(\mathbf{q})], \frac{1}{q_j} \mathbf{e}_j - \frac{1}{q_n} \mathbf{e}_n \right\rangle \\
&= \left(\frac{1}{q_j} \mathbf{e}_j - \frac{1}{q_n} \mathbf{e}_n \right)^\top \mathcal{P}_{\mathbf{q}^\perp} \mathbb{E}[\mathbf{x} \cdot \nabla h_\mu(\mathbf{x}^\top \mathbf{q})] \\
&= \left(\frac{1}{q_j} \mathbf{e}_j - \frac{1}{q_n} \mathbf{e}_n \right)^\top \mathbb{E}[\mathbf{x} \cdot \nabla h_\mu(\mathbf{x}^\top \mathbf{q})].
\end{aligned}$$

Let

$$Z = Z_1 + Z_2, \quad Z_1 = q_i x_i \sim \mathcal{N}(0, (b_i q_i)^2), \quad Z_2 = \mathbf{q}_{-i}^\top \mathbf{x}_{-i} \sim \mathcal{N}(0, \|\mathbf{q}_{-i} \odot \mathbf{b}_{-i}\|^2).$$

Notice that for every $i \in [n]$, we have

$$\begin{aligned} & \frac{1}{q_i} \mathbf{e}_i^\top \mathbb{E} [\mathbf{x} \cdot \nabla h_\mu(\mathbf{x}^\top \mathbf{q})] \\ &= \frac{1}{q_i^2} \frac{1}{\mu} \mathbb{E} [Z_1^2 \mathbb{1}_{|Z_1+Z_2| \leq \mu}] + \frac{1}{q_i^2} \frac{1}{\mu} \mathbb{E} [Z_1 Z_2 \mathbb{1}_{|Z_1+Z_2| \leq \mu}] + \frac{1}{q_i^2} \mathbb{E} [Z_1 \text{sign}(Z_1 + Z_2) \mathbb{1}_{|Z_1+Z_2| \geq \mu}]. \end{aligned}$$

By Lemma B.7, we have

$$\begin{aligned} \mathbb{E} [Z_1^2 \mathbb{1}_{|Z_1+Z_2| \leq \mu}] &= -\sqrt{\frac{2}{\pi}} \mu \mathbb{E}_{\mathcal{I}} \left[\frac{q_i^4 \mathbb{1}_{i \in \mathcal{I}}}{\|\mathbf{q}_{\mathcal{I}}\|^3} \exp \left(-\frac{\mu^2}{2 \|\mathbf{q}_{\mathcal{I}}\|^2} \right) \right] \\ &\quad + \mathbb{E} [q_i^2 \mathbb{1}_{i \in \mathcal{I}} \mathbb{P}(|Z| \leq \mu)], \\ \mathbb{E} [Z_1 Z_2 \mathbb{1}_{|Z_1+Z_2| \leq \mu}] &= -\sqrt{\frac{2}{\pi}} \mu \mathbb{E}_{\mathcal{I}} \left[\frac{q_i^2 \mathbb{1}_{i \in \mathcal{I}} \|\mathbf{q}_{-i}\|_{\mathcal{I}}^2}{\|\mathbf{q}_{\mathcal{I}}\|^3} \exp \left(-\frac{\mu^2}{2 \|\mathbf{q}_{\mathcal{I}}\|^2} \right) \right] \\ \mathbb{E} [Z_1 \text{sign}(Z_1 + Z_2) \mathbb{1}_{|Z_1+Z_2| \geq \mu}] &= \sqrt{\frac{2}{\pi}} \mathbb{E}_{\mathcal{I}} \left[\frac{q_i^2 \mathbb{1}_{i \in \mathcal{I}}}{\|\mathbf{q}_{\mathcal{I}}\|} \exp \left(-\frac{\mu^2}{2 \|\mathbf{q}_{\mathcal{I}}\|^2} \right) \right]. \end{aligned}$$

Combining the results above, we obtain

$$\frac{1}{q_i} \mathbf{e}_i^\top \mathbb{E} [\mathbf{x} \cdot \nabla h_\mu(\mathbf{x}^\top \mathbf{q})] = \frac{1}{\mu} \mathbb{E} [\mathbb{1}_{i \in \mathcal{I}} \mathbb{P}(|Z| \leq \mu)].$$

Therefore, we have

$$\begin{aligned} & \left\langle \text{grad} \mathbb{E} [\tilde{f}(\mathbf{q})], \frac{1}{q_j} \mathbf{e}_j - \frac{1}{q_n} \mathbf{e}_n \right\rangle \\ &= \frac{1}{\mu} (\mathbb{E} [\mathbb{1}_{j \in \mathcal{I}} \mathbb{P}(|Z| \leq \mu)] - \mathbb{E} [\mathbb{1}_{n \in \mathcal{I}} \mathbb{P}(|Z| \leq \mu)]) \\ &= \frac{\theta}{\mu} \sqrt{\frac{2}{\pi}} \mathbb{E}_{\mathcal{I}} \left[\frac{1}{\sqrt{q_j^2 + \|\mathbf{q}_{\mathcal{I} \setminus j}\|^2}} \int_0^\mu \exp \left(-\frac{t^2}{q_j^2 + \|\mathbf{q}_{\mathcal{I} \setminus j}\|^2} \right) dt \right] \\ &\quad - \frac{\theta}{\mu} \sqrt{\frac{2}{\pi}} \mathbb{E}_{\mathcal{I}} \left[\frac{1}{\sqrt{q_n^2 + \|\mathbf{q}_{\mathcal{I} \setminus n}\|^2}} \int_0^\mu \exp \left(-\frac{t^2}{q_n^2 + \|\mathbf{q}_{\mathcal{I} \setminus n}\|^2} \right) dt \right] \\ &= \frac{\theta(1-\theta)}{\mu} \sqrt{\frac{2}{\pi}} \mathbb{E}_{\mathcal{I}} \left[\frac{1}{\sqrt{q_j^2 + \|\mathbf{q}_{\mathcal{I} \setminus \{j,n\}}\|^2}} \int_0^\mu \exp \left(-\frac{t^2}{q_j^2 + \|\mathbf{q}_{\mathcal{I} \setminus \{j,n\}}\|^2} \right) dt \right] \\ &\quad - \frac{\theta(1-\theta)}{\mu} \sqrt{\frac{2}{\pi}} \mathbb{E}_{\mathcal{I}} \left[\frac{1}{\sqrt{q_n^2 + \|\mathbf{q}_{\mathcal{I} \setminus \{j,n\}}\|^2}} \int_0^\mu \exp \left(-\frac{t^2}{q_n^2 + \|\mathbf{q}_{\mathcal{I} \setminus \{j,n\}}\|^2} \right) dt \right] \\ &= \frac{\theta(1-\theta)}{\mu} \mathbb{E}_{\mathcal{I}} \left[\text{erf} \left(\frac{\mu}{\sqrt{q_j^2 + \|\mathbf{q}_{\mathcal{I} \setminus \{j,n\}}\|^2}} \right) - \text{erf} \left(\frac{\mu}{\sqrt{q_n^2 + \|\mathbf{q}_{\mathcal{I} \setminus \{j,n\}}\|^2}} \right) \right] \end{aligned}$$

where $\text{erf}(x)$ is the Gaussian error function

$$\text{erf}(x) = \frac{1}{\sqrt{2\pi}} \int_{-x}^x \exp(-t^2/2) dt = \sqrt{\frac{2}{2\pi}} \int_0^x \exp(-t^2/2) dt, \quad x \geq 0.$$

When $\mu \leq \frac{1}{\sqrt{3n}}$ such that $\frac{\mu}{\sqrt{q_n^2 + \|\mathbf{q}_{\mathcal{I} \setminus \{j,n\}}\|^2}} \leq 1$ for $\mathbf{q} \in \mathcal{S}_\xi^{n+}$, by Taylor approximation we have

$$\begin{aligned} & \text{erf}\left(\frac{\mu}{\sqrt{q_i^2 + \|\mathbf{q}_{\mathcal{I} \setminus \{j,n\}}\|^2}}\right) - \text{erf}\left(\frac{\mu}{\sqrt{q_n^2 + \|\mathbf{q}_{\mathcal{I} \setminus \{j,n\}}\|^2}}\right) \\ & \geq \frac{\mu}{2} \left[\frac{1}{\sqrt{q_i^2 + \|\mathbf{q}_{\mathcal{I} \setminus \{j,n\}}\|^2}} - \frac{1}{\sqrt{q_n^2 + \|\mathbf{q}_{\mathcal{I} \setminus \{j,n\}}\|^2}} \right] = \frac{\mu}{4} \int_{q_i^2}^{q_n^2} \frac{1}{(t^2 + \|\mathbf{q}_{\mathcal{I} \setminus \{j,n\}}\|^2)^{3/2}} dt. \end{aligned}$$

Therefore, we have

$$\begin{aligned} & \left\langle \text{grad } \mathbb{E}[\tilde{f}(\mathbf{q})], \frac{1}{q_j} \mathbf{e}_j - \frac{1}{q_n} \mathbf{e}_n \right\rangle \\ & \geq \frac{\theta(1-\theta)}{4} \int_{q_i^2}^{q_n^2} \frac{1}{(t^2 + \|\mathbf{q}_{\mathcal{I} \setminus \{j,n\}}\|^2)^{3/2}} dt \\ & \geq \frac{\theta(1-\theta)}{4} (q_n^2 - \|\mathbf{q}_{-n}\|_\infty^2) \geq \frac{\theta(1-\theta)}{4} \frac{\xi}{1+\xi} q_n^2 \geq \frac{\theta(1-\theta)}{4n} \frac{\xi}{1+\xi}. \end{aligned}$$

This gives the desired result. ■

G Gradient Concentration

In this section, under the same settings of Appendix E, we uniformly bound the deviation between the empirical process $\text{grad } \tilde{f}(\mathbf{q})$ and its mean $\mathbb{E}[\text{grad } \tilde{f}(\mathbf{q})]$ over the sphere. Namely, we show the following results.

Proposition G.1 *For every $i \in [n]$ and any $\delta \in (0, 1)$, when*

$$p \geq C \delta^{-2} n \log\left(\frac{\theta n}{\mu \delta}\right), \quad (63)$$

we have

$$\sup_{\mathbf{q} \in \mathbb{S}^{n-1}} \left| \left\langle \text{grad } \tilde{f}(\mathbf{q}) - \mathbb{E}[\text{grad } \tilde{f}(\mathbf{q})], \mathbf{e}_i \right\rangle \right| \leq \delta$$

holds with probability at least $1 - np^{-c_1 \theta n} - n \exp(-c_2 p \delta^2)$, for any \mathbf{e}_i . Here, c_1 , c_2 , and C are some universal positive numerical constants.

Remarks. Here, our bound is loose by roughly a factor of n because of the looseness in handling the probabilistic dependency due to the convolution measurement. We believe this bound can be improved by an order of $\mathcal{O}(n)$ using more advanced probability tools, such as decoupling and chaining [DIPG12, KMR14, QZEW17].

Proof First, note that

$$\tilde{f}(\mathbf{q}) = \frac{1}{np} \sum_{i=1}^p H_\mu(\mathbf{C}_{\mathbf{x}_i} \mathbf{q}), \quad \text{grad } \tilde{f}(\mathbf{q}) = \frac{1}{np} \mathcal{P}_{\mathbf{q}^\perp} \sum_{i=1}^p \mathbf{C}_{\mathbf{x}_i}^\top \nabla h_\mu(\mathbf{C}_{\mathbf{x}_i} \mathbf{q}). \quad (64)$$

Thus, we have

$$\begin{aligned} & \left\langle \text{grad } \tilde{f}(\mathbf{q}) - \mathbb{E} [\text{grad } \tilde{f}(\mathbf{q})], \mathbf{e}_n \right\rangle \\ &= \frac{1}{np} \sum_{i=1}^p \sum_{j=0}^{n-1} \left[\left\langle \mathcal{P}_{\mathbf{q}^\perp} s_j [\tilde{\mathbf{x}}_i], \mathbf{e}_n \right\rangle \nabla h_\mu \left(s_j [\tilde{\mathbf{x}}_i]^\top \mathbf{q} \right) - \mathbb{E} \left[\left(\mathbf{e}_n^\top \mathcal{P}_{\mathbf{q}^\perp} \mathbf{x} \right) \nabla h_\mu (\mathbf{x}^\top \mathbf{q}) \right] \right]. \end{aligned}$$

This is a summation of dependent random variables, which is very difficult to show measurement concentration in general. We alleviate this difficulty by only considering a partial summation of independent random variables, namely,

$$\mathcal{L}(\mathbf{q}) = \frac{1}{p} \frac{1}{\|\mathbf{P}_{\mathbf{q}^\perp} \mathbf{e}_n\|} \sum_{i=1}^p \left[\left\langle \mathcal{P}_{\mathbf{q}^\perp} \mathbf{x}_i, \mathbf{e}_n \right\rangle \nabla h_\mu (\mathbf{x}_i^\top \mathbf{q}) - \mathbb{E} \left[\left(\mathbf{e}_n^\top \mathcal{P}_{\mathbf{q}^\perp} \mathbf{x} \right) \nabla h_\mu (\mathbf{x}^\top \mathbf{q}) \right] \right],$$

where $\mathbf{x}_i \sim_{i.i.d.} \mathcal{BG}(\theta)$. Note that the bound of $\mathcal{L}(\mathbf{q})$ automatically gives an upper bound of

$$\left\langle \text{grad } \tilde{f}(\mathbf{q}) - \mathbb{E} [\text{grad } \tilde{f}(\mathbf{q})], \mathbf{e}_n \right\rangle$$

in distribution. To uniformly control $\mathcal{L}(\mathbf{q})$ over the sphere, we first consider controlling $\mathcal{L}(\mathbf{q})$ for a fixed $\mathbf{q} \in \mathbb{S}^{n-1}$. For each $\ell = 1, 2, \dots$, we have the moments

$$\mathbb{E} \left[\left| \left\langle \mathcal{P}_{\mathbf{q}^\perp} \mathbf{x}_i, \mathbf{e}_n \right\rangle \nabla h_\mu (\mathbf{x}_i^\top \mathbf{q}) \right|^\ell \right] \leq \mathbb{E} \left[\left| \mathbf{e}_n^\top \mathcal{P}_{\mathbf{q}^\perp} \mathbf{x}_i \right|^\ell \right] = \mathbb{E} \left[|Z_i|^\ell \right],$$

where conditioned on the Bernoulli distribution, we have $Z_i \sim \mathcal{N} \left(0, \left\| (\mathcal{P}_{\mathbf{q}^\perp} \mathbf{e}_n)_{\mathcal{J}} \right\|^2 \right)$. By Lemma B.1, we have

$$\mathbb{E} \left[\left| \left\langle \mathcal{P}_{\mathbf{q}^\perp} \mathbf{x}_i, \mathbf{e}_n \right\rangle \nabla h_\mu (\mathbf{x}_i^\top \mathbf{q}) \right|^\ell \right] \leq \mathbb{E}_{\mathcal{J}} \left[(\ell-1)!! \left\| (\mathcal{P}_{\mathbf{q}^\perp} \mathbf{e}_n)_{\mathcal{J}} \right\|^\ell \right] \leq \frac{\ell!}{2} \left\| \mathbf{P}_{\mathbf{q}^\perp} \mathbf{e}_n \right\|^\ell,$$

where we used the fact that $|\nabla h_\mu(z)| \leq 1$ for any z . Thus, we are controlling the concentration of summation of sub-Gaussian r.v., for which we have

$$\mathbb{P}(|\mathcal{L}(\mathbf{q})| \geq t) \leq \exp \left(-C \frac{pt^2}{2} \right).$$

Next, we turn this point-wise concentration into a uniform bound for all $\mathbf{q} \in \mathbb{S}^{n-1}$ via a standard covering argument. Let $\mathcal{N}(\varepsilon)$ be an ε -net of the sphere, whose cardinality can be controlled by

$$|\mathcal{N}(\varepsilon)| \leq \left(\frac{3}{\varepsilon} \right)^{n-1}.$$

Thus, we have

$$\mathbb{P} \left(\sup_{\mathbf{q} \in \mathcal{N}(\varepsilon)} |\mathcal{L}(\mathbf{q})| \geq t \right) \leq \left(\frac{3}{\varepsilon} \right)^{n-1} \exp \left(-\frac{pt^2}{2+2t} \right).$$

For any point $\mathbf{q} \in \mathbb{S}^{n-1}$, it can be written as $\mathbf{q} = \mathbf{q}' + \mathbf{e}$, where $\mathbf{q}' \in \mathcal{N}(\varepsilon)$ and $\|\mathbf{e}\| \leq \varepsilon$. Now we control the all points over the sphere through the Lipschitz property of \mathcal{L} .

$$\begin{aligned}
& \sup_{\mathbf{q} \in \mathbb{S}^{n-1}} |\mathcal{L}(\mathbf{q})| \\
&= \sup_{\mathbf{q}' \in \mathcal{N}(\varepsilon), \|\mathbf{e}\| \leq \varepsilon} |\mathcal{L}(\mathbf{q}' + \mathbf{e})| \\
&\leq \underbrace{\sup_{\mathbf{q}' \in \mathcal{N}(\varepsilon)} |\mathcal{L}(\mathbf{q}')| + \sup_{\mathbf{q}' \in \mathcal{N}(\varepsilon), \|\mathbf{e}\| \leq \varepsilon} \left| \mathbb{E} \left[(\mathbf{e}_n^\top \mathcal{P}_{(\mathbf{q}'+\mathbf{e})^\perp} \mathbf{x} - \mathbf{e}_n^\top \mathcal{P}_{(\mathbf{q}')^\perp} \mathbf{x}) \nabla h_\mu(\mathbf{x}^\top \mathbf{q}') \right] \right|}_{\mathcal{L}_1} \\
&\quad + \underbrace{\sup_{\mathbf{q}' \in \mathcal{N}(\varepsilon), \|\mathbf{e}\| \leq \varepsilon} \left| \mathbb{E} \left[(\mathbf{e}_n^\top \mathcal{P}_{(\mathbf{q}'+\mathbf{e})^\perp} \mathbf{x}) (\nabla h_\mu(\mathbf{x}^\top (\mathbf{q}' + \mathbf{e})) - \nabla h_\mu(\mathbf{x}^\top \mathbf{q}')) \right] \right|}_{\mathcal{L}_2} \\
&\quad + \underbrace{\sup_{\mathbf{q}' \in \mathcal{N}(\varepsilon), \|\mathbf{e}\| \leq \varepsilon} \left| \frac{1}{p} \sum_{i=1}^p [\mathbf{e}_n^\top \mathcal{P}_{(\mathbf{q}'+\mathbf{e})^\perp} \mathbf{x}_i - \mathbf{e}_n^\top \mathcal{P}_{(\mathbf{q}')^\perp} \mathbf{x}_i] \nabla h_\mu(\mathbf{x}_i^\top \mathbf{q}') \right|}_{\mathcal{L}_3} \\
&\quad + \underbrace{\sup_{\mathbf{q}' \in \mathcal{N}(\varepsilon), \|\mathbf{e}\| \leq \varepsilon} \left| \frac{1}{p} \sum_{i=1}^p (\mathbf{e}_n^\top \mathcal{P}_{(\mathbf{q}'+\mathbf{e})^\perp} \mathbf{x}_i) [\nabla h_\mu(\mathbf{x}_i^\top (\mathbf{q}' + \mathbf{e})) - \nabla h_\mu(\mathbf{x}_i^\top \mathbf{q}')] \right|}_{\mathcal{L}_4}.
\end{aligned}$$

By Lipschitz continuity and the fact that $\nabla h_\mu(z) \leq 1$ for any z , we obtain

$$\begin{aligned}
\mathcal{L}_1 &\leq \sup_{\mathbf{q}' \in \mathcal{N}(\varepsilon), \|\mathbf{e}\| \leq \varepsilon} \sqrt{\theta} \|(\mathcal{P}_{(\mathbf{q}'+\mathbf{e})^\perp} - \mathcal{P}_{(\mathbf{q}')^\perp}) \mathbf{e}_n\| \leq 3\sqrt{\theta}\varepsilon \\
\mathcal{L}_2 &\leq \sup_{\mathbf{q}' \in \mathcal{N}(\varepsilon), \|\mathbf{e}\| \leq \varepsilon} \frac{1}{\mu} \mathbb{E} [\|\mathbf{x}\| \|\mathbf{x}^\top \mathbf{e}\|] \leq \frac{\theta n}{\mu} \varepsilon.
\end{aligned}$$

For each \mathbf{x}_i , we know that $\mathbf{x}_i = \mathbf{g}_i \odot \mathbf{b}_i$ with $\mathbf{g}_i \sim \mathcal{N}(\mathbf{0}, \mathbf{I})$ and $\mathbf{b}_i \sim_{i.i.d.} \mathcal{B}(\theta)$. By Gaussian concentration inequality, we know that for each \mathbf{x}_i ,

$$\mathbb{P}(\|\mathbf{x}_i\| - \sqrt{\theta n} \geq t) \leq \mathbb{P}(\|\mathbf{x}_i\| - \mathbb{E}[\|\mathbf{x}_i\|] \geq t) \leq \exp\left(-\frac{t^2}{2\|\mathbf{b}_i\|_\infty}\right) \leq \exp\left(-\frac{t^2}{2}\right).$$

Therefore, by a union bound, we have

$$\max_{1 \leq i \leq p} \|\mathbf{x}_i\| \leq 5\sqrt{\theta n \log p}$$

holds with probability at least $1 - p^{-8\theta n}$. Therefore, w.h.p we have

$$\begin{aligned}
\mathcal{L}_3 &\leq \left(\max_{1 \leq i \leq p} \|\mathbf{x}_i\| \right) \sup_{\mathbf{q}' \in \mathcal{N}(\varepsilon), \|\mathbf{e}\| \leq \varepsilon} \|\mathcal{P}_{(\mathbf{q}'+\mathbf{e})^\perp} - \mathcal{P}_{(\mathbf{q}')^\perp}\| \leq 15\sqrt{\theta n \log p} \varepsilon, \\
\mathcal{L}_4 &\leq \frac{1}{\mu} \left(\max_{1 \leq i \leq p} \|\mathbf{x}_i\|^2 \right) \sup_{\mathbf{q}' \in \mathcal{N}(\varepsilon), \|\mathbf{e}\| \leq \varepsilon} \|\mathbf{e}\| \leq 25 \frac{\theta n \log p}{\mu} \varepsilon.
\end{aligned}$$

Combining the bounds above, choose $\varepsilon = \frac{\mu t}{c\theta n \log p}$, we have

$$\sup_{\mathbf{q} \in \mathbb{S}^{n-1}} |\mathcal{L}(\mathbf{q})| \leq \sup_{\mathbf{q}' \in \mathcal{N}(\varepsilon)} |\mathcal{L}(\mathbf{q}')| + c \frac{\theta n \log p}{\mu} \varepsilon \leq 2t$$

holds with probability at least

$$1 - p^{-8\theta n} - \exp\left(-C\frac{pt^2}{2} + c'n \log\left(\frac{\theta n}{\mu t}\right)\right).$$

Thus, applying a union bound, we obtain the desired result holding for every $i \in [n]$. ■

Similarly, we also show the following result.

Corollary G.2 *For any $\delta \in (0, 1)$, when*

$$p \geq C\delta^{-2}n^2 \log\left(\frac{\theta n}{\mu\delta}\right), \quad (65)$$

we have

$$\begin{aligned} \sup_{\mathbf{q} \in \mathbb{S}^{n-1}} \left\| \text{grad } \tilde{f}(\mathbf{q}) - \mathbb{E} \left[\text{grad } \tilde{f}(\mathbf{q}) \right] \right\| &\leq \delta, \\ \sup_{\mathbf{q} \in \mathbb{S}^{n-1}} \left\| \nabla \tilde{f}(\mathbf{q}) - \mathbb{E} \left[\nabla \tilde{f}(\mathbf{q}) \right] \right\| &\leq \delta, \end{aligned}$$

hold with probability at least $1 - p^{-c_1\theta n} - n \exp(-c_2p\delta^2)$. Here, c_1 , c_2 , and C are some universal positive numerical constants.

Proof From Proposition G.1, we know that when $p \geq C_0\varepsilon^{-2}n \log\left(\frac{\theta n}{\mu\varepsilon}\right)$,

$$\begin{aligned} &\sup_{\mathbf{q} \in \mathbb{S}^{n-1}} \left\| \text{grad } \tilde{f}(\mathbf{q}) - \mathbb{E} \left[\text{grad } \tilde{f}(\mathbf{q}) \right] \right\|^2 \\ &\leq \sum_{i=1}^n \sup_{\mathbf{q} \in \mathbb{S}^{n-1}} \left| \left\langle \text{grad } \tilde{f}(\mathbf{q}) - \mathbb{E} \left[\text{grad } \tilde{f}(\mathbf{q}) \right], \mathbf{e}_i \right\rangle \right|^2 \leq n\varepsilon^2. \end{aligned}$$

holds with probability at least $1 - p^{-c_1\theta n} - n \exp(-c_2p\delta^2)$. Therefore, by letting $\delta = \sqrt{n}\varepsilon$, w.h.p. we have

$$\sup_{\mathbf{q} \in \mathbb{S}^{n-1}} \left\| \text{grad } \tilde{f}(\mathbf{q}) - \mathbb{E} \left[\text{grad } \tilde{f}(\mathbf{q}) \right] \right\| \leq \delta,$$

whenever $p \geq C\delta^{-2}n^2 \log\left(\frac{\theta n}{\mu\delta}\right)$. By a similar argument, we can also provide the same bound for

$$\sup_{\mathbf{q} \in \mathbb{S}^{n-1}} \left\| \nabla \tilde{f}(\mathbf{q}) - \mathbb{E} \left[\nabla \tilde{f}(\mathbf{q}) \right] \right\|$$

.

■

Corollary G.3 *For each $i \in [n]$ and any $\delta \in (0, 1)$, when $p \geq C\delta^{-2}n \log\left(\frac{\theta n}{\mu\delta}\right)$, we have*

$$\sup_{\mathbf{q} \in \mathbb{S}^{n-1}} \left| \left\langle \text{grad } \tilde{f}(\mathbf{q}), \mathbf{e}_i \right\rangle \right| \leq 1 + \delta,$$

hold with probability at least $1 - np^{-c_1\theta n} - n \exp(-c_2p\delta^2)$. Here, c_1 , c_2 , and C are some universal positive numerical constants.

Proof For any $\mathbf{q} \in \mathbb{S}^{n-1}$ and every $i \in [n]$, we have

$$\mathbb{E} \left[\left| \langle \text{grad } \tilde{f}(\mathbf{q}), \mathbf{e}_i \rangle \right| \right] = \mathbb{E} \left[\left| (\mathbf{e}_i^\top \mathcal{P}_{\mathbf{q}^\perp} \mathbf{x}) \cdot \nabla h_\mu(\mathbf{x}^\top \mathbf{q}) \right| \right] \leq \mathbb{E} \left[\left\| \mathbf{e}_i^\top \mathcal{P}_{\mathbf{q}^\perp} \mathbf{x} \right\| \right] \leq 1.$$

Thus, we have

$$\begin{aligned} & \sup_{\mathbf{q} \in \mathbb{S}^{n-1}} \left| \langle \text{grad } \tilde{f}(\mathbf{q}) - \mathbb{E} [\text{grad } \tilde{f}(\mathbf{q})], \mathbf{e}_i \rangle \right| \\ & \geq \sup_{\mathbf{q} \in \mathbb{S}^{n-1}} \left(\left| \langle \text{grad } \tilde{f}(\mathbf{q}), \mathbf{e}_i \rangle \right| - \mathbb{E} \left[\left| \langle \text{grad } \tilde{f}(\mathbf{q}), \mathbf{e}_i \rangle \right| \right] \right) \\ & \geq \sup_{\mathbf{q} \in \mathbb{S}^{n-1}} \left| \langle \text{grad } \tilde{f}(\mathbf{q}), \mathbf{e}_i \rangle \right| - \sup_{\mathbf{q} \in \mathbb{S}^{n-1}} \mathbb{E} \left[\left| \langle \text{grad } \tilde{f}(\mathbf{q}), \mathbf{e}_i \rangle \right| \right]. \end{aligned}$$

Therefore, by using the result in Proposition G.1, we obtain the desired result. \blacksquare

Corollary G.4 For any $\delta \in (0, 1)$, when p satisfies (65), we have

$$\sup_{\mathbf{q} \in \mathbb{S}^{n-1}} \left\| \text{grad } \tilde{f}(\mathbf{q}) \right\| \leq \sqrt{\theta n} + \delta,$$

hold with probability at least $1 - p^{-c_1 \theta n} - n \exp(-c_2 p \delta^2)$. Here, c_1 , c_2 , and C are some universal positive numerical constants.

Proof For any $\mathbf{q} \in \mathbb{S}^{n-1}$, we have

$$\mathbb{E} \left[\left\| \text{grad } \tilde{f}(\mathbf{q}) \right\| \right] = \mathbb{E} \left[\left\| \mathcal{P}_{\mathbf{q}^\perp} \mathbf{x} \nabla h_\mu(\mathbf{x}^\top \mathbf{q}) \right\| \right] \leq \mathbb{E} \left[\left\| \mathbf{x} \right\| \right] \leq \sqrt{\theta n}.$$

Note that

$$\begin{aligned} \sup_{\mathbf{q} \in \mathbb{S}^{n-1}} \left\| \text{grad } \tilde{f}(\mathbf{q}) - \mathbb{E} [\text{grad } \tilde{f}(\mathbf{q})] \right\| & \geq \sup_{\mathbf{q} \in \mathbb{S}^{n-1}} \left(\left\| \text{grad } \tilde{f}(\mathbf{q}) \right\| - \mathbb{E} \left[\left\| \text{grad } \tilde{f}(\mathbf{q}) \right\| \right] \right) \\ & \geq \sup_{\mathbf{q} \in \mathbb{S}^{n-1}} \left\| \text{grad } \tilde{f}(\mathbf{q}) \right\| - \sup_{\mathbf{q} \in \mathbb{S}^{n-1}} \mathbb{E} \left[\left\| \text{grad } \tilde{f}(\mathbf{q}) \right\| \right]. \end{aligned}$$

Thus, by using the result in Corollary G.2, we obtain the desired result. \blacksquare

H Preconditioning

In this section, given the Riemannian gradient of $\tilde{f}(\mathbf{q})$ in (10) and its preconditioned variant

$$\begin{aligned} \text{grad } \tilde{f}(\mathbf{q}) &= \frac{1}{np} \mathcal{P}_{\mathbf{q}^\perp} \sum_{i=1}^p \mathbf{C}_{\mathbf{x}_i}^\top \nabla h_\mu(\mathbf{C}_{\mathbf{x}_i} \mathbf{q}), \\ \text{grad } f(\mathbf{q}) &= \frac{1}{np} \mathcal{P}_{\mathbf{q}^\perp} \sum_{i=1}^p (\mathbf{R} \mathbf{Q}^{-1})^\top \mathbf{C}_{\mathbf{x}_i}^\top \nabla h_\mu(\mathbf{C}_{\mathbf{x}_i} (\mathbf{R} \mathbf{Q}^{-1}) \mathbf{q}), \end{aligned}$$

with

$$\mathbf{R} = \mathbf{C}_a \left(\frac{1}{\theta np} \sum_{i=1}^p \mathbf{C}_{\mathbf{y}_i}^\top \mathbf{C}_{\mathbf{y}_i} \right)^{-1/2}, \quad \mathbf{Q} = \mathbf{C}_a (\mathbf{C}_a^\top \mathbf{C}_a)^{-1/2},$$

we prove that they are very close via a perturbation analysis by using the Lipschitz property of first-order derivative of Huber loss.

Proposition H.1 Suppose $\theta \geq \frac{1}{n}$. For any $\delta \in (0, 1)$, whenever

$$p \geq C \frac{\kappa^8 n}{\mu^2 \theta \delta^2 \sigma_{\min}^2} \log^4 n \log \left(\frac{\theta n}{\mu} \right),$$

we have

$$\sup_{\mathbf{q} \in \mathbb{S}^{n-1}} \left\| \text{grad } \tilde{f}(\mathbf{q}) - \text{grad } f(\mathbf{q}) \right\| \leq \delta$$

holds with probability at least $1 - c_1 p^{-c_2 n \theta} - n^{-c_3} - n e^{-c_4 \theta n p}$. Here, κ and σ_{\min} denote the condition number and minimum singular value of \mathbf{C}_a , and c_1, c_2, c_3, c_4 and C are some positive numerical constants.

Proof Notice that

$$\mathbf{RQ}^{-1} = \mathbf{C}_a \left(\frac{1}{\theta n p} \sum_{i=1}^p \mathbf{C}_{\mathbf{y}_i}^\top \mathbf{C}_{\mathbf{y}_i} \right)^{-1/2} (\mathbf{C}_a^\top \mathbf{C}_a)^{1/2} \mathbf{C}_a^{-1}.$$

Thus, we have

$$\begin{aligned} & \sup_{\mathbf{q} \in \mathbb{S}^{n-1}} \left\| \text{grad } \tilde{f}(\mathbf{q}) - \text{grad } f(\mathbf{q}) \right\| \\ & \leq \frac{1}{np} \left\| \mathcal{P}_{\mathbf{q}^\perp} (\mathbf{I} - (\mathbf{RQ}^{-1}))^\top \sum_{i=1}^p \mathbf{C}_{\mathbf{x}_i}^\top \nabla h_\mu(\mathbf{C}_{\mathbf{x}_i} \mathbf{q}) \right\| \\ & \quad + \frac{1}{np} \left\| \mathcal{P}_{\mathbf{q}^\perp} (\mathbf{RQ}^{-1})^\top \sum_{i=1}^p \mathbf{C}_{\mathbf{x}_i}^\top [\nabla h_\mu(\mathbf{C}_{\mathbf{x}_i} \mathbf{q}) - \nabla h_\mu(\mathbf{C}_{\mathbf{x}_i} (\mathbf{RQ}^{-1}) \mathbf{q})] \right\| \\ & \leq \|\mathbf{I} - \mathbf{RQ}^{-1}\| \left\| \nabla \tilde{f}(\mathbf{q}) \right\| + \|\mathbf{RQ}^{-1}\| \left\| \frac{1}{np} \sum_{i=1}^p \mathbf{C}_{\mathbf{x}_i}^\top [\nabla h_\mu(\mathbf{C}_{\mathbf{x}_i} \mathbf{q}) - \nabla h_\mu(\mathbf{C}_{\mathbf{x}_i} (\mathbf{RQ}^{-1}) \mathbf{q})] \right\| \\ & \leq \|\mathbf{I} - \mathbf{RQ}^{-1}\| \left\| \nabla \tilde{f}(\mathbf{q}) \right\| + \frac{1}{\mu \sqrt{n}} \|\mathbf{RQ}^{-1}\| \left(\max_{1 \leq i \leq p} \|\mathbf{x}_i\| \|\mathbf{F} \mathbf{x}_i\|_\infty \right) \|\mathbf{I} - \mathbf{RQ}^{-1}\|. \end{aligned} \quad (66)$$

Here, by Lemma H.4, for any given $\varepsilon \in (0, 1)$, when $p \geq C \frac{\kappa^8}{\theta \varepsilon^2 \sigma_{\min}^2(\mathbf{C}_a)} \log^3 n$, we have

$$\|\mathbf{RQ}^{-1} - \mathbf{I}\| \leq \varepsilon, \quad \|\mathbf{RQ}^{-1}\| \leq 1 + \varepsilon, \quad (67)$$

holding with probability at least $1 - p^{-c_1 n \theta} - n^{-c_2}$. On the other hand, by Gaussian concentration inequality and a union bound, we have

$$\max_{1 \leq i \leq p} \|\mathbf{x}_i\| \leq 4\sqrt{n \log p}, \quad \max_{1 \leq i \leq p} \|\mathbf{F} \mathbf{x}_i\|_\infty \leq 4\sqrt{n \log p}, \quad (68)$$

hold with probability at least $1 - p^{-c_3 n}$. By Corollary G.4, when $p \geq C_2 \theta^{-1} n \log \left(\frac{\theta n}{\mu} \right)$, we have

$$\sup_{\mathbf{q} \in \mathbb{S}^{n-1}} \left\| \text{grad } \tilde{f}(\mathbf{q}) \right\| \leq 2\sqrt{\theta n} \quad (69)$$

holds with probability at least $1 - p^{-c_4 \theta n} - n e^{-c_5 \theta n p}$. Plugging the bounds in (67) and (68) into (66), we obtain

$$\sup_{\mathbf{q} \in \mathbb{S}^{n-1}} \left\| \text{grad } \tilde{f}(\mathbf{q}) - \text{grad } f(\mathbf{q}) \right\| \leq \varepsilon \left[2\sqrt{\theta n} + \frac{16\sqrt{n \log p}}{\mu} \cdot (1 + \varepsilon) \right].$$

By a change of variable, we obtain the desired result. ■

Lemma H.2 When $\theta \geq 1/n$,

$$\left\| \frac{1}{\theta np} \sum_{i=1}^p \mathbf{C}_{\mathbf{x}_i}^\top \mathbf{C}_{\mathbf{x}_i} - \mathbf{I} \right\| \leq t \quad (70)$$

holds with probability at least $1 - p^{-c_1 n \theta} - n \exp \left(-c_2 \min \left\{ \frac{pt^2}{\theta \log p}, \frac{pt}{\sqrt{\theta \log p}} \right\} \right)$ for some numerical constants $c_1, c_2 > 0$.

Proof Notice that

$$\mathbf{C}_{\mathbf{x}_i}^\top \mathbf{C}_{\mathbf{x}_i} = \mathbf{F}^* \text{diag} \left(|\mathbf{F} \mathbf{x}_i|^{\odot 2} \right) \mathbf{F}.$$

Then

$$\begin{aligned} \left\| \frac{1}{\theta np} \sum_{i=1}^p \mathbf{C}_{\mathbf{x}_i}^\top \mathbf{C}_{\mathbf{x}_i} - \mathbf{I} \right\| &= \left\| \mathbf{F}^* \left(\text{diag} \left(\frac{1}{\theta np} \sum_{i=1}^p |\mathbf{F} \mathbf{x}_i|^{\odot 2} \right) - \mathbf{F}^{-1} (\mathbf{F}^*)^{-1} \right) \mathbf{F} \right\| \\ &= \left\| \frac{1}{\theta np} \sum_{i=1}^p |\mathbf{F} \mathbf{x}_i|^{\odot 2} - \mathbf{1} \right\|_{\infty}. \end{aligned} \quad (71)$$

Let $\mathbf{x}_i = \mathbf{b}_i \odot \mathbf{g}_i$ with $\mathbf{b}_i \sim_{i.i.d.} \mathcal{B}(\theta)$ and $\mathbf{g}_i \sim \mathcal{N}(\mathbf{0}, \mathbf{I})$, and let us define events

$$\mathcal{E}_{i,j} \doteq \left\{ \|\mathbf{b}_i \odot \mathbf{f}_j\|^2 \leq 5n\sqrt{\theta \log p} \right\}, \quad 1 \leq i \leq p, 1 \leq j \leq n.$$

We use $\mathcal{E}_j = \bigcap_{i=1}^p \mathcal{E}_{i,j}$. For each individual i and j , by the Hoeffding's inequality, we have

$$\mathbb{P}(\mathcal{E}_{i,j}^c) \leq \exp(-8n\theta \log p)$$

For each $j = 1, \dots, n$, by conditional probability and union bound, we have

$$\begin{aligned} \mathbb{P} \left(\left| \frac{1}{\theta np} \sum_{i=1}^p |\mathbf{f}_j^* \mathbf{x}_i|^2 - 1 \right| \geq t \right) &\leq \mathbb{P} \left(\bigcup_{i=1}^p \mathcal{E}_{i,j}^c \right) + \mathbb{P} \left(\left| \frac{1}{\theta np} \sum_{i=1}^p |\mathbf{f}_j^* \mathbf{x}_i|^2 - 1 \right| \geq t \mid \mathcal{E}_j \right) \\ &\leq \sum_{i=1}^p \mathbb{P}(\mathcal{E}_{i,j}^c) + \mathbb{P} \left(\left| \frac{1}{\theta np} \sum_{i=1}^p |\mathbf{f}_j^* \mathbf{x}_i|^2 - 1 \right| \geq t \mid \mathcal{E}_j \right) \\ &\leq pe^{-8n\theta \log p} + \mathbb{P} \left(\left| \frac{1}{\theta np} \sum_{i=1}^p |\mathbf{f}_j^* \mathbf{x}_i|^2 - 1 \right| \geq t \mid \mathcal{E}_j \right). \end{aligned} \quad (72)$$

For the second term, since $\mathbf{x}_i \sim \mathcal{BG}(\theta)$, we have

$$\mathbf{f}_j^* \mathbf{x}_i = \sum_{k=1}^n f_{ji} b_{ik} g_{ik} \sim \mathcal{N} \left(0, \|\mathbf{b}_i \odot \mathbf{f}_j\|^2 \right)$$

for all $\ell \geq 1$, by Lemma B.1, we have

$$\begin{aligned} \mathbb{E} \left[(\theta n)^{-\ell} |\mathbf{f}_j^* \mathbf{x}_i|^{2\ell} \mid \mathcal{E}_{i,j} \right] &= \frac{(2\ell-1)!!}{(\theta n)^\ell} \mathbb{E} \left[\|\mathbf{b} \odot \mathbf{f}\|^{2\ell} \mid \mathcal{E}_{i,j} \right] \\ &\leq \frac{\ell!}{2} 10^\ell \theta^{-\ell/2} \log^{\ell/2} p. \end{aligned}$$

Thus, by Bernstein inequality in Lemma B.3, we have

$$\begin{aligned} \mathbb{P} \left(\left| \frac{1}{\theta np} \sum_{i=1}^p |\mathbf{f}_j^* \mathbf{x}_i|^2 - 1 \right| \geq t \mid \mathcal{E}_j \right) &\leq \exp \left(-\frac{pt^2}{200\theta \log p + 20\sqrt{\theta \log pt}} \right) \\ &\leq \exp \left(-\min \left\{ \frac{pt^2}{400\theta \log p}, \frac{pt}{40\sqrt{\theta \log p}} \right\} \right). \end{aligned} \quad (73)$$

Plugging (73) into (72), we obtain

$$\left| \frac{1}{\theta np} \sum_{i=1}^p |\mathbf{f}_j^* \mathbf{x}_i|^2 - 1 \right| \leq t$$

holds with high probability for each $j = 1, \dots, n$. We apply a union bound to control the ℓ_∞ -norm in (71), and hence get the desired result. \blacksquare

Lemma H.3 For any $\varepsilon \in (0, 1)$, when $p \geq C\theta^{-1}\varepsilon^{-2} \log^3 n$, we have

$$\begin{aligned} \left\| \frac{1}{\theta np} \sum_{i=1}^p \mathbf{C}_{\mathbf{y}_i}^\top \mathbf{C}_{\mathbf{y}_i} \right\| &\leq (1 + \varepsilon) \|\mathbf{C}_a\|^2 \\ \left\| \left(\frac{1}{\theta np} \sum_{i=1}^p \mathbf{C}_{\mathbf{y}_i}^\top \mathbf{C}_{\mathbf{y}_i} \right)^{-1/2} - (\mathbf{C}_a^\top \mathbf{C}_a)^{-1/2} \right\| &\leq \frac{4\kappa^2 \varepsilon}{\sigma_{\min}^2(\mathbf{C}_a)} \end{aligned}$$

holds with probability at least $1 - p^{-c_1 n^\theta} - n^{-c_2}$. Here, κ is the condition number of \mathbf{C}_a , and $\sigma_{\min}(\mathbf{C}_a)$ is the smallest singular value of \mathbf{C}_a .

Proof For any $\varepsilon \in (0, 1)$, from Lemma H.2, when $p \geq C\theta^{-1}\varepsilon^{-2} \log^3 n$ we know that the event

$$\mathcal{E}(\varepsilon) \doteq \left\{ \left\| \frac{1}{\theta np} \sum_{i=1}^p \mathbf{C}_{\mathbf{x}_i}^\top \mathbf{C}_{\mathbf{x}_i} - \mathbf{I} \right\| \leq \varepsilon \right\}$$

holds with probability at least $1 - p^{-c_1 n^\theta} - n^{-c_2}$. Conditioned on the event $\mathcal{E}(\varepsilon)$, let us denote

$$\mathbf{A} = \mathbf{C}_a^\top \mathbf{C}_a > \mathbf{0},$$

and let $\sigma_{\max}(\mathbf{A})$, $\sigma_{\min}(\mathbf{A})$ be the largest and smallest singular values of \mathbf{A} , respectively. Then we observe,

$$\begin{aligned} \frac{1}{\theta np} \sum_{i=1}^p \mathbf{C}_{\mathbf{y}_i}^\top \mathbf{C}_{\mathbf{y}_i} &= \mathbf{C}_a^\top \mathbf{C}_a + \underbrace{\mathbf{C}_a^\top \left[\frac{1}{\theta np} \sum_{i=1}^p \mathbf{C}_{\mathbf{x}_i}^\top \mathbf{C}_{\mathbf{x}_i} - \mathbf{I} \right] \mathbf{C}_a}_{\mathbf{\Delta}} \\ &= \mathbf{A} + \mathbf{\Delta}, \quad \|\mathbf{\Delta}\| \leq \varepsilon \cdot \sigma_{\max}(\mathbf{A}). \end{aligned}$$

Therefore, we have

$$\left\| \frac{1}{\theta np} \sum_{i=1}^p \mathbf{C}_{\mathbf{y}_i}^\top \mathbf{C}_{\mathbf{y}_i} \right\| \leq \|\mathbf{A}\| + \|\mathbf{\Delta}\| \leq (1 + \varepsilon) \|\mathbf{C}_a\|^2.$$

By Lemma B.12, whenever

$$\|\mathbf{\Delta}\| \leq \frac{1}{2} \sigma_{\min}(\mathbf{A}) \implies \varepsilon \leq \frac{1}{2} \frac{\sigma_{\min}(\mathbf{A})}{\sigma_{\max}(\mathbf{A})} = \frac{1}{2\kappa^2},$$

we know that

$$\begin{aligned} \left\| \left(\frac{1}{\theta np} \sum_{i=1}^p \mathbf{C}_{\mathbf{y}_i}^\top \mathbf{C}_{\mathbf{y}_i} \right)^{-1/2} - (\mathbf{C}_a^\top \mathbf{C}_a)^{-1/2} \right\| &= \left\| (\mathbf{A} + \mathbf{\Delta})^{-1/2} - \mathbf{A}^{-1/2} \right\| \\ &\leq \frac{4 \|\mathbf{\Delta}\|}{\sigma_{\min}^2(\mathbf{A})} \leq \frac{4\varepsilon \sigma_{\max}(\mathbf{A})}{\sigma_{\min}^2(\mathbf{A})} = \frac{4\kappa^2 \varepsilon}{\sigma_{\min}^2(\mathbf{C}_a)}. \end{aligned}$$

■

Lemma H.4 Let $\theta \in (1/n, 1/3)$, and given a $\delta \in (0, 1)$. Whenever

$$p \geq C \frac{\kappa^8}{\theta \delta^2 \sigma_{\min}^2(\mathbf{C}_a)} \log^3 n,$$

we have

$$\begin{aligned} \|\mathbf{RQ}^{-1} - \mathbf{I}\| &\leq \delta, & \|\mathbf{RQ}^{-1}\| &\leq 1 + \delta, \\ \|(\mathbf{RQ}^{-1})^{-1} - \mathbf{I}\| &\leq 2\delta, & \|(\mathbf{RQ}^{-1})^{-1}\| &\leq 1 + 2\delta \end{aligned}$$

hold with probability at least $1 - p^{-c_1 n \theta} - n^{-c_2}$.

Proof First, by Lemma H.3, for a given $\varepsilon \in (0, 1)$, when $p \geq C_1 \theta^{-1} \varepsilon^{-2} \log^3 n$, we have

$$\begin{aligned} \|\mathbf{RQ}^{-1} - \mathbf{I}\| &= \left\| \mathbf{I} - \mathbf{C}_a \left(\frac{1}{\sqrt{\theta np}} \sum_{i=1}^p \mathbf{C}_{\mathbf{y}_i}^\top \mathbf{C}_{\mathbf{y}_i} \right)^{-1/2} (\mathbf{C}_a^\top \mathbf{C}_a)^{1/2} \mathbf{C}_a^{-1} \right\| \\ &\leq \kappa \cdot \|\mathbf{C}_a\| \cdot \left\| \left(\frac{1}{\theta np} \sum_{i=1}^p \mathbf{C}_{\mathbf{y}_i}^\top \mathbf{C}_{\mathbf{y}_i} \right)^{-1/2} - (\mathbf{C}_a^\top \mathbf{C}_a)^{-1/2} \right\| \\ &\leq \kappa \|\mathbf{C}_a\| \frac{4\kappa^2 \varepsilon}{\sigma_{\min}^2(\mathbf{C}_a)} \leq \frac{4\kappa^4 \varepsilon}{\sigma_{\min}(\mathbf{C}_a)}, \end{aligned}$$

and

$$\|\mathbf{RQ}^{-1}\| \leq 1 + \|\mathbf{I} - \mathbf{RQ}^{-1}\| \leq 1 + \frac{4\kappa^4 \varepsilon}{\sigma_{\min}(\mathbf{C}_a)}$$

hold with probability at least $1 - p^{-c_1 n \theta} - n^{-c_2}$. Similarly, by Lemma H.3,

$$\begin{aligned} \|\mathbf{I} - (\mathbf{RQ}^{-1})^{-1}\| &= \left\| \mathbf{I} - \mathbf{C}_a (\mathbf{C}_a^\top \mathbf{C}_a)^{-1/2} \left(\frac{1}{\sqrt{\theta np}} \sum_{i=1}^p \mathbf{C}_{\mathbf{y}_i}^\top \mathbf{C}_{\mathbf{y}_i} \right)^{1/2} \mathbf{C}_a^{-1} \right\| \\ &\leq \kappa \cdot \left\| \frac{1}{\theta np} \sum_{i=1}^p \mathbf{C}_{\mathbf{y}_i}^\top \mathbf{C}_{\mathbf{y}_i} \right\|^{1/2} \cdot \left\| \left(\frac{1}{\theta np} \sum_{i=1}^p \mathbf{C}_{\mathbf{y}_i}^\top \mathbf{C}_{\mathbf{y}_i} \right)^{-1/2} - (\mathbf{C}_a^\top \mathbf{C}_a)^{-1/2} \right\| \\ &\leq \kappa \cdot \frac{4\kappa^2 \varepsilon}{\sigma_{\min}^2(\mathbf{C}_a)} \cdot (1 + \varepsilon)^{1/2} \|\mathbf{C}_a\| \leq \frac{8\kappa^4 \varepsilon}{\sigma_{\min}(\mathbf{C}_a)}, \end{aligned}$$

and

$$\|(\mathbf{RQ}^{-1})^{-1}\| \leq 1 + \|\mathbf{I} - (\mathbf{RQ}^{-1})^{-1}\| \leq 1 + \frac{8\kappa^4 \varepsilon}{\sigma_{\min}(\mathbf{C}_a)}$$

Thus, replace $\delta = \frac{4\kappa^4 \varepsilon}{\sigma_{\min}(\mathbf{C}_a)}$, we obtain the desired result.

■

Table 2: Gradient for each different loss function

Loss function	$\nabla\varphi(\mathbf{q})$ for 1D problem (74)	$\nabla\varphi(\mathbf{Z})$ for 2D problem ²¹ (75)
ℓ^1 -loss	$\frac{1}{np} \sum_{i=1}^p \check{\mathbf{y}}_i \odot \text{sign}(\bar{\mathbf{y}}_i \odot \mathbf{q})$	$\frac{1}{n^2p} \sum_{i=1}^p \check{\bar{\mathbf{Y}}}_i \boxtimes \text{sign}(\bar{\mathbf{Y}}_i \boxtimes \mathbf{Z})$
Huber-loss	$\frac{1}{np} \sum_{i=1}^p \check{\mathbf{y}}_i \odot \nabla h_\mu(\bar{\mathbf{y}}_i \odot \mathbf{q})$	$\frac{1}{n^2p} \sum_{i=1}^p \check{\bar{\mathbf{Y}}}_i \boxtimes \nabla h_\mu(\bar{\mathbf{Y}}_i \boxtimes \mathbf{Z})$
ℓ^4 -loss	$-\frac{1}{np} \sum_{i=1}^p \check{\mathbf{y}}_i \odot (\bar{\mathbf{y}}_i \odot \mathbf{q})^{\odot 3}$	$-\frac{1}{n^2p} \sum_{i=1}^p \check{\bar{\mathbf{Y}}}_i \boxtimes (\bar{\mathbf{Y}}_i \boxtimes \mathbf{Z})^{\odot 3}$

I Algorithms and Implementation Details

It should be noted that the rotated problem in (9) and (10) are only for analysis purposes. In this section, we provide detailed descriptions of the actual implementation of our algorithms on optimizing the problem in the form of (4). First, we introduce the details Riemannian (sub)gradient descent method for 1D problem. Second, we discuss about subgradient methods for solving the LP rounding problem. Finally, we provide more details about how to solve problems in 2D.

For the purpose of implementation efficiency, we describe the problem and algorithms based on circulant convolution, which is slightly different from the main sections. Because our gradient descent method works for any sparse promoting loss function (other than Huber loss), in the following we describe the problem and the algorithm in a more general form rather than (4). However, it should be noted that our analysis in this work is only specified for Huber loss.

I.1 Riemannian (sub)gradient descent methods

Here, we consider (sub)gradient descent for optimizing a more general problem

$$\min_{\mathbf{q}} \varphi(\mathbf{q}) := \frac{1}{np} \sum_{i=1}^p \psi(C_{\mathbf{y}_i} \mathbf{P} \mathbf{q}), \quad \text{s.t. } \|\mathbf{q}\| = 1,$$

where $\psi(\mathbf{z})$ can be ℓ^1 -loss ($\psi(\mathbf{z}) = \|\mathbf{z}\|_1$), Huber-loss ($\psi(\mathbf{z}) = H_\mu(\mathbf{z})$), and ℓ^4 -loss ($\psi(\mathbf{z}) = -\|\mathbf{z}\|_4^4$). The preconditioning matrix \mathbf{P} can be written as

$$\mathbf{P} = \mathbf{C}_v, \quad v = \mathbf{F}^{-1} \left(\left(\frac{1}{\theta np} \sum_{i=1}^p |\hat{\mathbf{y}}_i|^{\odot 2} \right)^{\odot -1/2} \right),$$

where $\hat{\mathbf{y}}_i = \mathbf{F} \mathbf{y}_i$, so that

$$\mathbf{C}_{\mathbf{y}_i} \mathbf{P} = \mathbf{C}_{\mathbf{y}_i} \mathbf{C}_v = \mathbf{C}_{\mathbf{y}_i \odot v} = \mathbf{C}_{\bar{\mathbf{y}}_i}, \quad \bar{\mathbf{y}}_i = \mathbf{y}_i \odot v.$$

Therefore, our problem can be rewritten as

$$\min_{\mathbf{q}} \varphi(\mathbf{q}) := \frac{1}{np} \sum_{i=1}^p \psi(\bar{\mathbf{y}}_i \odot \mathbf{q}), \quad \text{s.t. } \|\mathbf{q}\| = 1. \quad (74)$$

²¹Here, for 2D problem, $\check{\mathbf{Z}}$ denotes a flip operator that flips a matrix $\mathbf{Z} \in \mathbb{R}^{n_1 \times n_2}$ both vertically and horizontally, i.e., $\check{\mathbf{Z}}_{i,j} = \mathbf{Z}_{n_1-i+1, n_2-j+1}$.

Algorithm 1 Riemannian (sub)gradient descent algorithm

Input: observation $\{\mathbf{y}_i\}_{i=1}^m$

Output: the vector \mathbf{q}_* ,

Precondition the data by $\bar{\mathbf{y}}_i = \mathbf{y}_i \circledast \mathbf{v}$, with $\mathbf{v} = \left(\frac{1}{\theta np} \sum_{i=1}^p |\mathbf{y}_i|^{\odot 2} \right)^{\odot -1/2}$.

Initialize the iterate $\mathbf{q}^{(0)}$ and stepsize $\tau^{(0)}$.

while not converged **do**

 Update the iterate by

$$\mathbf{q}^{(k+1)} = \mathcal{P}_{\mathbb{S}^{n-1}} \left(\mathbf{q}^{(k)} - \tau^{(k)} \text{grad } \varphi(\mathbf{q}^{(k)}) \right).$$

 Choose a new stepsize $\tau^{(k+1)}$, and set $k \leftarrow k + 1$.

end while

Starting from an initialization, we solve the problem via Riemannian (sub)gradient descent,

$$\mathbf{q}^{(k+1)} = \mathcal{P}_{\mathbb{S}^{n-1}} \left(\mathbf{q}^{(k)} - \tau^{(k)} \cdot \text{grad } \varphi(\mathbf{q}^{(k)}) \right),$$

where $\tau^{(k)}$ is the stepsize, and the Riemannian (sub)gradient is

$$\text{grad } \varphi(\mathbf{q}) = \mathcal{P}_{\mathbf{q}^\perp} \nabla \varphi(\mathbf{q}),$$

which is defined on the *tangent space*²² $T_{\mathbf{q}}\mathbb{S}^{n-1}$ at a point $\mathbf{q} \in \mathbb{S}^{n-1}$. [Table 2](#) lists the calculation of (sub)gradients $\nabla \varphi(\mathbf{q})$ for different loss functions. For each iteration, the projection operator $\mathcal{P}_{\mathbb{S}^{n-1}}(\mathbf{z}) = \mathbf{z} / \|\mathbf{z}\|$ retracts the iterate back to the sphere. Let \odot denotes entry-wise power/multiplication, the overall algorithm is summarized in [Algorithm 1](#).

Initialization. In our theory, we showed that starting from a random initialization drawn uniformly over the sphere,

$$\mathbf{q}^{(0)} = \mathbf{d}, \quad \mathbf{d} \sim \mathcal{U}(\mathbb{S}^{n-1}),$$

for Huber-loss, Riemannian gradient descent method provably recovers the target solution. On the other hand, we could also cook up a data-driven initialization by choosing a row of $\mathbf{C}_{\bar{\mathbf{y}}_i}$,

$$\mathbf{q}^{(0)} = \mathcal{P}_{\mathbb{S}^{n-1}} \left(\mathbf{C}_{\bar{\mathbf{y}}_i}^\top \mathbf{e}_j \right)$$

for some randomly chosen $1 \leq i \leq p$ and $1 \leq j \leq n$. By observing

$$\mathbf{C}_{\bar{\mathbf{y}}_i} \approx \mathbf{C}_{\mathbf{x}_i} \mathbf{C}_{\mathbf{a}} (\mathbf{C}_{\mathbf{a}}^\top \mathbf{C}_{\mathbf{a}})^{-1/2}, \quad \mathbf{q}^{(0)} \approx \mathcal{P}_{\mathbb{S}^{n-1}} \left((\mathbf{C}_{\mathbf{a}}^\top \mathbf{C}_{\mathbf{a}})^{-1/2} \mathbf{C}_{\mathbf{a}}^\top s_j [\tilde{\mathbf{x}}_i] \right),$$

we have

$$\mathbf{C}_{\bar{\mathbf{y}}_j} \mathbf{q}^{(0)} \approx \alpha \mathbf{C}_{\mathbf{x}_i} \mathbf{C}_{\mathbf{a}} (\mathbf{C}_{\mathbf{a}}^\top \mathbf{C}_{\mathbf{a}})^{-1} \mathbf{C}_{\mathbf{a}}^\top s_\ell [\tilde{\mathbf{x}}_i] = \alpha \mathbf{C}_{\mathbf{x}_j} s_\ell [\tilde{\mathbf{x}}_i].$$

This suggests that our particular initialization $\mathbf{q}^{(0)}$ is acting like $s_\ell [\tilde{\mathbf{x}}_i]$ in the rotated domain. It is sparse and possesses several large spiky entries more biased towards the target solutions. Empirically, we find this data-driven initialization often works better than random initializations.

Choice of stepsizes. For Huber and ℓ^4 losses, we can choose a fixed stepsize $\tau^{(k)}$ for all iterates to guarantee linear convergence. For subgradient descent of ℓ^1 -loss, it often achieves linear convergence when we choose a geometrically decreasing sequence of stepsize $\tau^{(k)}$ [[ZWR⁺18](#)]. Empirically, we find that the algorithm converges much faster when Riemannian linesearch is deployed (see [Algorithm 2](#)).

²² We refer the readers to Chapter 3 of [[AMS09](#)] for more details.

Algorithm 2 Riemannian linesearch for stepsize τ

Input: $\mathbf{a}, \mathbf{x}, \tau_0, \eta \in (0.5, 1), \beta \in (0, 1)$,
Output: $\tau, \mathcal{R}_{\mathbf{a}}^{\mathcal{M}}(-\tau \mathbf{P}_{T_{\mathcal{M}}} \nabla \psi_{\mathbf{x}}(\mathbf{a}))$
Initialize $\tau \leftarrow \tau_0$,
Set $\tilde{\mathbf{q}} = \mathcal{P}_{\mathbb{S}^{n-1}}(\mathbf{q} - \tau \text{grad } \varphi(\mathbf{q}))$
while $\varphi(\tilde{\mathbf{q}}) \geq \varphi(\mathbf{q}) - \tau \cdot \eta \cdot \|\text{grad } \varphi(\mathbf{q})\|^2$ **do**
 $\tau \leftarrow \beta \tau$,
 Update $\tilde{\mathbf{q}} = \mathcal{P}_{\mathbb{S}^{n-1}}(\mathbf{q} - \tau \text{grad } \varphi(\mathbf{q}))$.
end while

I.2 LP rounding

Due to preconditioning or smoothing effects of our choice of loss functions, the Riemannian (sub)gradient descent methods can only produce an approximate solution. To obtain the exact solution, we use the solution $\mathbf{r} = \mathbf{q}_\star$ produced by gradient methods as a warm start, and solve another phase-two LP rounding problem,

$$\min_{\mathbf{q}} \zeta(\mathbf{q}) := \frac{1}{np} \sum_{i=1}^p \|\bar{\mathbf{y}}_i \circledast \mathbf{q}\|_1 \quad \text{s.t.} \quad \langle \mathbf{r}, \mathbf{q} \rangle = 1.$$

Since the feasible set $\langle \mathbf{r}, \mathbf{q} \rangle = 1$ is essentially the tangent space of the sphere \mathbb{S}^{n-1} at \mathbf{q}_\star , whenever \mathbf{q}_\star is close enough to one of the target solutions, one should expect that the optimizer \mathbf{q}_r of LP rounding exactly recovers the inverse of the kernel \mathbf{a} up to a scaled-shift. To address this computational issue, we utilize a *projected subgradient method* for solving the LP rounding problem. Namely, we take

$$\begin{aligned} \mathbf{q}^{(k+1)} &= \mathbf{r} + (\mathbf{I} - \mathbf{r}\mathbf{r}^\top) \left(\mathbf{q}^{(k)} - \tau^{(k)} \mathbf{g}^{(k)} \right) \\ &= \mathbf{q}^{(k)} - \tau^{(k)} \mathcal{P}_{\mathbf{r}^\perp} \mathbf{g}^{(k)}, \end{aligned}$$

where $\mathbf{g}^{(k)}$ is the subgradient at $\mathbf{q}^{(k)}$ with

$$\mathbf{g}^{(k)} = \frac{1}{np} \sum_{i=1}^p \check{\bar{\mathbf{y}}}_i \circledast \text{sign}(\bar{\mathbf{y}}_i \circledast \mathbf{q}^{(k)}).$$

By choosing a geometrically shrinking stepsizes

$$\tau^{(k+1)} = \beta \tau^{(k)}, \quad \beta \in (0, 1).$$

we show that the subgradient descent linearly converges to the target solution. The overall method is summarized in [Algorithm 3](#).

I.3 Solving problems in 2D

Finally, we briefly discuss about technical details about solving the MCS-BD problem in 2D, which appears broadly in imaging applications such as image deblurring [[LWDF11](#), [ZWZ13](#), [SM12](#)] and microscopy imaging [[BPS⁺06](#), [HGM06](#), [RBZ06](#)].

Problem formulation. Given the measurements

$$\mathbf{Y}_i = \mathbf{A} \boxtimes \mathbf{X}_i, \quad 1 \leq i \leq p,$$

Algorithm 3 Projected subgradient method for solving the LP rounding problem

Input: observation $\{\mathbf{y}_i\}_{i=1}^m$, vector \mathbf{r} , stepsize τ_0 , and $\beta \in (0, 1)$.

Output: the solution \mathbf{q}_\star ,

Precondition the data by $\bar{\mathbf{y}}_i = \mathbf{y}_i \circledast \mathbf{v}$, with $\mathbf{v} = \left(\frac{1}{\theta n p} \sum_{i=1}^p |\mathbf{y}_i|^{\odot 2} \right)^{\odot -1/2}$.

Initialize $\mathbf{q}^{(0)} = \mathbf{r}$, $\tau^{(0)} = \tau_0$

while not converged **do**

 Update the iterate

$$\mathbf{q}^{(k+1)} = \mathbf{q}^{(k)} - \tau^{(k)} \mathcal{P}_{\mathbf{r}^\perp} \mathbf{g}^{(k)}.$$

 Set $\tau^{(k+1)} = \beta \tau^{(k)}$, and $k \leftarrow k + 1$.

end while

where \circledast denotes 2D convolution, $\mathbf{A} \in \mathbb{R}^{n \times n}$ is a 2D kernel, and $\mathbf{X}_i \in \mathbb{R}^{n \times n}$ is a sparse activation map, we want to recover \mathbf{A} and $\{\mathbf{X}_i\}_{i=1}^p$ simultaneously. We first precondition the data via

$$\bar{\mathbf{Y}}_i = \mathbf{Y}_i \circledast \mathbf{V}, \quad \mathbf{V} = \mathcal{F}^{-1} \left(\left(\frac{1}{\theta n^2 p} \sum_{i=1}^p |\mathcal{F}(\mathbf{Y}_i)|^{\odot 2} \right)^{\odot -1/2} \right),$$

where $\mathcal{F}(\cdot)$ denote the 2D DFT operator. By using the preconditioned data, we solve the following optimization problem

$$\min_{\mathbf{Z}} \varphi(\mathbf{Z}) := \frac{1}{n^2 p} \sum_{i=1}^p \psi(\bar{\mathbf{Y}}_i \circledast \mathbf{Z}), \quad \text{s.t. } \|\mathbf{Z}\|_F = 1, \quad (75)$$

where $\varphi(\cdot)$ is the loss function (e.g., ℓ^1 , Huber, ℓ^4 -loss), and $\|\cdot\|_F$ denotes the Frobenius norm. If the problem (75) can be solved to the target solution \mathbf{Z}_\star , then we can recover the kernel and the sparse activation map up to a signed-shift by

$$\mathbf{A}_\star = \mathcal{F}^{-1} \left(\mathcal{F}(\mathbf{V} \circledast \mathbf{Z}_\star)^{\odot -1} \right), \quad \mathbf{X}_i^\star = (\mathbf{Y}_i \circledast \mathbf{V}) \circledast \mathbf{Z}_\star, \quad 1 \leq i \leq p.$$

Riemannian (sub)gradient descent. Similar to the 1D case, we can optimize the problem (75) via Riemannian (sub)gradient descent,

$$\mathbf{Z}^{(k+1)} = \mathcal{P}_F \left(\mathbf{Z}^{(k)} - \tau^{(k)} \cdot \text{grad } \varphi(\mathbf{Z}^{(k)}) \right),$$

where the Riemannian (sub)gradient

$$\text{grad } \varphi(\mathbf{Z}) = \mathcal{P}_{\mathbf{Z}^\perp} \nabla \varphi(\mathbf{Z}).$$

The gradient $\nabla \varphi(\mathbf{Z})$ for different loss functions are recorded in Table 2. For any $\mathbf{W} \in \mathbb{R}^{n \times n}$, the normalization operator $\mathcal{P}_F(\cdot)$ and projection operator $\mathcal{P}_{\mathbf{Z}^\perp}(\cdot)$ are defined as

$$\mathcal{P}_F(\mathbf{W}) := \mathbf{W} / \|\mathbf{W}\|_F, \quad \mathcal{P}_{\mathbf{Z}^\perp}(\mathbf{W}) := \mathbf{W} - \|\mathbf{Z}\|_F^{-2} \langle \mathbf{Z}, \mathbf{W} \rangle \mathbf{Z}.$$

The initialization and stepsize $\tau^{(k)}$ can be chosen similarly as the 1D case.

LP rounding. Similar to 1D case, we solve a phase-two linear program to obtain exact solution. By using the solution \mathbf{Z}_\star produced by Riemannian gradient descent as a warm start $\mathbf{U} = \mathbf{Z}_\star$, we solve

$$\min_{\mathbf{Z}} \frac{1}{n^2 p} \sum_{i=1}^p \|\bar{\mathbf{Y}}_i \boxtimes \mathbf{Z}\|_1, \quad \text{s.t. } \langle \mathbf{U}, \mathbf{Z} \rangle = 1.$$

We optimize the LP rounding problem via subgradient descent,

$$\mathbf{Z}^{(k+1)} = \mathbf{Z}^{(k)} - \tau^{(k)} \mathcal{P}_{\mathbf{U}^\perp} \mathbf{G}^{(k)},$$

where we choose a geometrically decreasing stepsize $\tau^{(k)}$ and set the subgradient

$$\mathbf{G}^{(k)} = \frac{1}{n^2 p} \sum_{i=1}^p \check{\bar{\mathbf{Y}}}_i \boxtimes \text{sign}(\bar{\mathbf{Y}}_i \boxtimes \mathbf{Z}^{(k)}).$$